TECHNISCHE UNIVERSITÄT WIEN
Vienna University of Technology

ACIN
AUTOMATION & CONTROL INSTITUTE
INSTITUT FÜR AUTOMATISIERUNGS- & REGELUNGSTECHNIK

Hand Prosthesis Control via IMU-based Upper Limb Movement Tracking

DIPLOMARBEIT

ausgeführt zur Erlangung des akademischen Grades

DIPLOMINGENIEUR

in der Studienrichtung

ENERGIE- UND AUTOMATISIERUNGSTECHNIK

Angefertigt am Institut für Automatisierungs- und Regelungstechnik

Beurteilung:
Ao.Univ.–Prof. Dipl.–Ing. Dr.techn. Markus Vincze

Eingereicht von:

Klaus Schlachter

Matrikelnummer 0856968

29. August 2017

Wien, August 2017.

Technische Universität Wien
A-1040 Wien, Karlsplatz 13, Internet: http://www.tuwien.ac.at

Abstract

Usability and acceptance of multifunctional upper limb prosthesis are highly dependent on a user-friendly control. Improvement of the state of art is still required since conventional sEMG control only permits to position one joint at a time, and it is usually the angular velocity instead of the position that is controlled. This is not intuitive, and also takes much time to position all joints. In this thesis a control scheme for a simultaneous and direct position control of several joints based on upper limb movement tracking should be implemented and tested. Tracking of the arm movement should be realized by an IMU placed on the forearm.

At first, this work summarizes state of the art algorithms which are used in position and orientation tracking systems using inertial measurements. Further essential error sources and their contributions to the tracking error are described (error propagation). Identification of the sensor measurement noise allows an estimation of the uprising drifts as a function of the tracking duration. This estimation of the uprising drifts is meant to provide a basis for the present and further work. Compared to an orientation-based control scheme, a position-based control scheme requires more restrictive requirements on the usage, as position tracking with adequate accuracy is only possible for short periods of time of a couple of seconds. Therefore in the following, an orientation-based control scheme is developed.

To evaluate the proposed control concept, a test framework is implemented in Matlab/Simulink. Within one test scenario the subjects are prompted to reposition a virtual prosthesis from different start configurations into its neutral configuration; within another scenario the subjects steer a cursor into subsequently appearing targets (circles of different sizes) with the coordinate axes representing the position of two joints. The two control concepts are then compared via a comparison of real-time performance metrices such as the completion time and the path efficiency, and through a qualitative survey via a questionnaire and discussions with the participants.

User tests were conducted with five disabled and twelve able-bodied subjects. It is shown that the proposed control scheme allows to position two joints simultaneously and faster compared to a conventional sEMG control. The five amputated subjects perceived the novel control concept as being more intuitive and quoted that it allows a more precise positioning of joints. The subjects considered both a fast and precise control as an important criterion for prosthesis control. Three out of five quoted that an incorporation of the novel control scheme into daily life is “imaginable”, while two considered it as “rather imaginable”.

Zusammenfassung

Für die Steuerung von Myoprothesen der oberen Extremität besteht gegenüber dem aktuellen Stand der Technik insofern Verbesserungsbedarf, als zum Einen mittels sEMG Gelenke nur sequentiell und nicht gleichzeitig positioniert werden können und zum Anderen nicht die Gelenksposition, sondern die Gelenksgeschwindigkeit vorgegeben wird. Dies ist einerseits nicht sehr intuitiv, andererseits dauert es entsprechend lange, bis alle Gelenke richtig positioniert sind. In dieser Arbeit soll eine auf der Armbewegung basierende Steuerung zur direkten und simultanen Positionsvorgabe mehrerer Gelenke implementiert und getestet werden. Die Armbewegung soll dabei durch eine am Unterarm angebrachte IMU erfasst werden.

In der vorliegenden Arbeit werden zunächst – basierend auf einer Literaturrecherche – die aktuellen Algorithmen von Orientierungs- und Positionstrackingsystemen mittels inertialer Sensorik zusammengefasst. Die essentiellen Fehlerquellen und deren Einfluss auf den Schätzfehler werden beschrieben (Fehlerfortpflanzung). Eine Identifikation der Sensoreigenschaften erlaubt anschließend eine Abschätzung der erzielbaren Genauigkeit in Abhängigkeit der Trackingdauer. Dies soll als Basis für die vorliegende, aber auch für zukünftige Arbeiten dienen. Für eine positionsbasierte Steuerung sind im Allgemeinen restriktivere Anforderungen nötig, da eine sinnvolle Positionsschätzung nur für wenige Sekunden möglich ist. Daher wird im Folgenden eine orientierungsbasierte Steuerung entworfen.

Für die Evaluierung der vorgeschlagenen Steuerung wird eine Testumgebung in Matlab/Simulink implementiert. In einem Testszenario werden die Probanden aufgefordert, zwei Gelenke einer virtuellen Prothese ausgehend von verschieden Startkonfigurationen in die neutrale Position zurückzuführen. In einem zweiten Testszenario muss ein Cursor in nacheinander am Bildschirm auftauchende Ziele (Kreise unterschiedlicher Größe) gesteuert werden, wobei die beiden Koordinatenachsen die Position zweier Gelenke repräsentieren. Ein Vergleich der beiden Steuervarianten erfolgt anschließend durch objektive Kennzahlen wie der benötigten Zeit und der Pfadeffizienz sowie durch eine qualitative Befragung der Testteilnehmer in Form von Fragebögen.

Im Zuge von Anwendertests mit fünf amputierten und zwölf nicht-amputierten Probanden konnte gezeigt werden, dass die neuartige Steuerung eine simultane und im Vergleich zur sEMG-Steuerung schnellere Positionierung zweier Gelenke ermöglicht. Die fünf Prothesenträger bewerteten die neuartige Steuerung als intuitiver einsetzbar und gaben zudem an, Gelenke mit der neuartigen Steuerung genauer positionieren zu können. Sowohl eine genaue als auch schnelle Positionierung stellte für die befragten Probanden ein wichtiges Kriterium an eine Steuerung dar. Drei der fünf Befragten bewerteten eine Nutzung der Steuerung im Alltag als „vorstellbar“, zwei als „eher vorstellbar“.

Acknowledgment

First of all, I want to express my sincere gratitude to all of the people who encouraged and supported me, thereby contributing to the success of this thesis. Sincere thanks go to my advisor Professor Markus Vincze for his effort, continuous support and very helpful advice. Thank you also for always finding the time on short notice to meet with me, give me feedback, and answer questions that arose. I would also like to thank the employees of Otto Bock who made this thesis possible in the first place. Especially, I want to thank Markus Schachinger, Georg Brandmayr, Raphael Mayer and Sebastian Amsüss for the numerous interesting and stimulating discussions, and their support in various technical matters. I would like to especially thank Georg Brandmayr for the review of the final work. Very special thanks go to all my colleagues who provided me with their time and participated in the user tests.

Special thanks and love go to my parents, who supported me emotionally and financially throughout all the years of education, which also went along with putting their own wishes to the side at some points in time. With their confidence and patience, they fulfilled the basic requirements for a successful completion of my studies.

Moreover, I am very grateful to all of the friends, who provided me with their support and helped me stay focused and motivated, but also gave me necessary distractions. Very special thanks go to Alina for the numerous hours of proof-reading and providing me with feedback in various stages of writing.

Contents

List of Figures

Nomenclature

$\boldsymbol{A}_{BA}$	basis transformation matrix (from frame A to frame B)
$\boldsymbol{q}_{BA}$	rotation quaternion: ${}_B\boldsymbol{x} = \boldsymbol{q}_{BA} \cdot {}_A\boldsymbol{x} \cdot (\boldsymbol{q}_{BA})^{(*)}$
${}_A\boldsymbol{e}_x$	basis vector with respect to frame A
${}_A\boldsymbol{x}$	vector with respect to frame A
${}_B\boldsymbol{\omega}_{AB}$	angular velocity of frame B relative to frame A resolved in frame B

1 Introduction

Modern upper-limb prostheses restore many hand functions and can improve the quality of life of people with forearm disabilities. In order to reintegrate activities like carrying a plate, holding a book or driving a car into daily life, modern upper-limb prostheses are designed as complex mechatronic systems with several degrees of freedom and allow multiple movements such as wrist flexion/extension, wrist pronation/supination as well as executing different grasp types. Usability and acceptance of such multifunctional prostheses highly depend on a user-friendly control; therefore fast, reliable and intuitive control methods are required. The design of the control of such multifunctional prostheses is challenging and substantial improvement is still required.

Conventional commercial solutions mostly use two sEMG sensors, placed on the skin surface on opposite sides of the forearm. This allows to control the angular velocity of one joint. The angular velocity is typically proportional to the signal power and the rotation direction is defined by the strongest signal. In order to control another joint, mode switching is necessary (e.g. by co-contraction of the muscles related to both sEMG sensors). The control of the angular velocity instead of the angle of a joint and also the sequential control of single joints instead of a simultaneous control is not intuitive and takes much time. These aspects lead to the development of alternative control concepts. Besides or in addition to the approach of the use of more than two electrodes and pattern recognition in this thesis alternative control concepts - based on tracking of the forearm's orientation or position using IMU data - should be drawn up. These IMU-based control concepts should overcome the major challenges of pattern recognition concepts toward clinical usability and robustness which are [1]:

- Training of classifiers have to be conducted for each user separately because of their unique signals.
- Major challenges toward clinical robustness:
  - different arm positions: In daily life the limb is used in different positions which causes different load on the muscles from which sEMG data is recorded.
  - variation in force: Contractions performed at different force levels may be very different from one another and therefore present a challenge to pattern classifiers.
  - transient changes: Short- and long-term variations in the recording environment during use, external interference, electrode impedance changes, electrode shift and lift and muscle fatigue may alter the sEMG signals and present challenges to clinical robustness.

While pattern recognition has the ability to avoid mode switching, still typically only one degree of freedom is manipulated at a time. These aspects lead to the motivation to develop alternative control concepts which should meet the following characteristics:

- intuitive and simultaneous control of several degrees of freedom
- reliability (irrespective of the limb position)
- robustness to changes in the recording environment, e.g. the temperature
- as little individual training as possible

1.1 General Objectives

IMU-based sensors have developed very quickly throughout the last decade; with MEMS technology going through some major changes, IMU sensors of small size, low weight and low energy consumption are now offered for relatively low cost. In recent times they are used in various fields for new approaches to human computer interaction. With prosthesis control being one of those, the present work is meant to determine the potential of hand prosthesis control via IMU-based upper limb movement tracking.

Thus, the main goals of this thesis are: at first to investigate upper limb movement tracking concepts in terms of their usability for a prospective prosthesis control. Further a control concept should be implemented and control of a virtual prosthesis should be enabled. On the basis of this implementation the pros and cons with respect to a conventional sEMG solution should be examined. The basic idea of an IMU-based control scheme is illustrated in Fig. (1.1). The sEMG electrodes are used to allow the user to activate and deactivate the orientation-based control mode. When enabled, the forearm orientation is linked to joints' angles and thus joints can be positioned by moving the forearm.

1.2 Line of Solution

At first a literature research on methods which are used in arm tracking systems was carried out. Further the achievable accuracy regarding orientation and position tracking using the predefined sensor (Bosch BMX055) was examined. As next step, real-time data of the IMU was integrated in Matlab/Simulink and an orientation-based control of a virtual prosthesis was implemented. Based on a literature research a test framework was implemented and the proposed orientation-based control concept as well as the conventional sEMG solution by Ottobock were integrated into the framework. As a last step user tests were conducted in order to compare these two different control methods as well

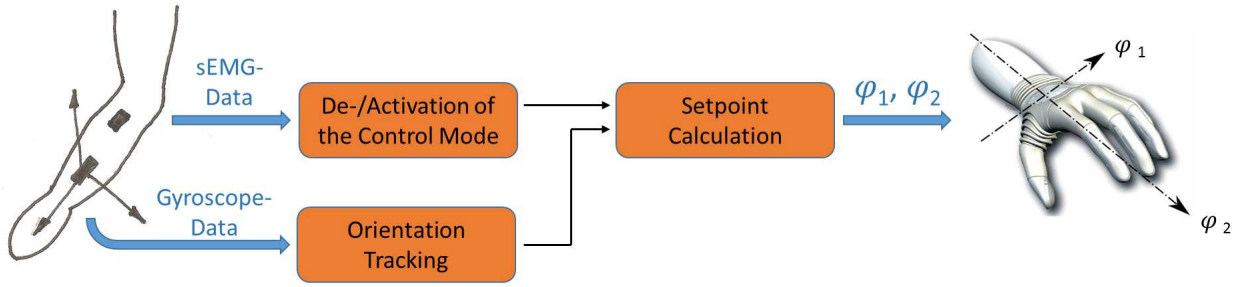

Figure 1.1: Orientation-based control scheme. When activated, the orientation of the forearm is linked to the joint angles of the wrist. Activation and deactivation of the control mode is intended to be provided via sEMG. By moving the forearm the user is then able to bend $\dot{\varphi}_1$ and rotate $\dot{\varphi}_2$ the wrist simultaneously.

as to gather feedback from prosthesis users. The work in this project can be divided into following milestones:

- Literature review on arm tracking systems
- Real-time integration of IMU data in Matlab/Simulink
- Implementation of a control concept
- Implementation of a test framework
- Planning of user tests (test protocols, questionnaires)
- Evaluation of the conducted user tests

A sensor casing which can be fixed on the forearm using hook-and-loop tape was developed in prior work [2].

1.3 Structure of the Thesis

This thesis is organized as follows. In Chapter 2 the main mathematical concepts used for representation of rotations are presented.

Chapter 3 at first describes the arm-kinematics and the typical physical limitations of people with forearm amputations. Subsequently, the conventional sEMG control concept is described. This concept acts later on as a reference to determine pros and cons of the IMU-based control scheme. Chapter 3 then focuses on following concepts and its limitations:

- Orientation tracking based on integration of the angular velocities
- Position tracking based on double-integration of the accelerations

Finally, the evaluation of human-computer interfaces using the Target Achievement Control Test is discussed [3].

Chapter 4 briefly describes prior work [2] on which this work is based. The chapter also serves as delimitation between the already existing work and the present one.

Chapter 5 at first describes the implementation of the proposed control scheme which utilizes the orientation of the forearm. Subsequently the implemented test framework is presented. This framework allows to compare two control methods via a comparison of real-time performance metrics such as completion time and path efficiency.

In Chapter 6 the underlying noise process of the accelerometer and gyroscope is identified via an Allan variance analysis. Further it is investigated how essential error sources propagate through orientation and position tracking solutions. Subsequently the results of the conducted user tests are presented.

Chapter 7 reflects the result followed by an outlook on future possibilities on the use of the introduced control scheme and further perspectives on its development.

2 Theoretical Background

This chapter begins with the definition of coordinate frames which are commonly used in inertial navigation systems. Subsequently, the concepts of rotation matrices and quaternions are introduced and the kinematic equation is stated. In literature different conventions for representing quaternions are used and conventions regarding rotations are sometimes ambiguous (active vs. passive). Although this has no fundamental meaning, it makes formulations look different and changes the interpretation of quantities. Therefore, in this chapter it was paid heed to a clear definition of the terms and an unambiguous notation. In the end of this chapter the notation used in this work is summarized.

2.1 Coordinate Frame Definitions

In inertial navigation, there are several coordinate frames which are commonly used. The coordinate frames used within this thesis are defined as in [4]:

- Body frame denoted by B: Its origin and its axes are fixed with respect to the object described by the navigation solution.
- Sensor frame denoted by S: Its origin is fixed with respect to the IMU and its axes coincide with the sensitive axes of the sensor (the measurements are resolved in the sensor frame).
- Local navigation frame denoted by N: Its origin is fixed with the object described by the navigation solution; its axes are fixed with respect to the earth and the z-axis coincides with the orientation of the gravity vector and is pointing upwards.
- Local tangent-plane frame denoted by L: Its origin is fixed with respect to the earth. Its axes coincide with the axes of the local navigation frame. Within this thesis it is regarded as an inertial reference frame.

2.2 Orientation Representation and Rotations

This part reviews the concepts of orientation representation using rotation matrices and quaternions.

Basis Transformation Matrix

A basis B for the vector space $\mathbb{R}^3$ is defined by an ordered list of three linear independent basis vectors $B = (\boldsymbol{b}_1, \boldsymbol{b}_2, \boldsymbol{b}_3)$. The coordinate vector of an element $\boldsymbol{v} \in \mathbb{R}^3$ with respect to the basis B is denoted as ${}_B\boldsymbol{v}$. The matrix with the basis vectors of one basis B with respect to another basis C as columns forms the *basis transformation matrix* [5]

$$\boldsymbol{A}_{CB} := [{}_C\boldsymbol{b}_1, {}_C\boldsymbol{b}_2, {}_C\boldsymbol{b}_3] \tag{2.1}$$

and describes how two bases B and C of the same vector space are related. The change of the basis of a vector $\boldsymbol{x}$ is given by

$$\begin{aligned} {}_C\boldsymbol{x} &= \boldsymbol{A}_{CB} \cdot {}_B\boldsymbol{x} && (2.2)\\ {}_B\boldsymbol{x} &= \boldsymbol{A}_{BC} \cdot_C \boldsymbol{x} = (\boldsymbol{A}_{CB})^{-1} \cdot {}_C\boldsymbol{x}\,. && (2.3) \end{aligned}$$

Rotations can be represented by the orientation of a body-fixed coordinate frame relative to a reference frame. Rotations are described by basis transformation matrices which are orthogonal and have the determinant +1. The property of orthogonality is equivalent to the property that the inverse of a rotation matrix is equal to its transpose

$$(\boldsymbol{A}_{CB})^{-1} = (\boldsymbol{A}_{CB})^T = \boldsymbol{A}_{BC}\,. \tag{2.4}$$

Angular Velocity

As illustrated in Fig. (2.1) the position vector of a point P relative to the inertial reference frame I can be written as:

$${}_I\boldsymbol{r}_{0P} = {}_I\boldsymbol{r}_{01} + \boldsymbol{A}_{IB} \cdot {}_B\boldsymbol{r}_{1P} \tag{2.5}$$

Assuming that point P is rigidly attached to the body-fixed frame, the velocity is given by

$$\frac{\mathrm{d}}{\mathrm{d}t}{}_I\boldsymbol{r}_{0P} =_I \boldsymbol{v}_P =_I \dot{\boldsymbol{r}}_{01} + \dot{\boldsymbol{A}}_{IB} \cdot {}_B\boldsymbol{r}_{1B}\,. \tag{2.6}$$

Modifying Eq. (2.6) in such a way that all vectors are represented with respect to the body-fixed frame leads to

$${}_B\boldsymbol{v}_P = \boldsymbol{A}_{BI} \cdot {}_I\dot{\boldsymbol{r}}_{01} + \underbrace{\boldsymbol{A}_{BI}\dot{\boldsymbol{A}}_{IB}}_{{}_B\widetilde{\boldsymbol{\omega}}_{IB}} \cdot {}_B\boldsymbol{r}_{1P} \tag{2.7}$$

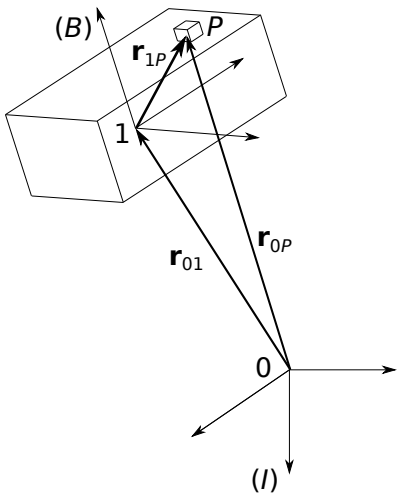

Figure 2.1: Coordinate systems

where ${}_B\widetilde{\boldsymbol{\omega}}_{IB}$ is the angular velocity tensor [6] associated with the angular velocity vector ${}_B\boldsymbol{\omega}_{IB} = [\omega_x, \omega_y, \omega_z]^T$:

$$ {}_B\widetilde{\boldsymbol{\omega}}_{IB} = \begin{bmatrix} 0 & -\omega_z & \omega_y \\ \omega_z & 0 & -\omega_x \\ -\omega_y & \omega_x & 0 \end{bmatrix} $$

The angular velocity vector is parallel to the instantaneous rotation axis and its magnitude represents the rate of rotation. From Eq. (2.7) follows the kinematic equation for rotation matrices[1]:

$$ \dot{\boldsymbol{A}}_{IB} = \boldsymbol{A}_{IB} \cdot {}_B\widetilde{\boldsymbol{\omega}}_{IB} \tag{2.8} $$

The quaternion skew field

A short introduction to quaternions is given here, and their algebraic structure is described since this provides an easy access to rules of calculation for further practical use.

Definition 2.1 *A quaternion* $\boldsymbol{q}$ *is defined as an ordered list of four real numbers* $\boldsymbol{q} = (a, b, c, d)$*, subjected to following rules of addition and multiplication. If*

$$ \boldsymbol{q_1} = (a_1, b_1, c_1, d_1), \boldsymbol{q_2} = (a_2, b_2, c_2, d_2) $$

then

[1] Applying tensor transformation rule ${}_I\widetilde{\boldsymbol{\omega}}_{IB} = \boldsymbol{A}_{IB} \cdot {}_B\widetilde{\boldsymbol{\omega}}_{IB} \cdot \boldsymbol{A}_{IB}$ and the relation $\boldsymbol{A}_{IB}\boldsymbol{A}_{BI} = \boldsymbol{I}$ leads to different forms of Eq. (2.8)

$$\begin{aligned} \boldsymbol{q_1} + \boldsymbol{q_2} &= (a_1 + a_2, b_1 + b_2, c_1 + c_2, d_1 + d_2) \\ \boldsymbol{q_1} \cdot \boldsymbol{q_2} &= (a_1a_2 - b_1b_2 - c_1c_2 - d_1d_2, a_1b_2 + b_1a_2 + c_1d_2 - d_1c_2, \\ &\quad a_1c_2 - b_1d_2 + c_1a_2 + d_1b_2, a_1d_2 + b_1c_2 - c_1b_2 + d_1a_2)\,. \end{aligned}$$

From this definition it follows that the set of quaternions, denoted as $\mathbb{H}$, forms a (associative) skew field[7] (a skew field has the same properties as a field except multiplication is allowed to be non-commutative).

A quaternion of the form $\boldsymbol{q} = (a, b, 0, 0)$ is associated with the complex number, defined as ordered pair (a, b) with the rule of multiplication

$$(a_1, b_1)(a_2, b_2) = (a_1a_2 - b_1b_2, a_1b_2 + b_1a_2)$$

and therefore quaternions can be understood as extension of complex numbers, further the set of quaternions of the form $(a, 0, 0, 0)$ is regarded as actually being the real number field (i.e. $(a, 0, 0, 0,) = a$). Along the lines of complex numbers, the conjugate of $\boldsymbol{q} = (a, b, c, d)$ is defined to be $\boldsymbol{q}^* = (a, -b, -c, -d)$ and the norm is defined as the product of a quaternion with its conjugate

$$\|\boldsymbol{q}\| = \boldsymbol{q}\ \boldsymbol{q^*} = (a^2 + b^2 + c^2 + d^2, 0, 0, 0)\,.$$

The square root of the norm $a^2 + b^2 + c^2 + d^2$ is called the length of a quaternion, denoted as $|\boldsymbol{q}|$. The inverse of $\boldsymbol{q}$ is its conjugate multiplied by the inverse of its norm

$$\boldsymbol{q}^{-1} = \frac{1}{\|\boldsymbol{q}\|}\boldsymbol{q}^*\,.$$

Within this thesis quaternions will be expressed as vectors $\boldsymbol{q} = [a, b, c, d]^T$.

Rotations are described by unity quaternions (their norm equals one). If the rotation vector $\boldsymbol{n}$ transfers the coordinate system C into the coordinate system B, then

$$\begin{pmatrix} 0 \\ {}_B\boldsymbol{x} \end{pmatrix} = \boldsymbol{q}_{BC} \cdot \begin{pmatrix} 0 \\ {}_C\boldsymbol{x} \end{pmatrix} \cdot (\boldsymbol{q}_{BC})^*\,, \tag{2.9}$$

with

$$\boldsymbol{q}_{BC} = \begin{bmatrix} \cos|\frac{\boldsymbol{n}}{2}| \\ -\frac{\boldsymbol{n}}{|\boldsymbol{n}|}\sin|\frac{\boldsymbol{n}}{2}| \end{bmatrix}\,.$$

Angular Velocity

The time derivative of the rotation quaternion is given by [8]

$$\dot{\boldsymbol{q}}_{IB} = \frac{1}{2}\boldsymbol{q}_{IB} \cdot \begin{pmatrix} 0 \\ {}_B\boldsymbol{\omega}_{IB} \end{pmatrix} \tag{2.10}$$

and can be rewritten in matrix form as [9]

$$\dot{\boldsymbol{q}}_{IB} = \frac{1}{2}\boldsymbol{\Omega}({}_B\boldsymbol{\omega}_{IB})\boldsymbol{q}_{NB} \tag{2.11}$$

where

$$\boldsymbol{\Omega}({}_B\boldsymbol{\omega}_{IB}) = \begin{bmatrix} 0 & -{}_B\boldsymbol{\omega}_{IB}^T \\ {}_B\boldsymbol{\omega}_{IB} & -{}_B\widetilde{\boldsymbol{\omega}}_{IB} \end{bmatrix} = \begin{bmatrix} 0 & -\omega_x & -\omega_y & -\omega_z \\ \omega_x & 0 & \omega_z & -\omega_y \\ \omega_y & -\omega_z & 0 & \omega_x \\ \omega_z & \omega_y & -\omega_x & 0 \end{bmatrix}. \tag{2.12}$$

In general, the solution of Eq. (2.10) and Eq. (2.7) is given by the Peano-Baker series as an infinite series [10]. A close form solution of the kinematic equations is unattainable [11] and therefore the equation must be integrated numerically in order to update the quaternion (or the rotation matrix).

2.3 Notation

For clarity, a summary of the used notation is given here. The left index of a vector denotes the coordinate frame in which the components of the vector are given (resolving axes). Basis transformation matrices and rotation quaternions are depicted with two indices. The second index indicates the *from* coordinate system and the first index the *to* coordinate system. Using this notation two corresponding indices are always nearby and create a chain of identifiers:

$${}_B\boldsymbol{x} = \boldsymbol{A}_{BA} \cdot {}_A\boldsymbol{x}\,, \tag{2.13}$$

$$\begin{pmatrix} 0 \\ {}_B\boldsymbol{x} \end{pmatrix} = \boldsymbol{q}_{BA} \cdot \begin{pmatrix} 0 \\ {}_A\boldsymbol{x} \end{pmatrix} \cdot (\boldsymbol{q}_{BA})^*\,. \tag{2.14}$$

To declare the angular rate unambiguously three indices are necessary. Exemplary, the angular rate ${}_B\boldsymbol{\omega}_{IB}$ denotes the angular velocity of frame B relative to frame I with respect to frame B. An IMU measures the angular rate ${}_S\boldsymbol{\omega}_{RS}$ of the sensor frame S relative to

an inertial reference frame N with respect to S. As no other angular rate measurement is in discussion, the indices are dropped. Thus, the kinematic equation is further written as

$$\dot{\boldsymbol{q}}_{NS} = \frac{1}{2}\boldsymbol{q}_{NS} \cdot \begin{pmatrix} 0 \\ \boldsymbol{\omega} \end{pmatrix} = \frac{1}{2}\boldsymbol{\Omega} \cdot \boldsymbol{q}_{NS} \tag{2.15}$$

where

$$\boldsymbol{\Omega} = \begin{bmatrix} 0 & -\boldsymbol{\omega}^T \\ \boldsymbol{\omega} & -\widetilde{\boldsymbol{\omega}} \end{bmatrix}. \tag{2.16}$$

3 State of the Art

3.1 Arm Kinematics and Hand Prostheses

The kinematics of the upper limb is usually modeled as a system of rigid segments connected by joints [12]. A basic model is illustrated in Fig. (3.1). The shoulder is modeled as a ball and socket joint which is free to rotate in all direction (triaxial). The elbow represents a joint with one degree of freedom allowing forearm flexion and extension. The movement in order to bring the palm up and down is produced in the forearm and is referred to as forehand supination (palm rotates to face up) and pronation (palm rotates to face down). In supination position the two forearm's bones are parallel. In order to bring the wrist into pronation position the two bones are shaped to an x-form. Since the wrist pro- and supination takes place near to the wrist, the capability to perform such a movement rapidly decreases with the amputation length of the forearm. The wrist joint allows flexion and extension as well as abduction and adduction (rotational movement within the palm plane).

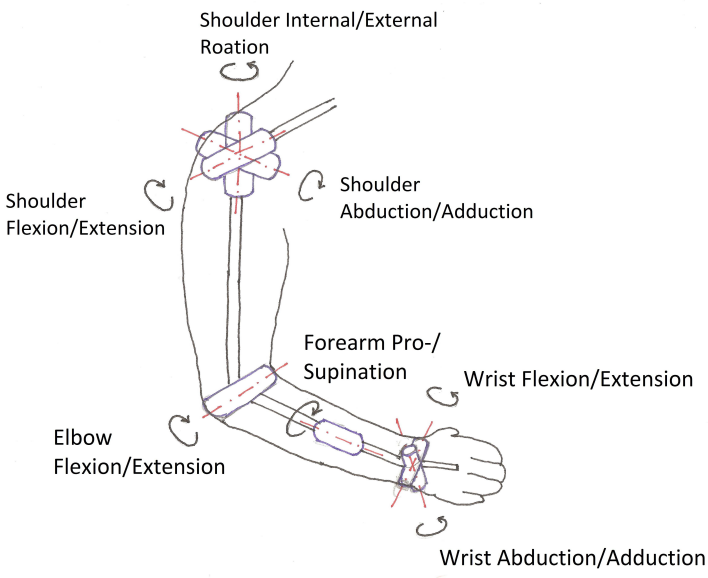

Figure 3.1: Kinematic model of the upper limb. Adapted from [13]

Hand prostheses' main task is to imitate the movements of a natural hand, i.e. to restore the ability to grasp and bend the wrist. Furthermore, prostheses for people with

forearm amputations need to restore not only the abovementioned abilities, but also need to overtake rotational movements originally done by the forearm, as the ability of wrist rotation decreases fast with the amputation length. Artificial wrist joints do usually not restore the ability for wrist abduction and adduction. In this thesis a control concept based on the forearm's orientation - which allows to bend (flexion/extension) and rotate (pronation/supination) an artificial wrist - is developed.

3.2 Four Channel Control

The novel control concept developed during this work is later compared to the commercially widely used four channel control solution of Ottobock which allows to position two joints using two sEMG signals. The sensors are mounted at the forearm on opposite sides; this allows the user to create sEMG-signals independently by contracting the flexor/extensor muscles. The control mode uses three parameters which are adjusted for each user; these are the two thresholds U_{on} and U_{high} and a time span t_S.

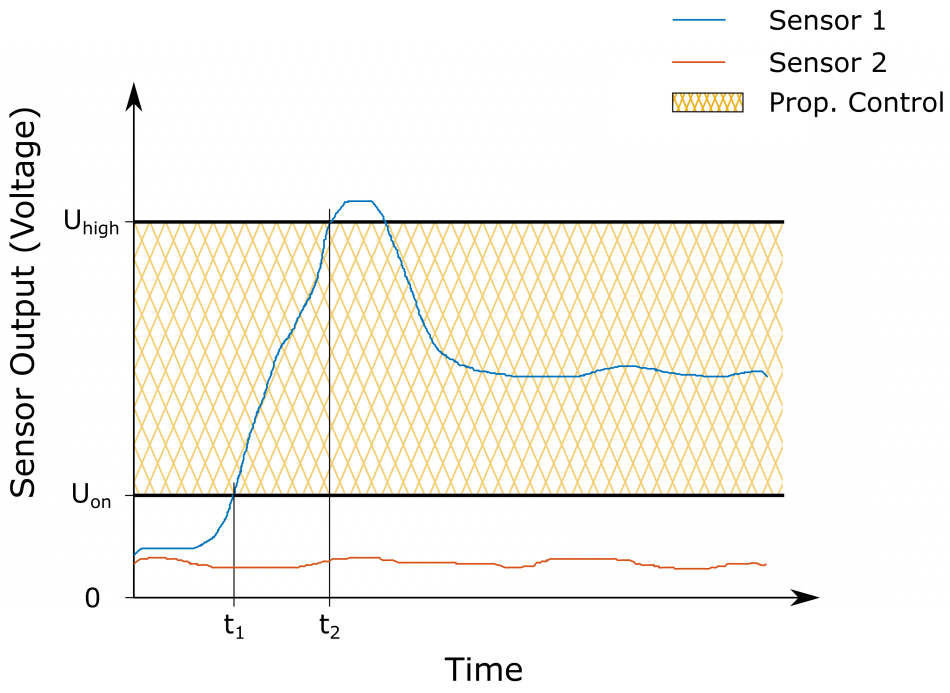

Figure 3.2: Illustration of the four-channel control

As illustrated in Fig. (3.2) the user rotates the wrist and closes the hand as follows:

- If the sensor output voltage U_1 or U_2 is between the thresholds U_{on} and U_{high} the user rotates the wrist with a velocity proportional to the voltage (activity level):

$$v = v_{max} \cdot \frac{U - U_{on}}{U_{high} - U_{on}}$$

The moving direction depends on the active signal, e.g. if activity is measured by the first sensor the wrist rotates the palm up and if activity is measured by the second sensor the wrist rotates in the opposite direction.

- In order to bend the wrist the user initially produces a fast muscle contraction. If the activity raises from threshold U_{on} to U_{high} within a defined time span t_s (typically 0.8s) the internal control state switches and the second joint (wrist bending) is now controlled. The active signal again defines the moving direction.
- If the user relaxes the muscles the controller switches back to the initial state and the user is able to rotate the wrist again.

3.3 Inertial Measurement Unit

Inertial measurement units (IMUs) are devices which combine gyroscopes and accelerometers, additionally magnetometers are included sometimes. This subsection shortly describes the working principles of MEMS gyroscopes and accelerometers. Subsequently, an overview of how IMUs are used in upper-limb prostheses is given.

3.3.1 Gyroscopes

Gyroscope technologies can be divided in three categories: spinning mass, vibration structure and optical gyroscopes. MEMS gyroscopes are vibrating structure gyroscopes. The structure is free to move in two perpendicular vibrating directions (modes). The sensing principle is based on the principle that the Coriolis force inducted by a rotation of the gyroscope transfers energy from one mode to the other mode. One mode is defined as the driving mode and is excited to enforce a sinusoidal vibration in the driving mode direction. When the gyroscope is rotated perpendicular to the driving mode direction the Coriolis force excites the sense mode. The reaction of the proof mass in the sense mode direction is measured and can is used to calculate the present angular velocity [14, 15].

3.3.2 Accelerometers

Accelerometers measure the force experienced by a proof mass and thus the accelerometer readings represent the acceleration relative to the free fall; i.e. an accelerometer resting on earth measures $[0, 0, g]^T$ if the z-axis of the sensor is pointing upwards. The force

is typically measured by a piezoresistive or capacitive principle [16]. The accelerometer readings $\boldsymbol{a}_m$ are given as

$$\boldsymbol{a}_m = \boldsymbol{q}_{SN} \cdot ({}_N\boldsymbol{a}_{LN} + \begin{pmatrix} 0 \\ 0 \\ g \end{pmatrix}) \cdot \boldsymbol{q}^*_{SN} \tag{3.1}$$

where $\boldsymbol{q}_{SN}$ represents the orientation of the sensor frame S relative to the local navigation frame N, and ${}_N\boldsymbol{a}_{LN}$ represents the acceleration of the sensor origin relative to an earth fixed reference point resolved in the local navigation frame.

3.3.3 Errors

The readings of MEMS gyroscopes and accelerometers are corrupted by various error terms which can be divided into systematic and random errors. The most important systematic errors are [17]:

- Scale factor errors: Deviations from the expected sensitivity. The occurring error is proportional to the measurement value.
- Scale factor non-linearity: The sensitivity depends on the magnitude of the measured quantity.
- Non-orthogonality: The sensor axes are not perfectly perpendicular (cross axes sensitivity).
- G-dependency: The bias changes depending on acceleration forces acting on the sensing axes. This effect applies mostly to MEMS gyroscopes.
- Constant bias: A constant difference between the observed and true value.

The most important random errors are [17]:

- Sensor Noise: The sensor noise is usually modeled as white noise. Integrating white noise leads to a random walk of orientation or velocity. The random walk is often stated in the data sheet.
- Bias Instability (In-run Bias): The bias changes randomly while the sensor is turned on; this is usually modeled as a bias random walk [18]. Also a temperature change and mechanical stress can cause a bias change.
- Bias Repeatability (Turn-on to Turn-on Bias): The bias term varies from when the sensor is turned off and on.

3.3.4 Calibration

Low-cost IMUs are usually poorly calibrated and therefore it is essential to account for the systematic errors if they are used for applications which are highly dependent on the sensor output quality. Calibration principles can be divided into two main groups - calibration by a specific routine and "in-run" calibration where the parameters are estimated during the normal use. This section deals with the former.

Sensor Error Model

In real IMU devices the sensitivity axes of the gyroscope and accelerometer are not perfectly perpendicular and do not perfectly coincide. A model which additionally accounts for measurement bias and scale factor errors can be stated as

$$\boldsymbol{a}_0 = \boldsymbol{T}_{SA} \cdot \boldsymbol{K}_a \cdot (\boldsymbol{a}_m - \boldsymbol{b}_a) \tag{3.2}$$
$$\boldsymbol{\omega}_0 = \boldsymbol{T}_{SG} \cdot \boldsymbol{K}_g \cdot (\boldsymbol{a}_m - \boldsymbol{b}_g) \tag{3.3}$$

where $\boldsymbol{b}$ represents the sensor bias, $\boldsymbol{K}$ the scale errors and $\boldsymbol{T}$ the projection of the sensor readings from the non-orthogonal sensing axes on an ideal orthogonal sensor frame S [19].

Aligning the x-axis of the orthogonal frame with the accelerometer's sensitivity axis and further assuming the sensing y-axis to be on the xy-plane of the orthogonal frame (see Fig. (3.3)), the parameters for a small angle approximation follow as

$$\boldsymbol{T}_{SA} = \begin{bmatrix} 1 & -\alpha_{yz} & \alpha_{zy} \\ 0 & 1 & -\alpha_{zx} \\ 0 & 0 & 1 \end{bmatrix}, \boldsymbol{T}_{SG} = \begin{bmatrix} 1 & -\beta_{yz} & \beta_{zy} \\ \beta_{xy} & 1 & -\beta_{zx} \\ -\beta_{ax} & \beta_{yx} & 1 \end{bmatrix}, \tag{3.4}$$

$$\boldsymbol{K}_{a/g} = \begin{bmatrix} k_{ax/gx} & 0 & 0 \\ 0 & k_{ax/gx} & 0 \\ 0 & 0 & k_{ax/gx} \end{bmatrix}, \boldsymbol{b}_{a/g} = \begin{bmatrix} b_{ax/gx} \\ b_{ay/gy} \\ b_{az/gz} \end{bmatrix}. \tag{3.5}$$

where α_{ij} and β_{ij} are the rotation angles of the i-th sensing axis around the j-th axis of S [19].

Calibration of IMUs can be carried out by measuring predefined accelerations and angular rates which are subsequently compared to the measurement data.

For accelerometer calibrations, it is exploited that a sensor in static state senses the gravity field [20]. Measurements in known positions can be directly compared to expected values. Supposing no axis misalignment and two measurements in opposite directions the scaling factor and bias term of one particular axis can be determined (two independent

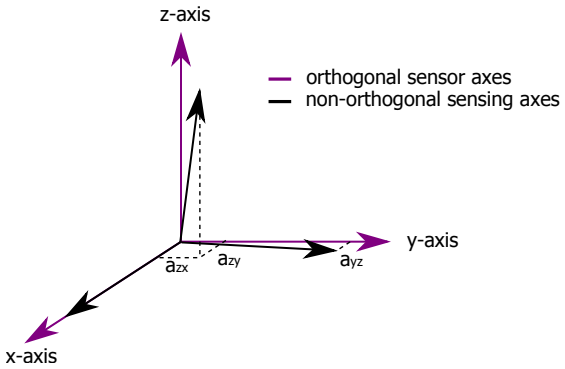

Figure 3.3: Construction of the orthogonal sensor frame

measurements for two unknowns) [9]. Another possibility is to capture the sensor readings in at least nine independent orientations. The scaling factor, bias term and axis misalignment are identified by optimization exploiting that the measured output should equal 1g in every arbitrary orientation.

The gyroscope bias can directly be measured when the sensor is at rest [21]. Measuring predefined angular velocities around the sensing axes provides information to determine the misalignment and sensitivity parameters but requires additional mechanical equipment as turntables [22]. Another possibility is to integrate the measured angular velocity while the sensor is rotated about a predefined angle [21].

In [23] a calibration procedure is proposed which accounts for non-coinciding sensing axes of the accelerometer and gyroscope without the use of external equipment. The calibration is based on measurements between static states. The gravity vector at the end of each interval is estimated based on the initial gravity vector by integrating the angular rates; the deviations are used as error measurement. Several such measurements are used to determine the calibration parameters by optimization.

3.3.5 IMUs and Upper Limb Prosthesis

The *DEKA arm* is a prosthetic arm which is controlled by feet movements. Sensing the feet's orientation provides eight different commands. For example wrist extension and flexion is controlled by bringing the toe of the left foot up and down respectively; an inner or outer rotation of the right foot activates grip selection (by backwards and forward cycling) [24].

The *i-limb quantum* bionic arm produced by *Touch Bionics* utilizes gesture control to switch between several grasp types. Gesture control can be activated by a defined sEMG signal when the forearm is held parallel to the ground. Subsequently, a specific grip is accessed by moving the forearm in one of four directions within the horizontal plane [25].

Woodward et al. [26] propose a system which utilizes grip switching based on specific arm

orientations. To change the grip type the user is required to bring the hand into relaxing position (close the hip) and subsequently to move the hand to the shoulder across the chest. The orientation change is sensed by an accelerometer.

Scheme et al. [27, 28] investigated the impact of variations in limb position on the robustness of pattern recognition based myoelectric control. A further study shows that the classification accuracy can be slightly improved by instrumenting the upper- and forearm with accelerometers.

Churko et al. [29] propose to use a virtual reality environment (VE) for early rehabilitation in stages before the patient can be fitted with a prosthesis. In order to measure the pose of the forearm to allow interaction within a VE an IMU and a linear displacement sensor are applied to the forearm.

Dermitzakis et al. [30] present a viability study which assesses gesture recognition using gyroscope data for the purpose of prosthesis control. Dynamic time warping is used to classify two-dimensional gesture paths as circles, triangles and squares. In total, a classifier for 22 gestures is trained and a high recognition rate could be achieved.

3.4 Orientation Tracking

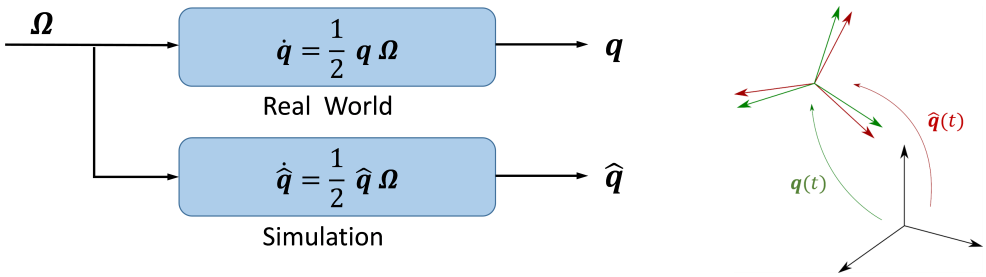

Figure 3.4: Orientation tracking using a simulator

Simulator. Orientation tracking is realized by integrating the kinematic equation (Fig. (3.4)). The error quaternion is defined as $\boldsymbol{e} = \hat{\boldsymbol{q}} * \boldsymbol{q}^{-1}$ and represents the rotation that brings the estimated body frame onto the true body frame. A simulator yields a stable but non-attractive solution (from the kinematic equation follows $\dot{\boldsymbol{e}} = 0$); i.e. a simulation error is conserved but is not growing inherently.

The most important error sources are the measurement noise and measurement bias. White noise leads to an angular random walk, whose standard deviation

$$\sigma_\theta = \sigma \cdot \sqrt{\delta t \cdot t} \tag{3.6}$$

grows with the square root of time [18]. Bias afflicted gyroscope measurement creates an angular error

$$\theta(t) = \epsilon \cdot t \tag{3.7}$$

which grows linearly over time. The constant bias term can be determined with little effort by measuring the sensor output under idle state. Temperature effects can be modeled but it takes a lot of calibration effort; in [31] a third order polynomial model is proposed.

In general the initial state $\boldsymbol{q}(0)$ is unknown, therefore additional sensor data is required in order to determine the orientation relative to an earth-fixed coordinate frame.

Vector Matching Approach. Sensor fusion algorithms are required to include the information obtained from an accelerometer and/or magnetometer. These algorithms are all based on the concept of vector matching and therefore require, in principle, the measurement of constant reference vectors (e.g. the Earth's magnetic and gravity field) [32, 33]. Including the measurement of the gravity field allows the determination of two degrees of freedom while the angle which represents a rotation around an axis parallel to the direction of the gravity field remains unobservable. When the gravity and the Earth's magnetic field are measured the orientation becomes fully observable [34].

In general, the constant reference assumption causes systematic errors when the component due to the gravity field (vertical reference) coexists with the component related to the body motion [35, 33] or when sources of magnetic fields as electrical devices nearby the IMU interfere with the Earth's magnetic field (horizontal reference) [36, 33].

In [33] an extended Kalman filter is developed defining the angular velocity measurement as external input; the measurement equation contains the accelerometer and magnetometer readings. In [37] Gauss-Newton optimization is used to determine a unique orientation solution from the accelerometer and magnetometer data. The obtained solution is treated as measurement available for the Kalman filter. This results in linear output equations which reduces the computational requirements for real-time implementations.

Madgwick published a complementary filter by fusing the orientation obtained from vector matching and the orientation obtained from angular rate integration [34, 38]. The filter is simple to tune as it contains only one parameter which represents the gyroscope measurement errors.

EKF filters can be made adaptive by setting the covariance matrix - representing the measurement noise - to very high values when the magnitude of the measured gravity or magnetic field differs from the excepted value, thus giving less weight to the reference vector measurements [39, 40]; a similar approach is possible for Madgwick filters.

Bias estimation. In [33] the gyroscope bias is included in the state vector of the EKF framework in order to estimate the measurement bias online; observability is shown analytically. A complementary filter can be augmented by an integral feedback of the error in the rate of change of orientation in order to account for gyroscope bias drift leading to an Lyapunov stable observer [41].

Angular Rate Integration

In order to update the attitude quaternion using a digital gyroscope the kinematic equation has to be discretized. As discussed before, a closed form solution is unattainable.

Euler forward approximation with a time step T_S leads to

$$\boldsymbol{q}(t_0 + T) = \boldsymbol{q}(t_0) + \frac{1}{2}\boldsymbol{W}\boldsymbol{q}(t_0)T_S\,. \tag{3.8}$$

It should be kept in mind that the addition operator appearing in integrating the kinematic differential equation is physically meaningless [42] and that the geometric properties of rotation quaternions are not preserved (as the vector $d\boldsymbol{q}/dt$ is always orthogonal to $\boldsymbol{q}$, integrating with a finite sample time T results in a updated quaternion which can not be on the unit sphere anymore) [42].

Constant velocity assumption. Assuming a constant angular velocity $\boldsymbol{\omega}$ the closed form solution can be stated as

$$\boldsymbol{q}(t_0 + T_S) = e^{\boldsymbol{W}T_S}\boldsymbol{q}(t_0)\,. \tag{3.9}$$

The exponential series $e^{\boldsymbol{W}T_S}$ of the skew-symmetric matrix $\boldsymbol{W}T_S$ may be computed by the Rodrigues formula [9]

$$e^{\boldsymbol{W}T_S} = \boldsymbol{I}\cos\frac{||\boldsymbol{\omega}||\cdot T_S}{2} + \frac{\boldsymbol{W}}{||\boldsymbol{\omega}||}\sin\frac{||\boldsymbol{\omega}||\cdot T_S}{2} \tag{3.10}$$

where $\boldsymbol{I}$ denotes the identity matrix. This can be expressed using quaternions as

$$\boldsymbol{q}(t_0 + T_S) = \tilde{\boldsymbol{q}}_n\boldsymbol{q}_n \tag{3.11}$$

with

$$\tilde{\boldsymbol{q}}_n = \begin{bmatrix} \cos\frac{||\boldsymbol{\omega}||\cdot T_S}{2} \\ \frac{\boldsymbol{\omega}}{||\boldsymbol{\omega}||}\sin\frac{||\boldsymbol{\omega}||\cdot T_S}{2} \end{bmatrix}. \tag{3.12}$$

Assuming a high sampling rate relative to the occurring angular velocities the constant velocity assumption is often reasonable.

3.5 Position Tracking and Error Propagation

Position tracking can be accomplished by double-integrating accelerations. As the accelerometer readings are sensed in the body frame, it is necessary to transform the measurements into a local-tangent-plane frame L. After removing the acceleration component related to gravity, the velocity ${}_L\boldsymbol{v}$ is tracked by integrating the acceleration ${}_L\boldsymbol{a}$ and the displacement ${}_L\boldsymbol{s}$ is obtained by integrating the estimated velocity:

$$ {}_L\boldsymbol{v}(t) =_L \boldsymbol{v}(t_0) + \int_{t_0}^{t} {}_L\boldsymbol{a}(\tau)\mathrm{d}\tau \tag{3.13} $$

$$ {}_L\boldsymbol{s}(t) =_L \boldsymbol{s}(t_0) + \int_{t_0}^{t} {}_L\boldsymbol{v}(\tau)\mathrm{d}\tau \tag{3.14} $$

The absence of any aiding sensor information to correct for velocity and position estimation errors leads to serious problems. In contrast to orientation tracking by integrating the angular rates, double-integration of the accelerometer readings leads to an unstable error dynamic, as an uncorrected error in the velocity estimation creates a steadily growing position error and thus a diverging solution. In generally, unstable systems are not suitable for technical purposes and it is well-excepted that the results obtained from double-integration of accelerometer readings are useless for long-term tracking. However, in the literature several examples of successfully used inertial position tracking systems without aiding sensors for short time spans can be found [43, 44, 45, 46].

This makes it all the more essential to be aware of the essential error sources and how they propagate through the integration scheme. This paragraph summarizes the main error sources.

Accelerometer Errors. White noise creates a random walk in velocity and a second-order random walk in position:

$$ \sigma_v(t) = \sigma \cdot \sqrt{T_s \cdot t} \tag{3.15} $$

$$ \sigma_s(t) = \sigma \cdot t^{3/2} \cdot \sqrt{\frac{T_S}{3}} \tag{3.16} $$

An accelerometer bias will lead to a quadratically growing position error.

Gyroscope Errors. When the orientation solution does not match the true body orientation, the accelerometer readings will not be correctly projected on the local-navigation frame and therefore are integrated in the wrong direction. Furthermore, an error of the estimated vertical causes that the Earth gravity can not be correctly removed anymore

which creates large errors in the horizontal plane. More precisely, a tilt error ϵ of the estimated vertical will cause that the Earth's gravity vector is projected onto the horizontal plane with the magnitude $g \cdot \sin\epsilon \approx g \cdot \epsilon$ (for small angles); the resultant error along the vertical axis becomes $g \cdot (1 - \cos\epsilon) \approx 0$. In a scenario in which the acceleration related to motion is much smaller than the gravity magnitude, that projection on the horizontal plane can be identified as the most critical error source related to the position tracking solution [18]. In detail, an angular error modeled as random walk creates a second-order random walk in velocity (grows proportionally to $t^{3/2}$) and a third-order random walk in position (grows proportionally to $t^{5/2}$) [47].

In order to correct for velocity errors, detection of inactivity periods can be used as pseudo measurements; when detected (e.g. based on the magnitude of accelerometer and gyroscope data) the velocity is zeroed [48]. In [49] the displacement during a hand movement is estimated by fitting a curve on the logged accelerations based on a hand movement model.

3.6 Allan Variance

The previous section describes how white noise and bias errors propagate through orientation and position tracking systems. The Allan technique is one of the most popular methods for identifying the random process in inertial sensor data.

Calculation

To estimate the Allan variance (AVAR), sensor readings have to be captured for a long time period in static state, typically throughout 12 hours. To calculate the AVAR, the sensor readings $(\omega_1, \omega_2, \dots)$ are divided into a series of successive clusters of length τ as shown in Fig. (3.5).

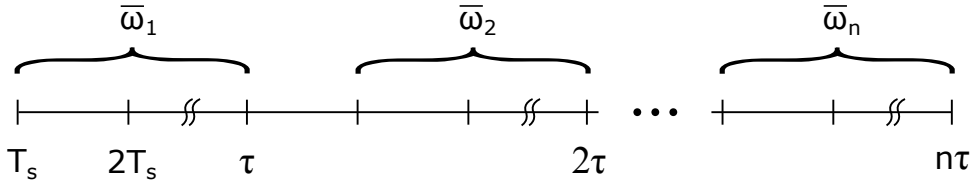

Figure 3.5: Non-overlapping Allan variance method

The AVAR is a function of the cluster length τ and is defined as

$$\sigma^2(\tau) = \frac{1}{2}\langle(\bar{\omega}_{k+1} - \bar{\omega}_k)^2\rangle \tag{3.17}$$

where $\bar{\omega}_k$ denotes the average value of the kth cluster ω_k and the angular brackets denote the expectation operator; the finite-sample variance is calculated as

$$\sigma^2(\tau) = \frac{1}{2 \cdot (n-1)} \sum_{k=1}^{n} (\bar{\omega}_{k+1}(\tau) - \bar{\omega}_k(\tau))^2 \tag{3.18}$$

with the number of clusters n. The reliability of the AVAR estimation increases with the number of clusters which are available for calculation (determined by the total length of the data stream and the averaging time τ). The resultant percentage error I of the AVAR estimation is given as [50]:

$$I = \frac{1}{\sqrt{2(n-1)}} \tag{3.19}$$

From Eq. (3.19) it follows that the number of clusters has to be not less than nine in order to ensure a percentage error less than 25%.

In order to increase the reliability of the AVAR estimation, overlapping clusters can be used. A good overview of the Allan variance technique can be found in [50]. The article also describes the different cluster sampling methods and the stochastic process identification.

Noise Identification

Different types of random processes cause different slopes in the double-logarithmic plot of the Allan Deviation (ADEV), which is defined as the square root of the AVAR. Typically, they also appear in different regions of the averaging time τ which allows to read out the different random processes directly from the graph [51]. Fig. (3.6) shows a typical ADEV plot and the appearance of different processes.

To identify the occurring stochastic processes, the ADEV graph is approximated by straight lines. The angular or velocity random walk is read out as the value of the line with a slope of -1/2 at averaging time $\tau = 1$.

The numeric value of the bias instability is the minimum value of the ADEV graph [50].

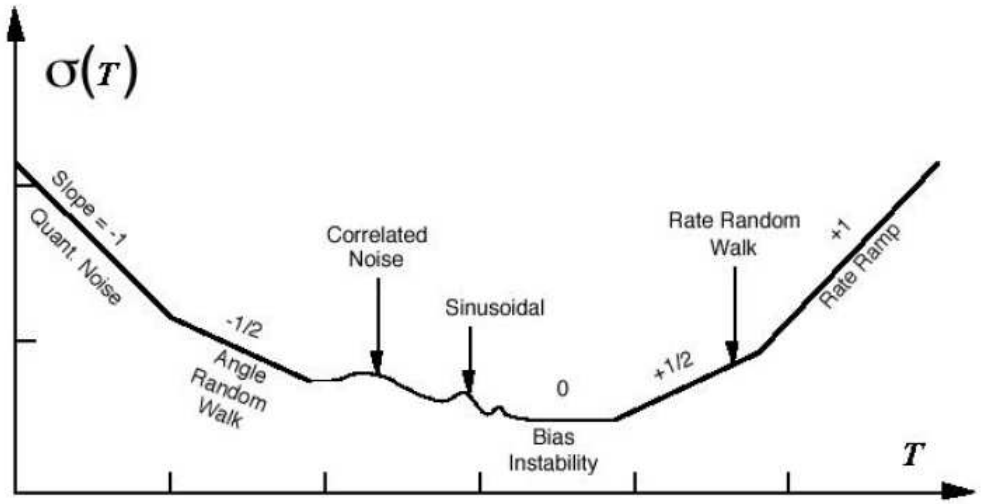

Figure 3.6: Sample plot of an Allan variance measurement and how different noise terms appear in the log-log plot (after IEEE 952 1997).

3.7 Evaluation of Prosthesis Control Schemes

Simon et al. [3] proposed the Target Achievement Control test (TAC test) for real-time evaluation of pattern recognition based control schemes. In this frequently used testing strategy, the control scheme is tested in a virtual environment as illustrated in Fig. (3.7). Starting from the initial state shown in Fig. (3.7)(a), the participant moves the virtual prosthesis into a requested posture, illustrated by the semi-transparent hand. When the target posture is reached within a predefined tolerance the hand turns green (Fig. (3.7)(b)). To successfully complete a trial the posture has to be maintained for a specific time span, the dwell time. A trial is considered as failed after reaching a maximum time without completing the task. The performance is assessed by several performance metrics:

- Completion Time: time from trial start to reaching the required posture
- Path Efficiency: quotient of the shortest possible path length to the actual traveled path length
- Overshoot Rate: rate of movements where the participant successfully reaches the target but does not maintain it for the required dwell time
- Completion Rate: percentage of the successfully completed trials of the test set

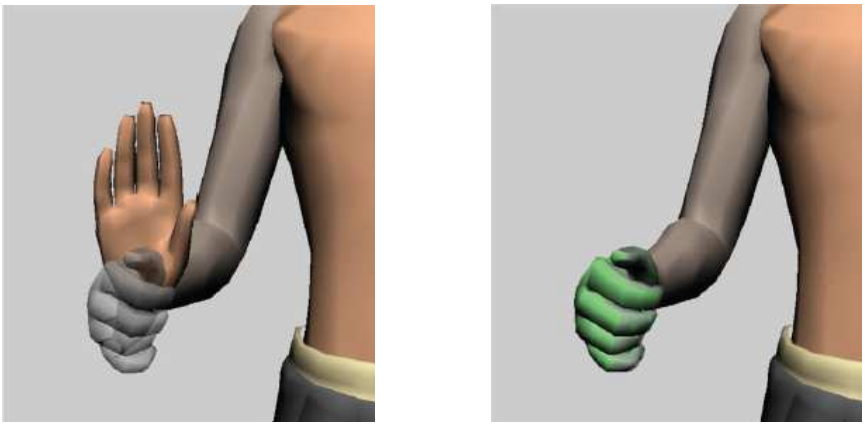

(a) initial state

(b) final state after correct execution

Figure 3.7: Target Achievement Control Test by Simon et al. [3]. The participant is intended to steer the virtual prosthesis from the initial state (a) into its neutral configuration (b), Source [3]

4 Existing Setup and Previous Work

Previous work. This work is based on a previous master thesis [2], in which a position estimation algorithm was developed in order to track arm displacements. For this purpose, the sensor casing – shown in Fig. (4.1) - was developed. It allows to mount the Bosch Application Board on the forearm using hook-and-loop tape. Sensor data is logged using the firmware provided by Bosch. The pre-gathered data is subsequently processed offline.

The gyroscope bias is determined by averaging the sensor's output in static state. The accelerometer is calibrated using a sensor model consisting of nine parameters. These parameters are determined using measurements of the sensor output in nine arbitrary orientations in static state (and utilizing the constant gravity magnitude condition). For this purpose, a simple apparatus was developed.

The developed position tracking algorithm determines the orientation using a Madgwick filter. Subsequently, the accelerometer readings are transformed into a local-navigation frame and the relative position is obtained by double-integrating. The Madgwick filter requires, in principle, the measurement of the constant gravity vector and therefore systematic errors occur during acceleration periods. These systematic errors are discussed in detail within the previous master thesis.

The present thesis re-uses the already developed sensor casing. Further, a similar method for accelerometer calibration is implemented but with the possibility to use an arbitrary number of measurements instead of an exact number of nine measurements. For this purpose, the existing apparatus was adopted and slightly extended.

This present thesis also investigates how the uprising stochastic errors limit the achievable accuracy of position tracking algorithms. This complements the examination of the systematic errors of the previous work.

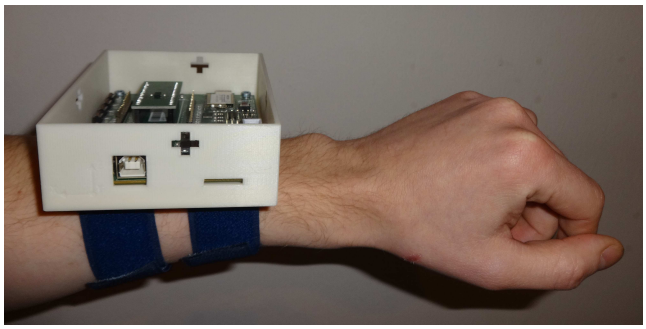

Figure 4.1: Sensor casing

5 Methods

5.1 Sensor Calibration

The predefined sensor is delivered uncalibrated, thus calibration should be conducted to increase the sensor output quality. The gyroscope bias can be directly measured in static state. To attain bias-free accelerometer measurements a more elaborate calibration procedure is required.

The accelerometer calibration is based on the sensor model described in Section 3.3.4. To identify the model parameters a series of measurements is recorded during which the sensor is aligned in different directions against the Earth's gravity vector in static state. For that purpose the existing mechanical equipment was adopted and slightly extended (by the plastic wedge pictured in Fig. (5.1)), making it possible to gather many independent measurements (Fig. (5.2)). Subsequently the model parameters are determined by minimizing the measurement error. The objective function defined in [20] exploits the magnitude of the measured reference equaling 1g. Explicitly, the objective function is defined to be

$$J = \frac{1}{N} \sum_i e_i^2 \tag{5.1}$$

where the error e_i is associated with the i-th measurement and represents the deviation from the expected magnitude

$$e_i = \boldsymbol{a}_{i,0}^T \boldsymbol{a}_{i,0} - g^2 \tag{5.2}$$

with the error compensated accelerometer measurement

$$\boldsymbol{a}_0 = \begin{bmatrix} 1 & -\alpha_{yz} & \alpha_{zy} \\ 0 & 1 & -\alpha_{zx} \\ 0 & 0 & 1 \end{bmatrix} \cdot \begin{bmatrix} k_x & 0 & 0 \\ 0 & k_y & 0 \\ 0 & 0 & k_z \end{bmatrix} \cdot (\boldsymbol{a}_m - \begin{bmatrix} b_x \\ b_y \\ b_z \end{bmatrix}) . \tag{5.3}$$

In this study the L-BFGS algorithm (a quasi-Newton method)[1] is used to solve the optimization problem. The initial parameter values are set to the parameters of an ideal sensor ($\alpha_i = 0$, $k_i = 1$, $b_i = 0$) and the gradient $\partial J / \partial \boldsymbol{p}$ is calculated analytically.

[1] an implementation under BDS-Licence is used, Copyright (c) 2009, Dirk-Jan Kroon

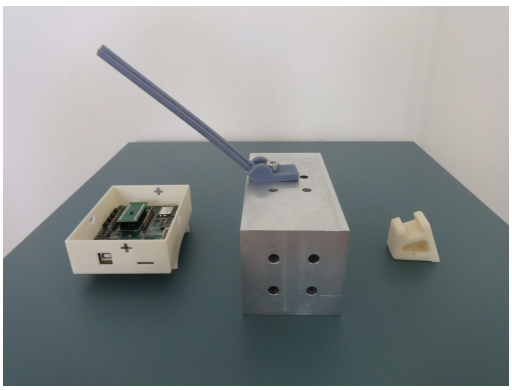

Figure 5.1: Calibration equipment consisting of the sensor casing, the calibration rig and the plastic wedge.

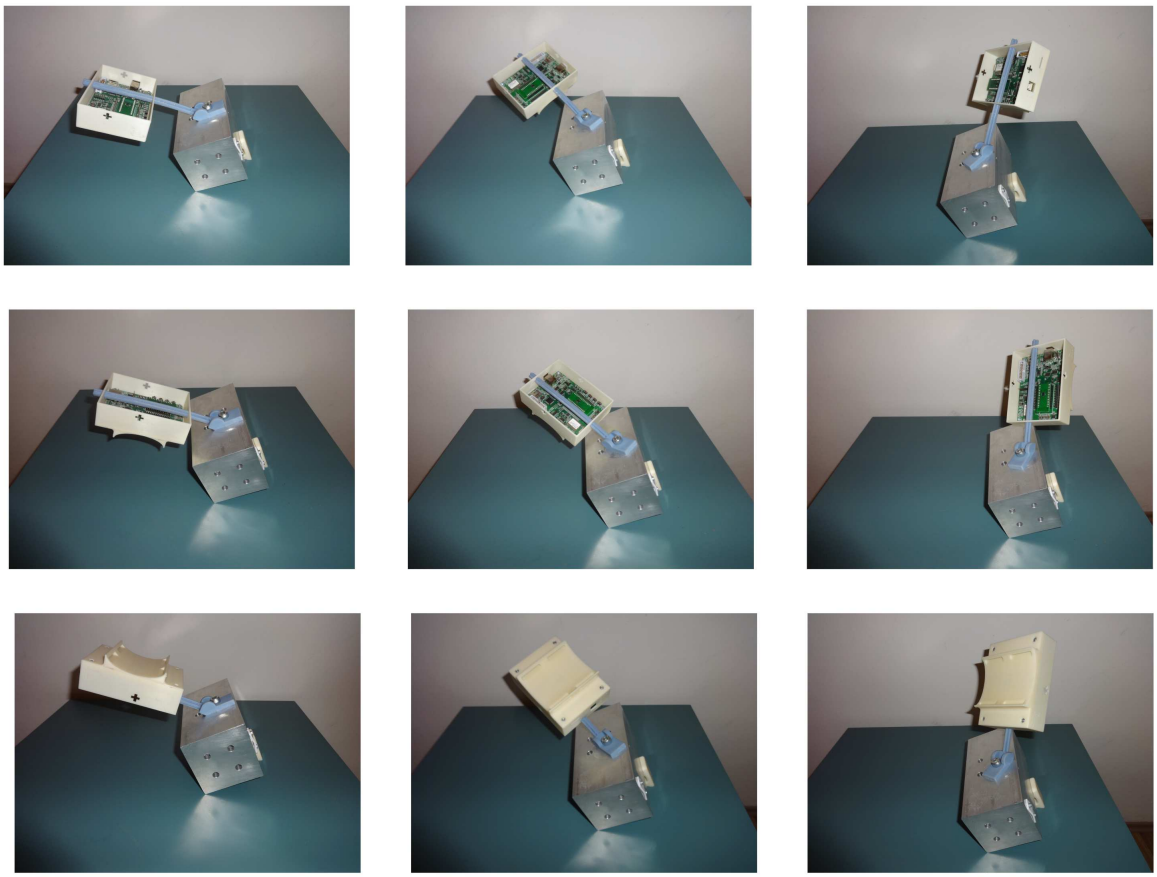

Figure 5.2: Example measurements of the gravity reference vector in different orientations in static state using the calibration equipment.

5.2 Error Determination

The underlying noise process of the accelerometer and gyroscope is identified via an AVAR analysis. Further the orientation and position tracking algorithms are applied to real data to verify if the identified noise processes allow a reasonable estimation of the uprising drifts.

The tracking solution is applied to 500 data streams obtained in static state. As the sensor readings are obtained in static state, the estimated velocities and positions equal the estimation errors (as the true values are zero).

The angular random walk (ARW) and velocity random walk (VRW) measurements represent the drift caused by white sensor noise. The standard deviations σ of the corresponding stochastic processes of the angle θ and the velocity v are given as

$$\sigma_\Theta(t) = \mathrm{ARW} \cdot \sqrt{t}\,, \qquad \sigma_v(t) = \mathrm{VRW} \cdot \sqrt{t}\,. \tag{5.4}$$

Further, double-integrating white accelerometer noise results in a second-order random walk in position s

$$\sigma_s(t) = \mathrm{VRW} \cdot \frac{1}{\sqrt{3}} \cdot t^{3/2}\,. \tag{5.5}$$

In the following, the implementations of the applied tracking algorithms are described.

Orientation Tracking. To update the orientation, the solution of the kinematic equation is approximated using the forward Euler method. After each integration step, the obtained quaternion is re-normalized. Thus, the update equations are given as:

$$\hat{\boldsymbol{q}}_{k+1} = \hat{\boldsymbol{q}}_k + \frac{1}{2}\boldsymbol{W}_k\hat{\boldsymbol{q}}_k T_S \tag{5.6}$$

$$\hat{\boldsymbol{q}}_{k+1} \leftarrow \hat{\boldsymbol{q}}_{k+1}\frac{1}{\left\|\hat{\boldsymbol{q}}_{k+1}\right\|} \tag{5.7}$$

Position Tracking. As discussed before, the orientation quaternion $\boldsymbol{q}$ obtained from integrating of the gyroscope readings represents the coordinate transformation from the sensor frame to the local navigation frame L. Thus, the g-corrected accelerations with respect to L are given as

$${}_L\boldsymbol{a} = \boldsymbol{q} \cdot \boldsymbol{a}_m \cdot \boldsymbol{q}^* - \begin{pmatrix} 0 \\ 0 \\ g \end{pmatrix} \tag{5.8}$$

where $\boldsymbol{a}_m$ denotes the accelerometer readings. Using forward Euler method to integrate the accelerations, the update equations for the velocity and position are given as

$$\boldsymbol{a}_k = \boldsymbol{q}_k \cdot \boldsymbol{a}_{m,k} \cdot \boldsymbol{q}_k^* - \begin{pmatrix} 0 & 0 & g \end{pmatrix}^T \tag{5.9}$$

$$\boldsymbol{v}_{k+1} = \boldsymbol{v}_k + \boldsymbol{a}_k \cdot T_s \tag{5.10}$$

$$\boldsymbol{s}_{k+1} = \boldsymbol{s}_k + \boldsymbol{v}_k \cdot T_s \,. \tag{5.11}$$

5.3 Orientation-Based two-DoF Control

5.3.1 Concept

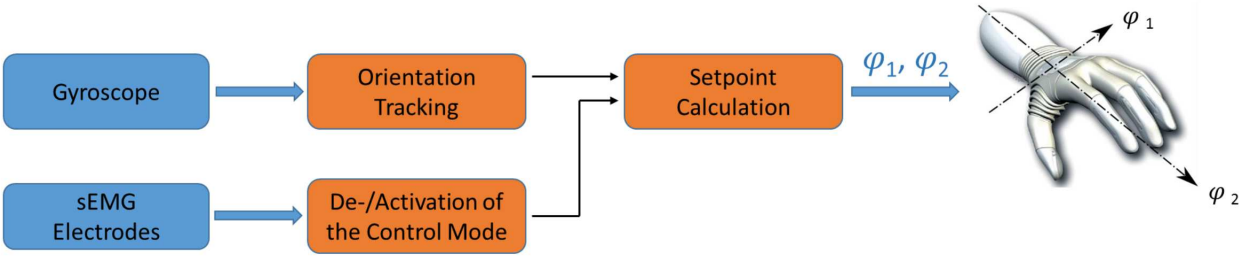

Figure 5.3: Orientation-based control concept

The user enables and disables the control mode via sEMG signals (e.g. by co-contraction of the muscles related to both sEMG sensors). When enabled, a relative change of the orientation of the forearm shifts the set-points for wrist flexion/extension φ_1 and supination/pronation φ_2. The orientation of the forearm is tracked by integrating the angular velocities measured by the gyroscope which is mounted on the forearm (see Fig. (5.3)).

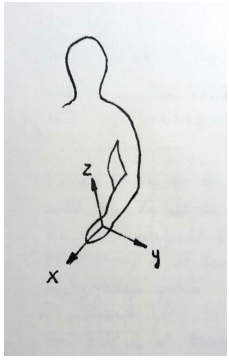

Figure 5.4: Arm-fixed frame

To define a mapping from the forearm orientation to wrist joint angles an auxiliary coordinate system fixed in the forearm as illustrated in Fig. (5.4) is used. The x-axis coincides with the forearm axis; the y-axis corresponds with the rotation axis during a elbow flexion/extension movement; the z-axis is defined as the rotation axis of a shoulder internal/external rotation when the elbow and the upper arm axes are perpendicular to each other.

The forearm orientation maps to prosthesis joint angles as follows:

- A rotation about the y-axis maps to wrist flexion/extension (Rotation about the y-axis corresponds to an elbow flexion/extension).
- A rotation about the z-axis maps to wrist rotation (corresponds to an internal/external shoulder rotation when the forearm is perpendicular to the upper arm and corresponds to a shoulder abduction/adduction when the arm is stretched).

The defined mapping used in two different arm positions is illustrated in Fig. (5.5).

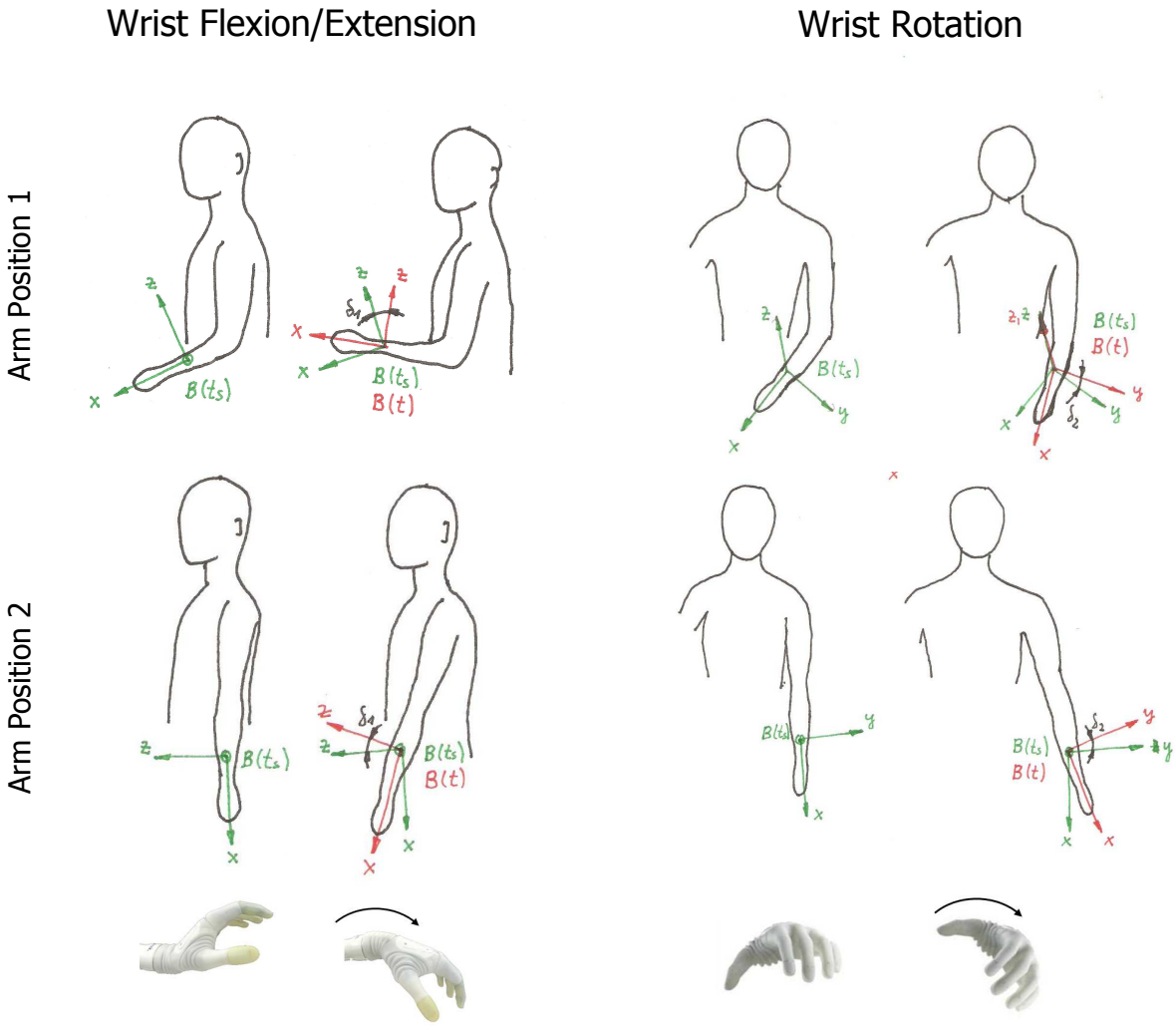

Figure 5.5: Orientation-based control scheme used in two different arm positions

5.3.2 Implementation

This subsection describes the implementation of the concept presented above. For clarity purposes, at first two points of time which are used in the implementation are defined. The time when the system is turned on (e.g. when the prosthesis is powered on) is denoted as t_0. At that time orientation tracking is initialized and started and no further reset of the estimated orientation occurs anymore. When the system is turned on, the orientation-based control mode can be enabled and disable by the user. The point of time when the user enables the orientation-based control is denoted as t_a (activation time).

Orientation Tracking

In order to track the orientation of the sensor frame using a gyroscope with a digital output the kinematic equation

$$\dot{\boldsymbol{q}} = \frac{1}{2}\boldsymbol{W}\boldsymbol{q} \tag{5.12}$$

from Chapter 2 has to be discretized. As highlighted before, an exact solution for Eq. (5.12) is unattainable and therefore a numerical integrating scheme has to be applied. Due to a high sample rate and low occurring angular velocities, it is reasonable to use a first-order integration scheme. Euler method leads to

$$\hat{\boldsymbol{q}}_{k+1} = \hat{\boldsymbol{q}}_k + \frac{1}{2}\boldsymbol{W}_k\hat{\boldsymbol{q}}_k T_S \tag{5.13}$$

where $\hat{\boldsymbol{q}}_k$ represents the current estimated orientation, $\boldsymbol{W}_k$ is the measured angular velocity tensor and T_S denotes the sample time. Since this kind of numerical integration cannot preserve the geometric property of rotation quaternions[2] renormalization is done after each integration step

$$\hat{\boldsymbol{q}}_k \frac{1}{\|\hat{\boldsymbol{q}}_k\|} \rightarrow \hat{\boldsymbol{q}}_k \,. \tag{5.14}$$

For the further implemented control scheme it is necessary to track the orientation of the forearm relative to the orientation at the time t_a when the orientation-based control mode was activated. However, the initial orientation when orientation tracking is started is irrelevant and therefore the initial value can be chosen arbitrarily and is set to $\boldsymbol{q}_0 = \begin{bmatrix} 1 & 0 & 0 & 0 \end{bmatrix}^T$.

[2]The set of rotation quaternions is given by the unit sphere $\mathcal{S}^3$ in $\mathbb{R}^4$. Since the vector $\mathrm{d}\boldsymbol{q}/\mathrm{dt}$ is always orthogonal to $\boldsymbol{q}$ a given $\boldsymbol{q}_k \in \mathcal{S}^3$ produces an approximation $\boldsymbol{q}_{k+1}$ which does not belong to $\mathcal{S}^3$.

Sensor Position Estimation

In order to realize the proposed control scheme the orientation of the sensor frame relative to the forearm has to be known. Measuring the the gravity vector while the user holds the forearm in different positions allows to determine the relative orientation of the accelerometer frame. These results are taken over for the gyroscope frame assuming that the sensor axes of the accelerometer and the gyroscope coincide.

The two conducted measurements are illustrated in Fig. (5.6). The user is instructed to hold the forearm parallel and subsequently normal to the floor for a specified time span. The time-averaged accelerometer data defines the x-axis ${}_S\boldsymbol{e}_x$ and z-axis ${}_S\boldsymbol{e}_z$ of the body-fixed forearm frame B resolved in the sensor frame S. The y-axis is calculated as the cross product of this two axes. The result is renormalized as the measured x- and z-axis cannot be assumed to be perfectly orthogonal

$$ {}_S\boldsymbol{e}_y = \frac{{}_S\boldsymbol{e}_z \times {}_S\boldsymbol{e}_x}{\|{}_S\boldsymbol{e}_z \times {}_S\boldsymbol{e}_x\|} \,. \tag{5.15} $$

The basis transformation matrix is then given as

$$ \boldsymbol{A}_{SB} = ({}_S\boldsymbol{e}_x, {}_S\boldsymbol{e}_y, {}_S\boldsymbol{e}_z) \,. \tag{5.16} $$

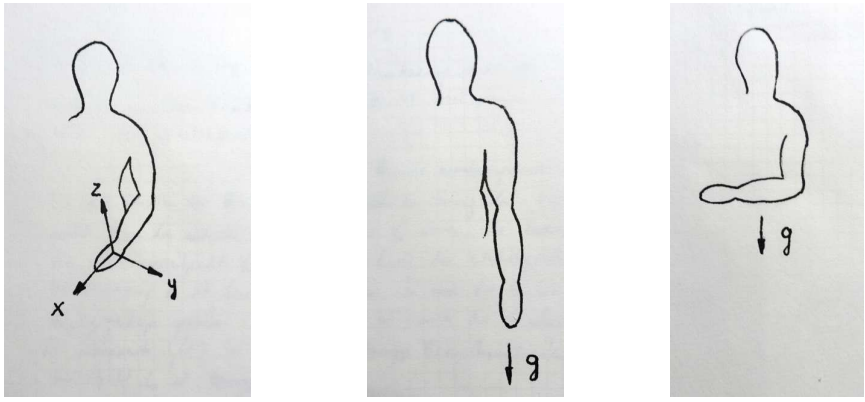

(a) (b) (c)

Figure 5.6: Image (a) shows the defined body-fixed forearm frame. Sensor position estimation relative to the forearm is conducted by two accelerometer measurements. Image (b) and (c) illustrate the measurement of the x- and z-axis of the forearm frame with respect to the sensor frame.

Set-point Calculation

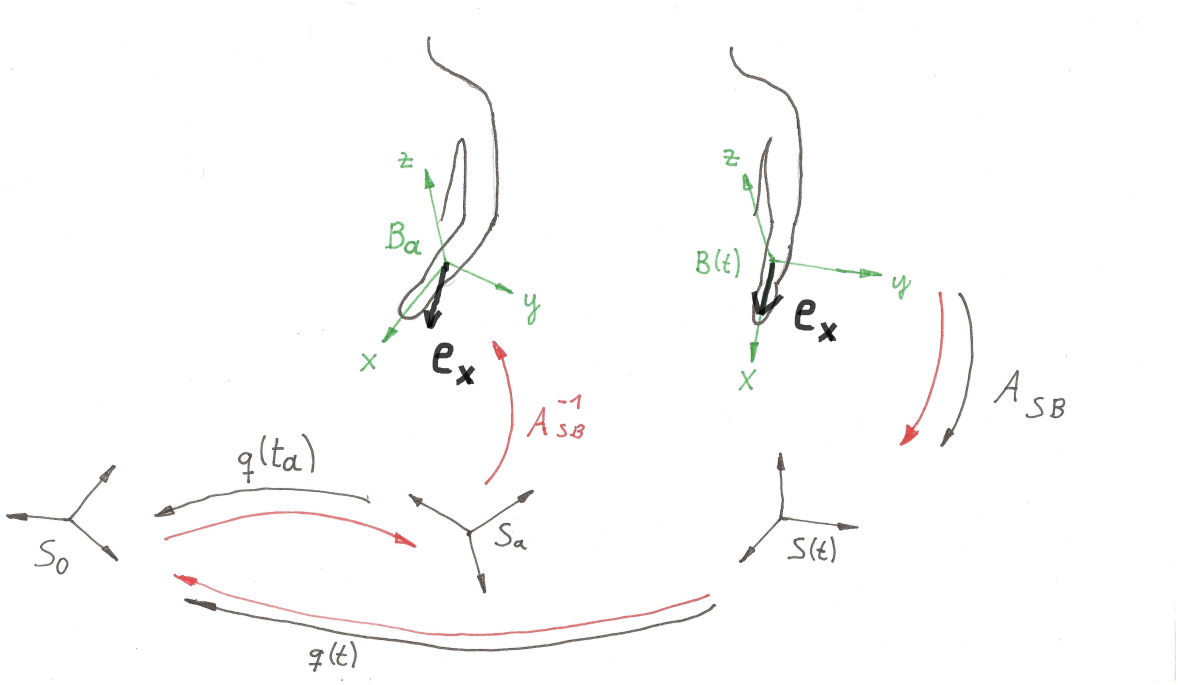

Figure 5.7: The red line indicates how the representation of the current forearm axis $\boldsymbol{e}_x$ with respect to the forearm frame B_a is calculated.

Based on the coordinate systems illustrated in Fig. (5.7) the mapping from the current orientation of the forearm to the set-points for wrist flexion/extension φ_1 and supination/pronation φ_2 is implemented as follows:

1. The representation of the current x-axis of the forearm frame $\boldsymbol{e}_x$ relative to the forearm frame B_a (represents the forearm orientation at activation time t_a) is calculated.

2. The y- and z-components of the current x-axis ${}_{Ba}\boldsymbol{e}_x$ with respect to B_a multiplied by a constant gain define the set-points for the wrist joints. For small angles the y- and z-components represent an approximation of the angles around the z- and y-axis respectively and therefore this corresponds to the concept as described before.

Since the initialization of the orientation tracking solution takes place when the system is powered on at the time t_0, the current estimated orientation $\hat{\boldsymbol{q}}(t)$ represents the current orientation of the sensor frame relative to t_0. When the user activates the orientation based control mode the current orientation of the sensor frame $\hat{\boldsymbol{q}}(t_a)$ is saved. The current

orientation of the sensor frame relative to the orientation at activation time is then given as the composition of these two relations:

$$\hat{\boldsymbol{q}}_{SaS(t)} = \hat{\boldsymbol{q}}(t_a)^{-1} \cdot \hat{\boldsymbol{q}}(t) \tag{5.17}$$

Due to the occurring drift, the estimation $\hat{\boldsymbol{q}}(t)$ becomes physically meaningless over long integration times. However the drift in $\hat{\boldsymbol{q}}_{SaS(t)}$ is proportional to the square root of the time span $t - t_a$. Since this time span represents the time which is needed to position the wrist joints, it will be rather short (most likely only a few seconds) and therefore the drift will remain within reasonable boarders.

Calculation of the representation of the current forearm axis with respect to the sensor frame at activation time S_a is performed as indicated by the red line in Fig. (5.7). First the forearm axis ${}_{B(t)}\boldsymbol{e}_x = \begin{pmatrix} 1 & 0 & 0 \end{pmatrix}^T$ is transformed into the current sensor frame

$${}_{S(t)}\boldsymbol{e}_x = \boldsymbol{A}_{SB} \begin{pmatrix} 1 \\ 0 \\ 0 \end{pmatrix} . \tag{5.18}$$

Subsequently its representation with respect to S_a is calculated

$$\begin{pmatrix} 0 \\ {}_{Sa}\boldsymbol{e}_x \end{pmatrix} = \hat{\boldsymbol{q}}_{SaS(t)} \cdot \begin{pmatrix} 0 \\ {}_{S(t)}\boldsymbol{e}_x \end{pmatrix} \cdot \left(\hat{\boldsymbol{q}}_{SaS(t)}\right)^{(*)} . \tag{5.19}$$

Back-transformation to the forearm frame finally results in the desired representation

$${}_{Ba}\boldsymbol{e}_x = (\boldsymbol{A}_{SB})^{-1}{}_{Sa}\boldsymbol{e}_x . \tag{5.20}$$

The y and z components of ${}_{Ba}\boldsymbol{e}_x$ define the angular set-points of pronation/supination φ_1 and flexion/extension φ_2 of the prosthesis. The mapping is realized by a gain k:

$$\begin{pmatrix} \varphi_1 \\ \varphi_2 \end{pmatrix} = k \cdot \begin{pmatrix} 0 & 1 & 0 \\ 0 & 0 & 1 \end{pmatrix} {}_{Ba}\boldsymbol{e}_x + \begin{pmatrix} \varphi_{1,0} \\ \varphi_{2,0} \end{pmatrix} \tag{5.21}$$

The term $\begin{pmatrix} \varphi_{1,0} & \varphi_{2,0} \end{pmatrix}^T$ represents the initial state of the wrist when the control mode was activated at t_a.

The gain k was set to five for all further investigations; this means that a rotation of one wrist joint by 90 degrees requires a forearm rotation by 18.3 degrees. At 90 degrees, the sensitivity of the proposed implementation decreases from 5 to 4.75. In Fig. (5.8) the resulting mapping as well as the sensitivity are shown.

To evaluate the proposed control concept, during this work user tests with a virtual prosthesis were conducted. For that purpose, the activation and deactivation of the orientation based control mode was enabled using a computer mouse. This allows to test the system without donning and adjusting sEMG electrodes.

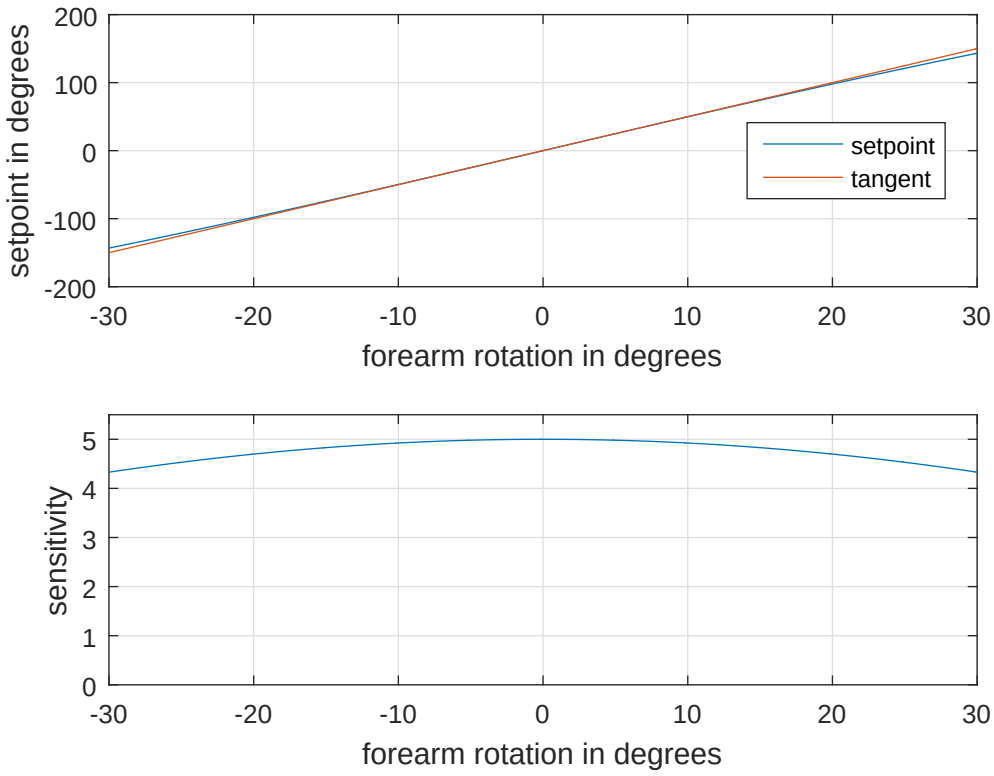

Figure 5.8: Sensitivity of the implemented control scheme.

5.4 Implementation of the Test Framework

The developed orientation-based control concept should be tested in order to establish a decision base regarding further investigations. For that purpose, the IMU control concept should be compared to the commercially available four-channel control (Chap. 3.2). Further the test framework should allow the participant to get an idea of how the control scheme could be used in everyday life. This is important to gain feedback from prosthetic users in order to estimate if the users can imagine to incorporate the control scheme into daily life and what individual advantages and disadvantages they see in the proposed control scheme.

A test framework was implemented which adopts the test procedure proposed by Simon et al. [3] (Chap. 3.7). On one hand, this allows to compare control schemes by performance metrics and on the other hand it gives the participant a first impression of the IMU control concept as it allows an interaction with a virtual prosthesis in real-time. The framework is implemented in Matlab/Simulink and requires three essential elements: the real-time connection of the sensor, implementation of the test logic and the visualization. The visualization was implemented in C# due to the better performance and bigger

possibilities compared to Matlab. Communication was realized via a TCP/IP network.

BMX055 Data Streaming

Bosch provides a generic API to interface with the Bosch Development Board. The API is hosted from Simulink via the provided .net DLL. The implemented Matlab System Block reads the sensor data through polling method. The block diagram in Fig. (5.9) illustrates the use of the generic API. The sample rate is set to 100 Hz as the embedded software of Ottobock also works at that frequency.

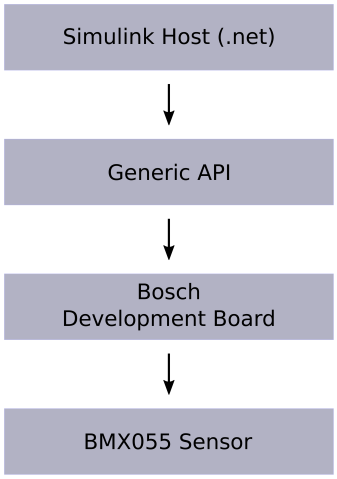

Figure 5.9: Real-time integration of the IMU in Matlab/Simulink

Test Implementation

To assess the proposed control scheme two tests were implemented. **The first test implementation** should serve to determine if the control scheme is applicable to position two joints in general. For that purpose, it is required to avoid the cognitive challenge which occurs if the configuration of a three-dimensional object has to be interpreted from a two-dimensional graphic. Also it should be as clear as possible which movement is necessary to fulfill the task. To achieve this, in this test the user is required to move a cursor into a target visualized as circle as shown in Fig. (5.10)(a). Fig (5.10)(b) illustrates how cursor movements correspond to prosthesis movements.

A feedback is provided by the color of the circle. Initially a red circle is shown; if the cursor is moved into the target the circle turns green. The targets are defined as part of the test preparation and are saved in a mat-file. Additionally, two parameters need to be set, namely, the time-span during which the cursor needs to dwell within the target to successfully end a trial (dwell time) and the maximum given time before an attempt is regarded as failure (timeout).

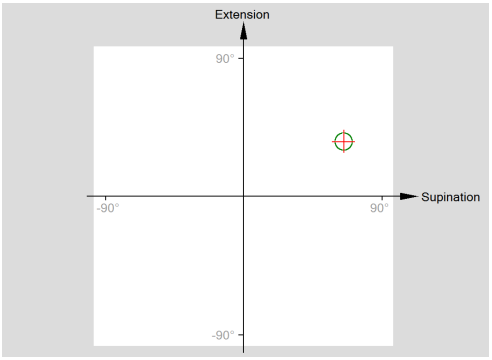

(a) Visualization of the first test implementation

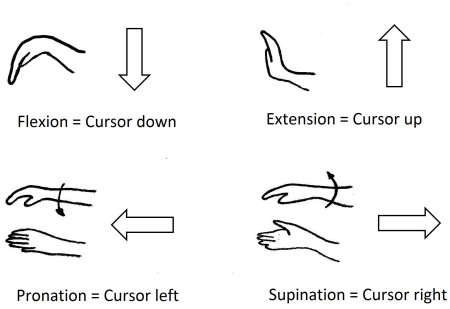

(b) Illustration of how cursor movements correspond with prosthesis joints

Figure 5.10: In the first test scenario the subject steers the cursor into the target represented by a circle. The right figure illustrates how cursor movements correspond with prosthesis movements.

The second test should explicitly allow to assess the applicability of the proposed control scheme for forearm prosthesis control. For this purpose, a test is implemented where a virtual prosthesis has to be controlled. As illustrated in Fig. (5.11) the participant has to move the virtual prosthesis from a given start-configuration into the neutral configuration indicated by the semi-transparent hand. The start-configurations are defined as part of the test preparation and are saved in a mat-file. As in the first test implementation, the dwell time and the timeout have to be set. Further the tolerance range of the neutral position needs to be defined. If the position of the virtual prosthesis is within the tolerance range the red square in the lower left turns green.

For the visualization of the second test concept, the implementation of a virtual hand prosthesis together with a TCP/IP interface was provided by Ottobock. This implementation was extended by the semi-transparent target gesture and by the colored square to provide a feedback if the virtual prosthesis is within the acceptable tolerance.

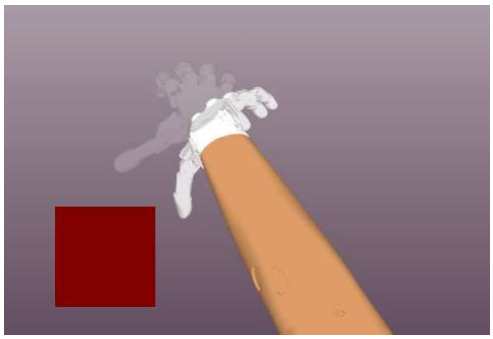

Figure 5.11: During this test, the virtual prosthesis has to be moved into the target configuration illustrated by the semi-transparent hand.

5.5 User Tests

User tests were conducted in order to first, evaluate the overall usability of the proposed control scheme (and possible upcoming problems regarding the implemented solution) and second. to assess pros and cons of the proposed control concept compared to a conventional two electrode sEMG control scheme. Additional tests were conducted focusing on the impact of their main differences. The proposed orientation based control scheme differs from conventional control with two sEMG electrodes in two essential points:

- proportional position control vs. proportional velocity control
- simultaneous vs. sequential control of wrist DoF (supination/pronation and flexion/extension)

To be able to compare the overall performance of wrist control of the novel control concept with the sEMG control concept, a test where two DoF had to be positioned was conducted. The users' feedback was captured via a questionnaire.

Subsequently, a test where one DoF had to be positioned was conducted in order to isolate the effect of proportional position mapping in comparison to proportional velocity mapping.

The final test investigated the learning effect. Therefore, participants were instructed to train with the virtual prosthesis once a day and to execute a test immediately afterwards. The development of the performance was measured. This third test's goal was to investigate if intuitive control of wrist joints using the proposed control scheme is possible after a certain time of use.

All in all, 17 people took part in the tests of which twelve subjects were able-bodied and five subjects were amputated. Except three externally recruited subjects with amputation, which were paid 10 Euro per hour, all of the participants were employees of Ottobock and took part in the test voluntarily.

General Test Conditions

All tests were conducted on a laptop with a 15″ screen. Participants sat about half a meter from the screen. In order to avoid any distractions during the test, only the test visualization was visible on the screen and was displayed in full screen mode. To avoid any interferences, only the test software was running and network access was disabled. All experiments took place in a quiet room with only the test conductor and the test participant in the room.

The IMU casing was always placed either on the users' prosthesis or on the dominant hand of the able-bodied subjects. The IMU unit was placed on the proximal third of

the forearm (respectively on the prosthesis). The IMU was placed at the upper side of the forearm to allow the participants to rest the arm on the desk or their thigh during breaks. The IMU casing was mounted carefully using hook-and-loop tape ensuring that the case was neither too lose nor caused any discomfort or pressure on the arm. During experiments with other input devices the IMU casing was removed so it would not bother during testing.

In order to complete a task successfully the cursor had to remain within the targets' borders a dwell time. Regarding the orientation-based control, the participants had to click on the left mouse button to enable the control mode; the mouse click also initiated an attempt. When once enabled it was not possible for the user to deactivate the control mode anymore. Regarding the four-channel control an attempt was initiated by the first myo-signal given by the participant. After a successful attempt or failure (maximum time was reached) the control mode was automatically disabled and a new target was shown on the screen. Experiments using the mouse were held under the same conditions.

Metrics

Completion time and path efficiency were measured. Path efficiency PE is defined as the coefficient of the shortest path from the start point to the target divided by the actual traveled path

$$PE = \frac{\text{shortest path}}{\text{actual path}}. \tag{5.22}$$

Completion time CT is defined as the elapsed time from first movement after showing a new target to its successful completion less dwell time

$$CT = t(s_0) - t(s_1), \tag{5.23}$$

i.e. the dwell time is not part of the measured completion time. The definition of these two performance metrics is illustrated in Fig. (5.12).

5.5.1 Two-DoF Tests

The main goals of this test are to assess if it's possible to use the proposed system to control two DoF in general and to evaluate the control quality regarding prosthesis control. In particular, following question should be answered:

- Is it possible to use the proposed system in a controlled way?
- How does the control performance compare to the conventional four-channel control?

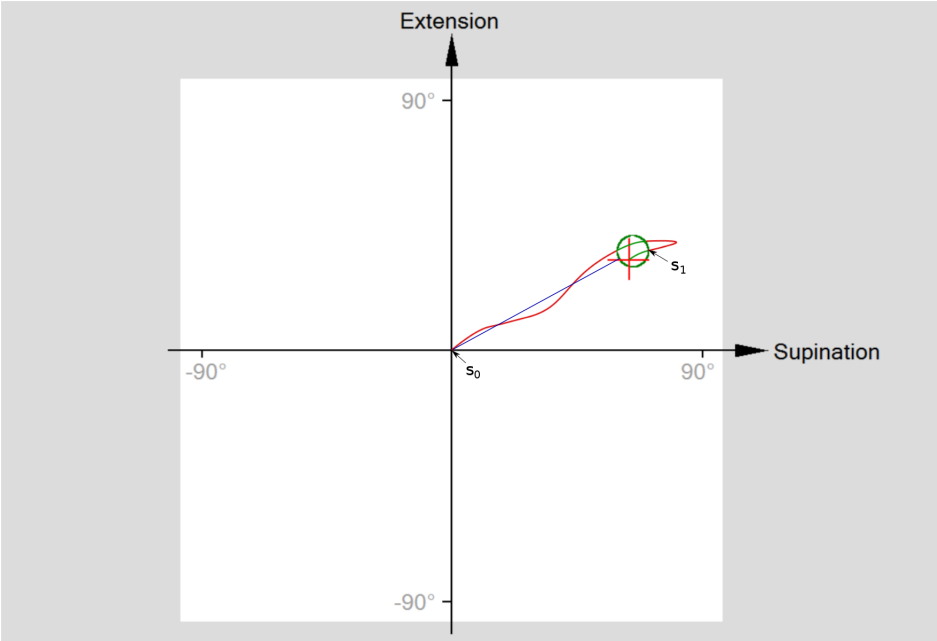

Figure 5.12: Measured metrics are completion time and path efficiency. Completion time CT is defined as the elapsed time from first movement at s_0 to final entering at s_1: $CT = t(s_1) - t(s_0)$. The length of the actual traveled path is defined as the length of the path from s_0 to s_1. Path efficiency means the coefficient of the actual path length divided by the shortest path (blue line).

- Is the mapping of orientation of the forearm to the prosthesis joint angles intuitively applicable?
- Could the users imagine to incorporate the control scheme in their daily life?

In order to answer the questions above two experiments were designed and conducted; in the first test targets had to be reached by moving a cursor horizontally and vertically, in the second test a virtual prosthesis had to be repositioned from a given start configuration. The participants' feedback was captured via a questionnaire. In order to gather expert-feedback also prosthesis users were recruited for this test.

The cursor test was primarily meant to answer (i) if it's possible to use the proposed system in a controlled way and (ii) how the control performance compares to the conventional four-channel control. To be able to answer the first question, additionally to the IMU and sEMG control scheme, the mouse was used as an input device. The mouse was chosen as a reference device to evaluate the overall performance as it is a highly accepted and sophisticated input device for cursor manipulations.

Subsequently, the repositioning task was conducted. The participants were instructed to reposition the virtual prosthesis from different given start-configurations back to its

neutral position. Goal of this test was to evaluate the applicability of the proportional map of forearm orientation to the prosthesis' joint angle. Interacting with the virtual prosthesis was also meant to give subjects the possibility to pre-estimate the proposed control schemes' advantages and disadvantages in everyday life and to assess its application in the participants daily life.

Participants

Twelve able-bodied (eleven males, one female) participants and five participants with amputation (all male) took part in the test. The able-bodied participants were aged between 21 to 51 (mean 27.9, std 9.1); eleven were right-handed, one was left-handed. The participants with amputation were aged between 28 to 35 (mean 30.2, std 2.9). From all participants with amputation the right hand was amputated.

All participants with amputation were fitted with a prosthesis by Ottobock and were wearing it for at least five hours a day. The first time that they were fitted with a prosthesis was between 1.5 to 9 years ago. Three participants used the four-channel control in daily life. Two participants did not use active wrist rotation at all. The quoted reason was a not reasonable reliability of the control scheme although both noted that an active control of wrist rotation would be useful in daily life.

Experimental Design

In order to make the test more reliable, same targets for every input device were used in experiments which were conducted using two or more input devices. In addition, all participants were confronted with the same targets which were saved beforehand and were randomly generated as part of the test preparation. The amount of targets is a compromise between mental exhaustion of the subject after a certain time of testing and the quantity of achieved data that is necessary for further analyses. To ensure an acceptable test duration for the participants the maximum length of the test session was set to one and a half hour.

The cursor test was conducted using IMU, sEMG and a mouse as input device. To provide some recover time the test was split into three runs per input device. One run consisted of 30 target. The targets were randomly generated with a continuous uniform distribution in size $U(1.8°, 9°)$, distance to the origin $U(22.5°, 72°)$ and angle to the horizontal $U(0, 2\pi)$. Every target was followed by a target located at the origin. This is done to ensure that (i) two immediately consecutive targets are separated in space by a minimum distance and (ii) to force the subject to keep the arm within a comfortable zone. An attempt was started with a mouse click by the subject. The dwell time was set to one second; timeout was set to 15 seconds.

The virtual prosthesis test was conducted using IMU and sEMG control. This test was also split into three runs per input device while one runs consisted of 20 start-configurations.

Experiment	Input Device	Targets per Run	Runs
Cursor Positioning Task	sEMG-based	30	3
	IMU-based	30	3
	Mouse	30	3
Repositioning Task	sEMG-based	20	3
	IMU-based	20	3

Table 5.1: Summary of the conducted experiments during the first user test with two-DoF control.

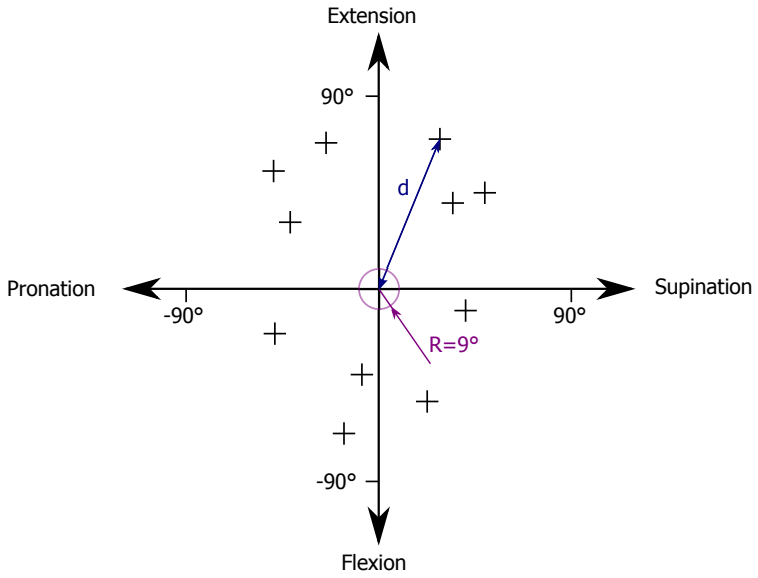

Figure 5.13: Example start configurations. Start configurations are randomly generated with an uniform distribution $U(22.5°, 72°)$ in the distance to the neutral position d and uniform distribution $U(0, 2\pi)$ in the angle φ. The virtual prosthesis has to be repositioned with a tolerance of $\pm 9°$ (indicated by the pink circle in the center).

The start-configurations were randomly generated with a continuous uniform distribution of the distance to the neutral configuration $U(22.5°, 72°)$ and of the angle $U(0, 2\pi)$. Fig. (5.13) illustrates a subsample of start configurations. Similar to the first experiment, an attempt was considered as successfully accomplished when the virtual prosthesis stayed in its neutral position within a tolerance of $\pm 9°$ for a defined dwell time of one second. The timeout was again set to fifteen seconds. Table 5.1 summarize the experimental design.

Questionnaire Design

In addition to the performance based test a questionnaire was used as a subjective measurement tool. Firstly, prosthesis users were asked about their previous experience with the control of prostheses. Furthermore, they were asked about their satisfaction with the

care, about occurring problems in daily life and any need for improvement. The other parts of the questionnaire - each related to a particular experiment - gave feedback regarding the control scheme and the test implementation (to identify possible software problems). In the last part the questions focused on a feedback on the difference and subjective comparison of the presented and established control systems. Here the prostheses users were additionally asked in how far this type of control would be of advantage or disadvantage for them and if they could imagine using it. The annex contains the full questionnaire: Here is a brief overview of the focus of the questions:

- Part 1: Demographics (sex, age, dominant hand), computer experience , time spent on the computer each day, experience with wearing prostheses, experience with the control of hand prostheses; disabled participants were additionally asked: date of the amputation, supplied with which prosthesis, how many hours is the prosthesis worn a day, which control scheme is used, satisfaction and need for improvement
- Part 2: After each experiment (except with the mouse), clarity of test procedure, sufficient time to familiarize yourself with the control scheme; precision, speed of the controller and if they were able to use the system in a controlled way
- Part 3: Comparison of control variants: comparison of speed, accuracy and comfort
- Part4: Personal estimation of the usability in everyday life; advantages and disadvantages of the presented control system; for which joints could an integration be imaginable; if a combination of sEMG and orientation-based control schemes could be useful

5.5.2 Single-DoF Test

As highlighted before - besides of the possibility of a simultaneous control of two DoF - the two considered control concepts inherently differ (i) by the physical quantity which is controlled (velocity or position) and (ii) by the way the user interacts with the control system (once by moving the forearm and once by contracting particular muscle groups).

The first user test assesses how the overall performance differs regarding the sEMG and IMU control schemes when two joints are positioned (wrist flexion and rotation). In order to assess the mentioned inherent major differences of the two control concepts a second user test was conducted. During this test the subjects had to fulfill tasks by manipulating one single DoF. This allows to assess the major inherent differences isolated from simultaneous control.

The results of this test are also of practical interest as a large number of users use a combination of an active control for wrist rotation and a passive joint for wrist flexion. This passive joint is typically built as flexible spring-loaded joint which can be fixed manually at a desired position. Therefore, it is also interesting to investigate how the

proposed control concept compares to a conventional four-channel control regarding a single-DoF control.

Participants

Four able-bodied participants (all male) took voluntarily part in the test. Their ages ranged from 21 to 26. Each subject was right-handed. All participants took part in the two-DoF test and therefore all of them were familiar with both control schemes.

Experimental Design

In order to assess the difference of a proportional velocity control versus a proportional position control (in combination with the way how the system is controlled by the user) all other impacts on the performance should be suppressed as much as possible. Therefore, this user test is only conducted using the cursor manipulation task. In order to obtain a single-DoF test all target were centered at the horizontal coordinate axis and vertical movements of the cursor were suppressed. In order to suppress vertical movements the signal pathway from the controller to the test implementation was cut off and the setpoint for the vertical position was set to zero degrees manually. Regarding the sEMG-based control an additional adaptation is necessary: Considering the case when a subjects unintentionally switches in the second control mode no cursor movement would occur. But still the internal state of the controller would have switched and the user would not be able to move the cursor anymore. The user would need to relax the muscles in order to switch back in the original state. The time needed for that would have an impact on the test results. Therefore, the second control mode was disabled within the embedded software using the Firmware of Ottobock.

The test was conducted using the sEMG-based and the IMU-based control schemes as input device. In order to make the test more reliable, the same targets were used for both input devices. In addition, all participants were confronted with the same targets which were again randomly generated and saved as part of the test preparation. As in the test before, the test was again split into three runs per input device with 30 targets per run. The targets were randomly generated with a uniform contribution in size $U(1.8°, 9°)$ and distance to the origin $U(22.5°, 72°)$ and were randomly located either on the left side (e.g. pronation) or the right side (e.g. supination) from the origin. For the same reasons as in the previous user test every first, randomly placed target, was followed by a second target located at the origin. The dwell time was again set to one second; and the time before an attempt was regarded as failure was again set to fifteen seconds.

5.5.3 Long Term Test

In order to assess how the performance develops under training, a user test was conducted in which the participants repeated the repositioning test daily after a short training procedure.

Participants

Two able-bodied participants (both male; aged 22 and 26) took part in the test. Both subjects were right-handed. The subjects took already part in both previous user tests and therefore were already familiar with the orientation-based control concept.

Experimental Design

This test was conducted on eight separate days during two consecutive working weeks. The training as well as the test were conducted with the implemented repositioning task of the virtual prosthesis. During the design it was payed attention to not exceed 20 minutes per day to keep the time effort for the participants reasonable. For each day new start configurations were randomly generated as part of the test preparation (two independent lists for the training and the test). Both participants were confronted with the same start configurations. The training as well as the test was conducted with 45 different start configurations which were split into three runs with fifteen tasks. As in the test described before, the start configurations were randomly generated with an uniform distribution in size $U(22.5°, 72°)$ and of the angle $U(0, 2\pi)$; an attempt was initiated by a left mouse click; the accepted tolerance of the neutral position was $\pm 9°$; dwell time was one second and timeout occurred after 15 seconds.

6 Evaluation

The first part of this chapter is designed to answer the question whether orientation and/or position tracking can be performed with acceptable accuracy using the predefined sensor. Regarding orientation tracking it is further of interest whether it is reasonable to include additional information obtained from the accelerometer and/or the magnetometer. In the context of prosthesis control, particularly the drifts occurring within a time span of a couple of seconds are of interest. For further investigations, five seconds are considered as a reasonable time span for positioning prosthesis joints.

To determine the uprising drifts, sensor noise processes of the gyroscope and accelerometer are identified via an AVAR measurement (see Chap. 3.6) and the quality of the calibration of the accelerometer is evaluated. The suitability of the estimated drifts based on the AVAR measurement is verified by data obtained by applying the tracking algorithms to real sensor data. The proposed control scheme is based on the orientation of the forearm and therefore the orientation tracking algorithm is additionally verified using an optical tracking system.

The second part of this chapter presents the results of the conducted user tests.

6.1 Orientation Tracking

6.1.1 Noise Process Identification

As the noise parameters vary with changing temperature, gyroscope data readings were logged in a thermal measurement chamber. Data history is acquired at 20°C at 100Hz for 12 hours. Fig. (6.1) shows the calculated ADEV plotted with the corresponding confident intervals (1σ-value). The angular random walk is determined by approaching the graph by a straight line with a slope of -1/2 and reading out the value at averaging time $\tau = 1$s. The numeric value of the bias instability is the minimum value of the ADEV graph (see Chap. 3.6) and appears in this particular graph at $\tau = 620$s. The results are summarized in Tab. (6.1).

	Angular Random Walk	Bias Instability (at 620s)
x Axis	$0.005\ ^\circ/\sqrt{s}$	$0.0011\ ^\circ/s$
y Axis	$0.007\ ^\circ/\sqrt{s}$	$0.0011\ ^\circ/s$
z Axis	$0.0037\ ^\circ/\sqrt{s}$	$0.0007\ ^\circ/s$

Table 6.1: Identified Gyroscope Noise Parameters.

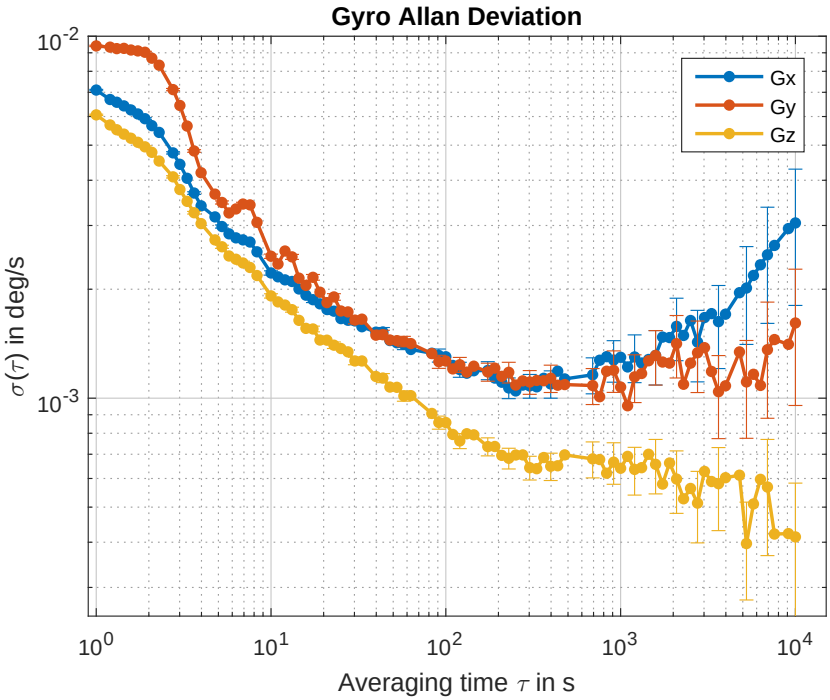

Figure 6.1: Allan Deviation plot of the gyroscope with confident intervals (1σ-values).

6.1.2 Error Propagation

The data history acquired for the AVAR analysis in the subchapter before is reused to survey whether the conducted analysis leads to suitable estimations of the uprising drifts. For this purpose, 500 data streams are applied to the first order integration scheme described in Chap. 5.2. The data streams accord to 500 subsequent bins with a length of 5s. One additional bin right before the first bin is used for bias calibration. Fig. (6.2) compares the expected drift based on the ARW measurement and the drift observed by integrating real sensor data. The first three figures show a snapshot of the observed drift after five seconds together with the expected and observed covariance ellipses. The last figure illustrates how the drift grows with time exemplary for the x-axis.

6.1.3 System Verification

The implemented control scheme is based on orientation tracking. To verify the implementation, the orientation tracking solution is compared to the results obtained by an optical tracking system. The sensor is placed on a white plate with two markers (at the upper left and lower right in the first picture in Fig. (6.3))[1]. A digital camera is used to

[1]Rotation symmetric markers are used as the matching algorithm used by Kinovea is rotation variant.

capture the scene while the sensor is rotated about the vertical axis by 90 degrees back and forth over 100s. Afterwards Kinovea (an open-source software for video analysis) is used to track the two markers and subsequently the coordinates of the tracked markers are used to calculate the tilt angle. Fig (6.4) (top) shows the angles derived from the movie analysis and from the inertial tracking algorithm. Fig. (6.4) (bottom) shows the difference of these two angles. The difference of the angles oscillates simultaneously with the absolute angle. Angles derived from the integration scheme turned out to be about 1.007 times larger.

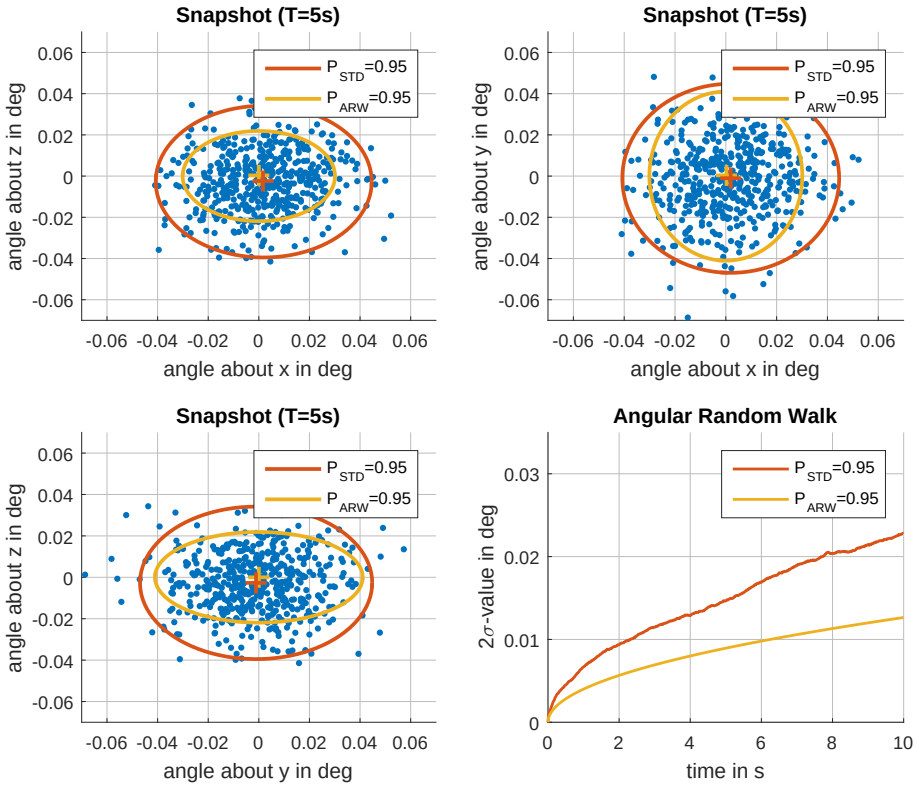

Figure 6.2: Orientation drift determined by integrating real data. The first three figures illustrate a snapshot after an integration time of 5s. The covariance ellipses illustrate the variance expected from the AVAR measurement (yellow) and the variance obtained from integrating of 500 data streams of real sensor data (red). The last figure illustrates how the variance increases over time exemplary for the angle about the x-axis.

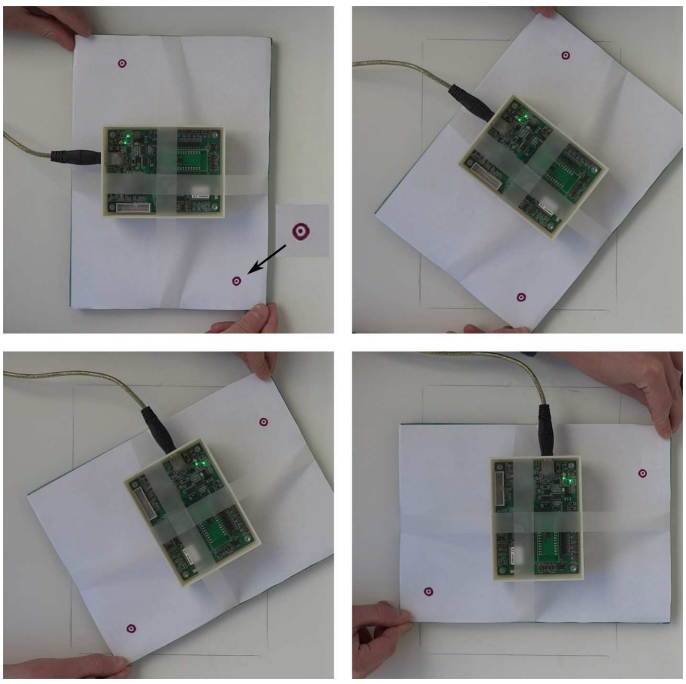

Figure 6.3: Setup to verify the inertial tracking solution with an optical tracking system. Two markers are used for optical tracking as shown in the upper left picture in more detail.

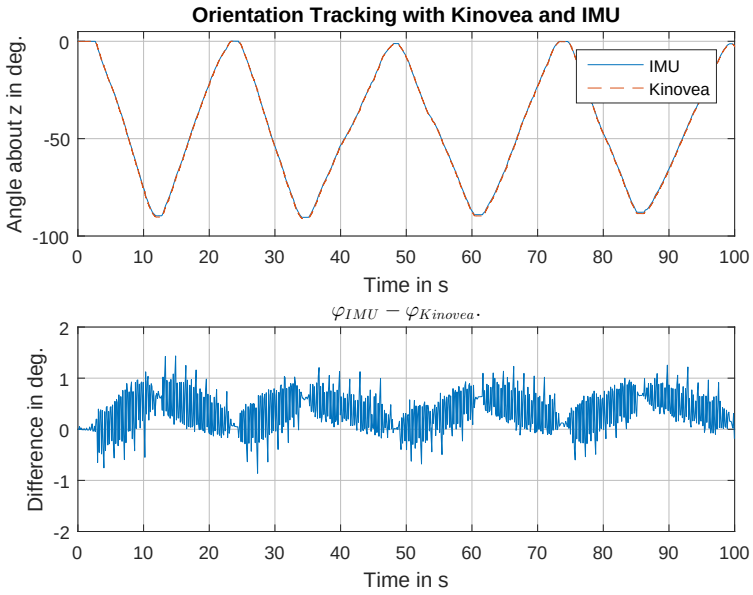

Figure 6.4: Comparison of the estimated angles around the vertical axis obtained by inertial tracking and optical tracking.

6.1.4 Bias Temperature Characteristic

To acquire a data history under changing temperature a measurement in a thermal measurement chamber is conducted. The output of three sensors is logged while the temperature was varied from -20°C to 50°C. The maximum temperature change is chosen to be 1°C/min and the temperature is held constant for an hour at the extremal values. This temperature profile is repeated three times. Fig. (6.5) shows the defined temperature profile and the temperature measured by the on-chip temperature sensor. The experiment is conducted two times on two different days. Fig. (6.6) shows the bias change plotted against the varied temperature. For each axis two characteristics are plotted - each related to the measurement on one day.

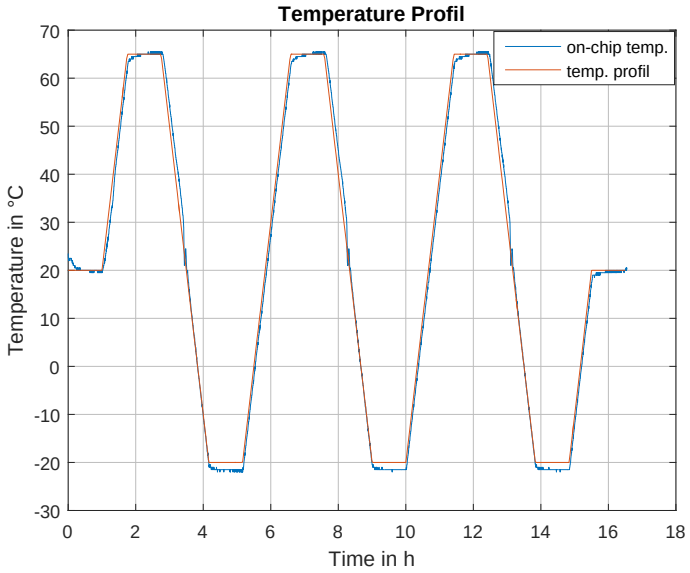

Figure 6.5: Temperature profile used to determine the bias-temperature characteristic. The red line shows the temperature set-point; the blue line shows the measured temperature by the on-chip sensor.

6.1.5 Discussion

The ARW measurement (which represents the white sensor noise) allows a suitable estimation of the uprising drifts for the considered time span of five seconds. The observed drift - obtained by applying the integration scheme to 500 data streams gathered in static state - is about 1.5 times higher but in the same range. As the drift was examined in static state, drifts due to calibration errors as e.g. scale non-linearity and axis-misalignment are not investigated.

The inertial tracking solution is verified with an optical tracking system. The evaluation shows that the integration scheme provides a meaningful solution for a long period of time.

The systematic error (Fig. (6.4)) observed between the optical and inertial solution could be either caused by the test setup (a non-perfectly aligned camera; the rotation axis does possibly not perfectly match the vertical sensing axis of the sensor) or by systematic errors of the sensor. Regarding a prosthesis control, the user builds a closed-loop to position a joint, and therefore the absolute accuracy (effected by systematic errors) is less important.

The investigation of the bias-temperature characteristic shows a different characteristic for each particular sensor. However the characteristic for each sensor is reproducible and therefore the on-chip temperature sensor could be used to account for this type of error. The observed bias-temperature dependency is of the size of several tenths of a deg/s. However, an assumed bias of 0.3 deg/s would result in a drift of 1.5 degrees within five seconds. Most likely, drifts of this scale will hardly be noticeable if at all perceptible regarding an orientation-based control scheme.

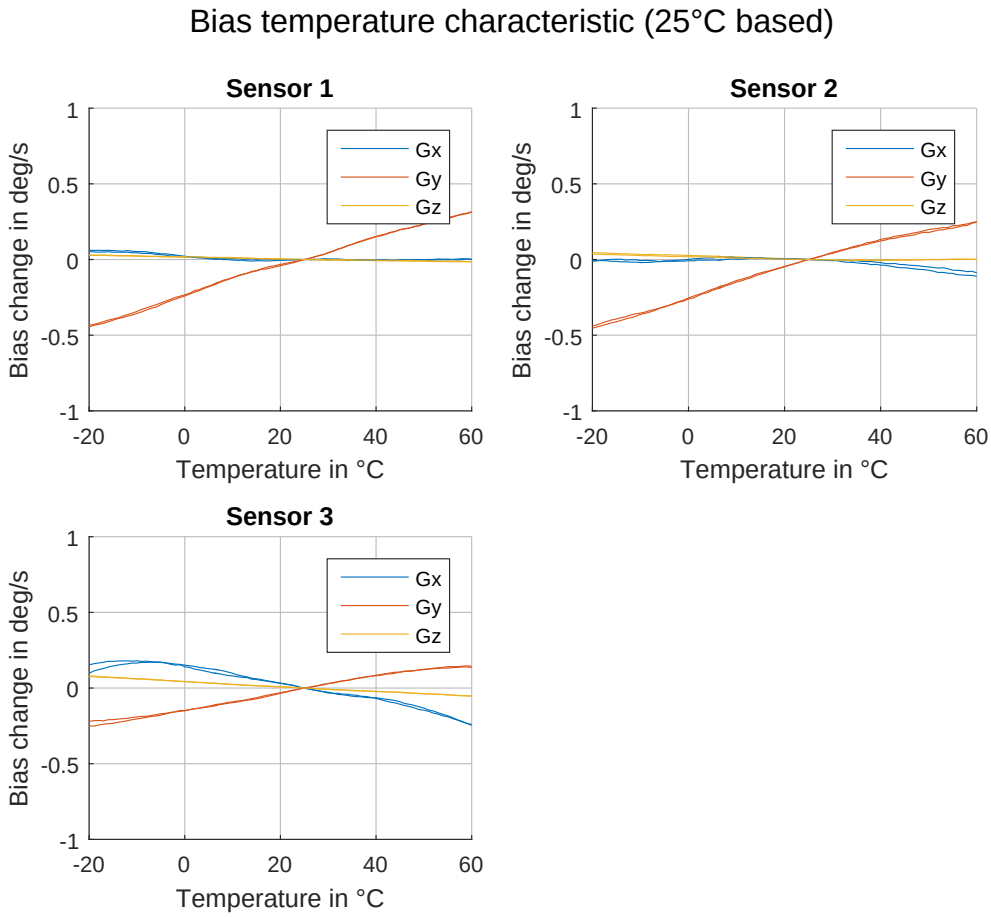

Figure 6.6: Bias-temperature characteristic determined for three sensors. The experiment is conducted two times at two different days resulting in the two characteristics plotted for each axis.

6.2 Position Tracking

6.2.1 Accelerometer Calibration

In order to estimate the relative position by double-integrating the accelerations, it is necessary to g-correct the measured data. Systematic errors as scale and bias errors distort the measurements and lead to a situation where gravity cannot be subtracted correctly anymore. Therefore systematic errors lead to high drifts in the velocity and position estimation. This subsection assesses the calibration method described in Chap. 5.1.

Since no ground truth data is available, it is not possible to verify the obtained model parameters directly. To assess the fit of the model, the deviations of the magnitude of error-corrected measurements from the magnitude of gravity are examined. For this purpose a subset of the recorded measurements is excluded from the calibration and used for the examination.

Three measurement series each with 70 measurements were used to examine the calibration quality. Each measurement series is split into a calibration-set consisting of 60 measurements and a test-set consisting of 10 measurements. Fig. (6.7) shows the resultant mean absolute error (MAE)

$$MAE = \frac{1}{N} \sum_{i} |(||\boldsymbol{a}_0|| - g)| \tag{6.1}$$

against the number of orientations which are used for calibration. The results indicate that including more than 40 to 50 measurements cannot significantly decrease the error anymore. The achieved results are stated in detail in Tab. (6.2).

	before calibration (MAE) in units of g	after calibration (MAE) in units of g
data-set 1	$0,032$	$5.1 \cdot 10^{-4}$
data-set 2	$0,034$	$7 \cdot 10^{-4}$
data-set 3	$0,033$	$6.9 * 10^{-4}$

Table 6.2: Results of the accelerometer calibration. The stated values are the mean average error (MAE) after calibration using 50 orientations and without any calibration.

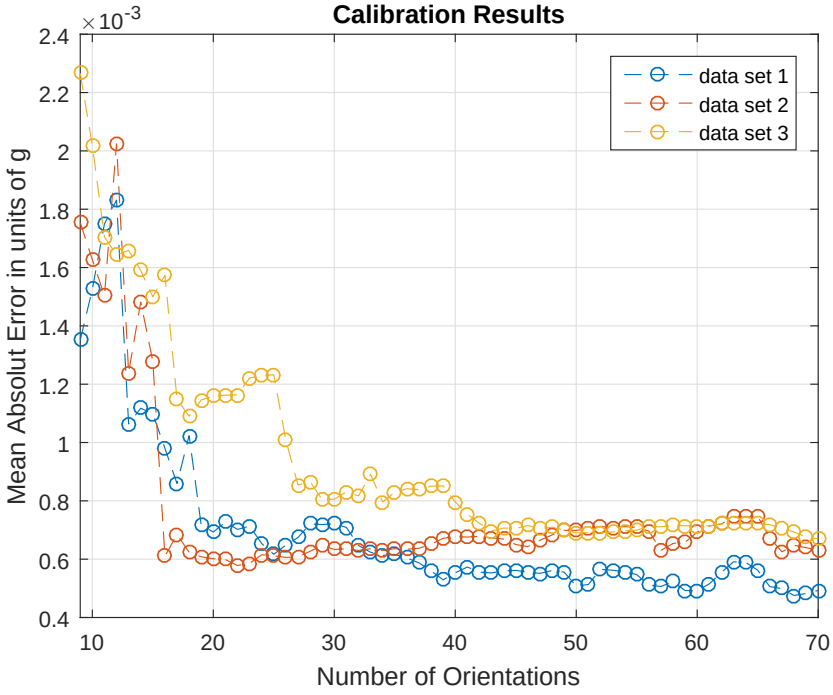

Figure 6.7: Results of the accelerometer calibration against the number of measurements used for calibration.

6.2.2 Noise Process Identification

The AVAR technique is applied to the data which was already obtained to analyze the gyroscope (data was acquired at 20°C at 100Hz during 12h). The ADEV is plotted in Fig. (6.8); the derived numerical values for the velocity random walk (VRW) and bias instability are summarized in Tab. (6.3).

	Velocity Random Walk	Bias Instability
x Axis	8.5 10^{-5} m/s$^2/\sqrt{\text{s}}$	1.3 10^{-4} m/s at 250s
y Axis	1.3 10^{-4} m/s$^2/\sqrt{\text{s}}$	3.1 10^{-4} m/s at 250s
z Axis	4.9 10^{-4} m/s$^2/\sqrt{\text{s}}$	2.3 10^{-4} m/s at 6000s

Table 6.3: Identified Accelerometer Noise Parameters.

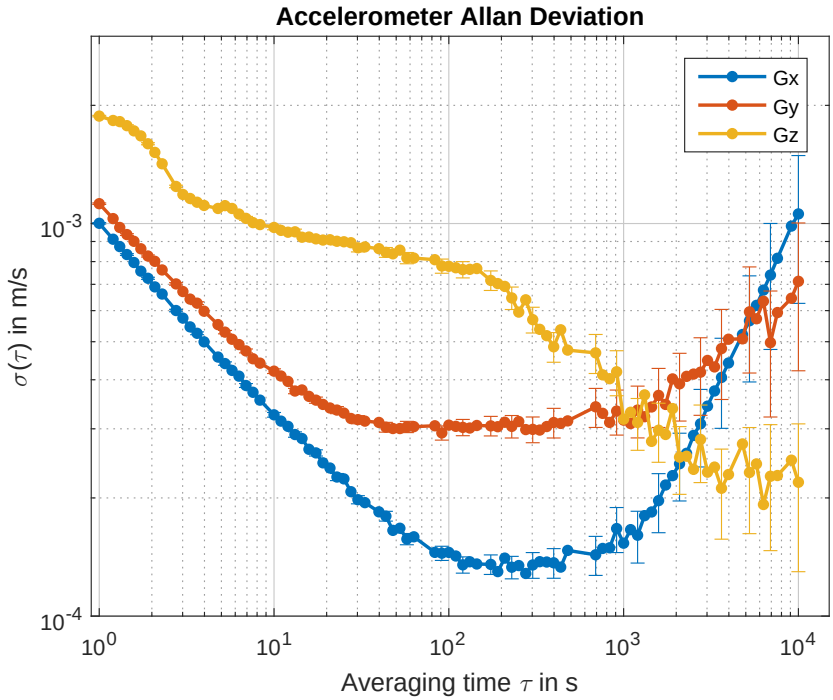

Figure 6.8: Allan Deviation plot of the accelerometer with confident intervals (1σ-values).

6.2.3 Error Propagation

Following the same proceedings as for the gyroscope, the uprising drifts are initially estimated using the VRW measurement (this corresponds with the assumption that white measurement noise is the dominant error source). This estimation is verified with data obtained by integrating 500 data streams (according to 500 subsequent bins with a length of 5s). The data is gathered in static state and therefore the true accelerations equal zero. A bin right before the first bin is used to determine the offset including the term caused by gravity. As stated in Chap. 5.2, white noise in the accelerometer readings leads to a first-order random walk in velocity and a second-order random walk in position. The corresponding standard deviations are

$$\sigma_v(t) = \mathrm{VRW} \cdot \sqrt{t}\ , \qquad \sigma_s(t) = \mathrm{VRW} \cdot \frac{1}{\sqrt{3}} \cdot t^{3/2}\ . \tag{6.2}$$

Fig. (6.9) compares the expected drift based on the VRW measurement and the drift observed by integrating real sensor data; Fig. (6.10) illustrates the uprising drift in position.

Finally, it is examined how noise related to the ARW and VRW terms propagate through a position tracking system. For this purpose, the position tracking algorithm is applied

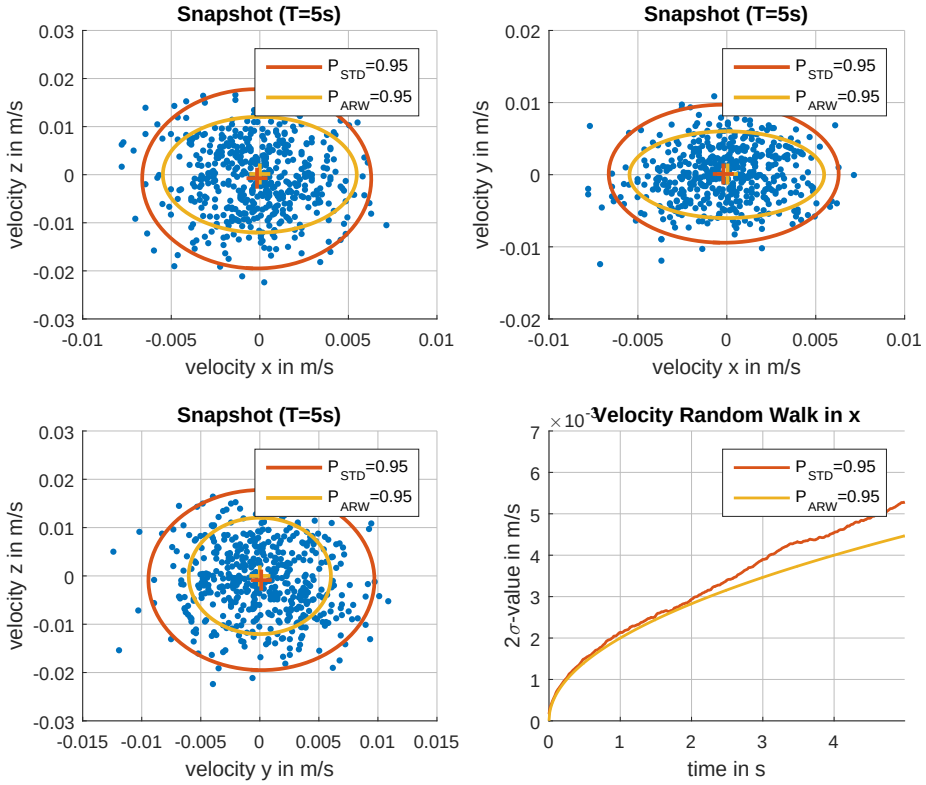

Figure 6.9: Drift of the estimated velocity which occurs when real accelerometer data is integrated. The covariance ellipses illustrate the expected variance based on the AVAR measurement (yellow) and the variance determined by integrating of 500 real sensor data streams (red). The last figure shows how drift grows with time exemplary in the x-direction.

to artificial sensor readings of a device in static state. The standard deviation of the corresponding white noise is given as

$$\sigma = \frac{\mathrm{RW}}{\sqrt{T_S}} \tag{6.3}$$

and noisy data is generated as

$$\boldsymbol{\omega}_k = \mathbf{0} + \boldsymbol{v}_{gyro}, \qquad \boldsymbol{a}_k = \begin{bmatrix} 0 \\ 0 \\ g \end{bmatrix} + \boldsymbol{v}_{acc} \tag{6.4}$$

with the measurement noise terms[2] $\boldsymbol{v}_{gyro}$ and $\boldsymbol{v}_{acc}$. Orientation is tracked by integrating

[2]White noise is generated using the Matlab random generator: σ·randn(1,stream_length).

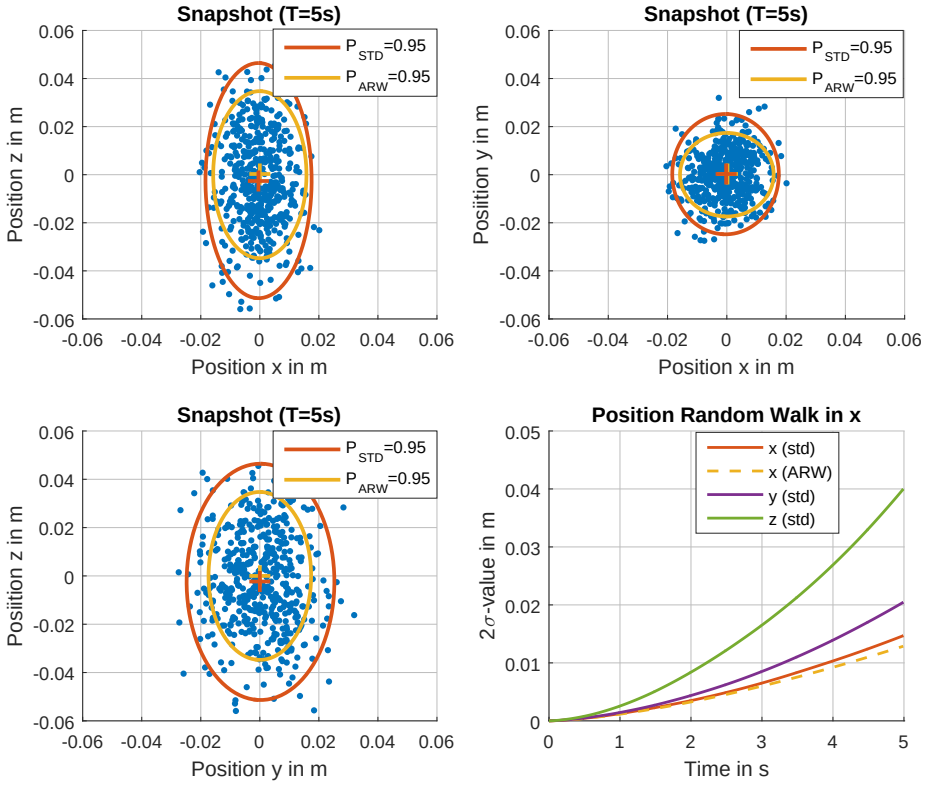

Figure 6.10: Drift of the estimated position which occurs when real accelerometer data is integrated. The covariance ellipses illustrate the expected variance based on the AVAR measurement (yellow) and the variance determined by integrating of 500 real sensor data streams (red). The last figure shows how drift grows with time (for x-axis additionally the expected drift based on the AVAR measurement is plotted).

the gyroscope readings. The accelerometer readings are transformed into the local navigation frame and subsequently integrated after subtracting the gravity vector. Fig. (6.11) shows the results exemplary by three (error) trajectories. The main drift occurs in the horizontal plane.

6.2.4 Discussion

The AVAR technique is used to determine the noise processes of the accelerometer. The evaluation shows that the VRW term allows a suitable estimation of the uprising velocity and position drifts. For the assessment of the quality of the accelerometer calibration no ground truth data is available and therefore an evaluation is conducted using the only available reference – the magnitude of the gravity vector. It is shown that the calibration considerably decreases the error of the measured magnitude (see Tab. (6.2)).

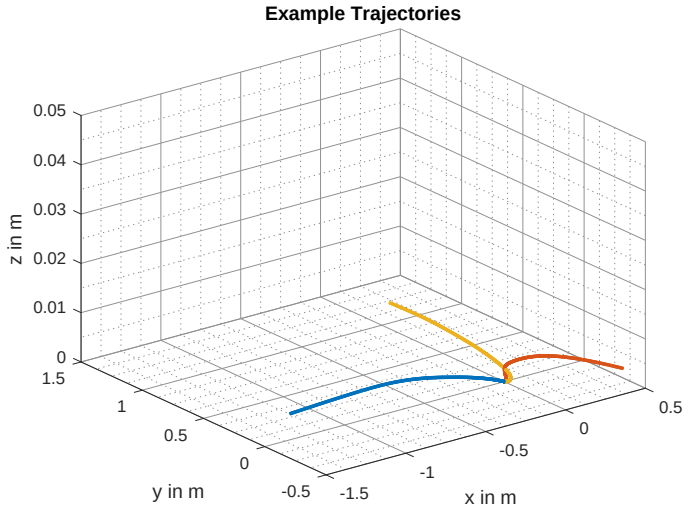

Figure 6.11: Three example error paths of the entire position tracking algorithm (5s integration time). The main drift occurs within the horizontal plane due to gyroscope noise.

The 2σ-values for the position error are determined to be 1.5cm, 2cm and 4cm in x, y and z direction after 5s. The accelerometer calibration reduced the magnitude error in static state to about 0.006 m/s^2. This value represents a residual bias after g-correction and leads to a displacement error of 7,5cm in 5s.

Finally, it is simulated how gyroscope and accelerometer noise propagate through a position tracking algorithm. For this purpose, it is assumed that the initial orientation is known exactly. The solution shows that the gyroscope noise represents the dominant error source, which causes errors in the range of 1m within the horizontal plane. This error is caused by the projection of the gravity vector onto the horizontal plane which arises when the estimated vertical is rotated against the true vertical (Chap. 3.5), and could be reduce by applying a vector matching approach for orientation estimation (Chap. 3.4).

Within the considered time span of 5s, the drift caused by the accelerometer's characteristics would be in the range of several centimeters what would cause a partly arbitrary behavior of a potential control scheme. This leads to the conclusion that a control scheme based on position tracking (regarding a steering time of 5s and the predefined sensor) is hardly feasible. Restricting the time span to e.g. 2s, the accelerometers' characteristics causes a drift in the range of millimeters. However, several challenges remain: Restrictive requirements on the usage would be necessary, like the request to keep the forearm at rest right before enabling the control mode (to allow short integration times and zero velocity updates). Further it would be necessary to include accelerometer readings in the orientation estimation algorithm which also implies that a compromise between stochastic and systematic errors has to be found; this compromise depends on whether slow or fast movements should be tracked.

6.3 User Tests

6.3.1 Two-DoF Tests

Experimental Protocol

All participants followed the same test procedure, which took about 90 minutes. The four-channel control was tested first. The adjustment process of the four-channel control was taken over by an Ottobock employee who was conversant with the procedure. Afterwards it was explained how to control the cursor using the four-channel control. During a short training process the participant was asked to move the cursor into a certain position which was indicated by the test conductor pointing on a sport on the screen with a pencil. After ten of those tasks the participants were asked if they feel comfortable using the four-channel control and they were offered to try out to control the cursor without guidance. Immediately after the training process, the cursor test took place using the four-channel control. Three runs were executed, one run contained 30 trials, resulting in 90 trials in total. After each run the participants had the opportunity to take a short break. Subsequently, the participant was asked to answer the relevant part of the questionnaire.

Next it was explained how to control the virtual prosthesis using the four-channel control. This was followed by a guided training session where the participant was asked to fulfill particular movements (rotation and flexion/extension in particular direction). After a couple of minutes of this guided practice the participants were asked if they feel comfortable using the control scheme and they were offered to try out to control the virtual prosthesis without guidance. Subsequently, the test procedure was explained. The subsequently performed experiment consisted of three runs each containing 20 trials, resulting in 60 trials at all. Afterwards, the sEMG electrodes were removed and the participant answered the next part of the questionnaire.

After a break of a couple of minutes the IMU casing was placed either on the users' prosthesis or on the dominant hand of the able-bodied subjects. After calibrating the sensor position (p. 32) it was explained how to fulfill cursor movements using the orientation-based control scheme. Able-bodied participants held the mouse in their dominant hand; participants with amputation held the mouse in their healthy hand (as already explained, the mouse was used to enable the orientation-based control mode). A training procedure was provided by requesting the participant to move the cursor toward spots on the screen which were indicated by the test conductor. Before the experiment, the participants were instructed to start each attempt by clicking the left mouse button. It was pointed out that the time before activating the control mode is not inflicting the evaluation. Again the test part consisted of three runs with 30 trials per run.

This was followed by the repositioning task of the virtual prosthesis using the orientation-based control. The same guided training as with the four-channel control was performed. The participants were instructed to start each attempt with a left mouse click and one

more time it was pointed out that the time before activating the control mode is not inflicting the evaluation and that before starting an attempt it is possible to rearrange the arm in a comfortable position if necessary. Three runs were executed, one run contained 20 trials. After each run a break was offered. Subsequently, the participant was asked to answer the part of the questionnaire regarding the repositioning task using the orientation-based control and regarding the comparison of the orientation-based control and the four-channel control.

After removing the IMU casing and a break of a couple of minutes the cursor positioning task was conducted using a computer mouse. Also during this experiment, the participants started an attempt by a left mouse click. The experiment included three runs with 30 trials per run.

Participants were monitored during performing the test to ensure that no software problems occurred and to answer questions that may have come up. A summary of the test procedure is shown in Fig. (6.12).

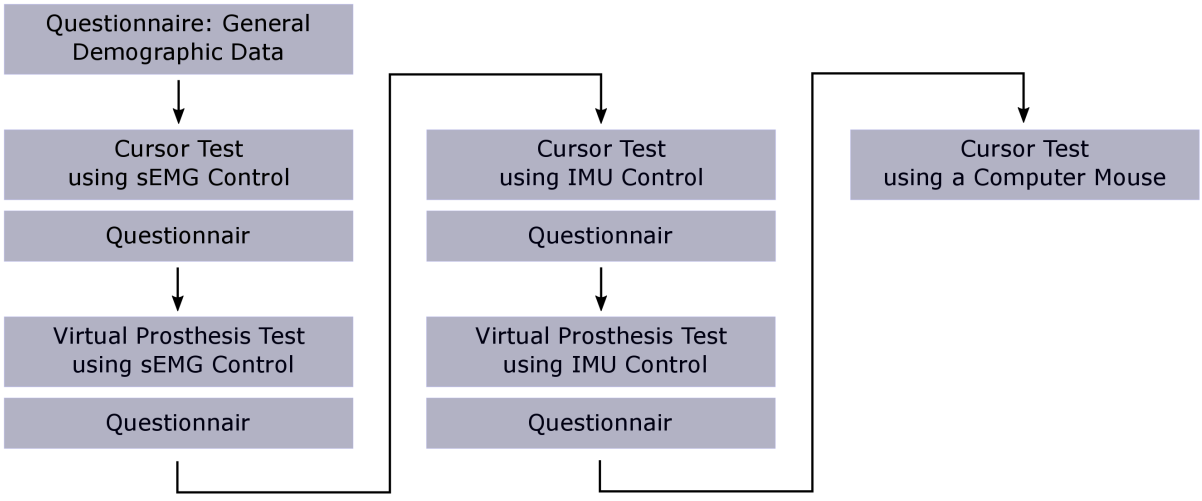

Figure 6.12: Summary of the test procedure.

Performance Evaluation

Fig. (6.13)(a) and Fig. (6.13)(b) compare the results of the cursor positioning task using the orientation-based control scheme and a computer mouse. The completion time and the path efficiency are reported. For each metric a boxplot including all trials (15 participants x 90 trials) and a boxplot of the mean values achieved by each participant (15 data points) are shown.

It is reasonable to assume that prosthesis users are more confident using the four-channel control due to their experience compared to able-bodied participants. Therefore, results concerning the four-channel control are reported separately for able-bodied and disabled participants. Fig. (6.14) compares the results of the cursor positioning task using the orientation-based and the four-channel control scheme. As the two DoF have to be positioned sequentially using the four-channel control (in contrast to the orientation-based control scheme), only the completion time is used as performance indicator.

Fig. (6.15)(a) and Fig. (6.15)(b) report the results of the repositioning task of the virtual prosthesis using the orientation-based and the four-channel control scheme. The completion time and the path efficiency are reported. The path efficiency allows to assess if the participants made use of the possibility to position both DoF simultaneously.

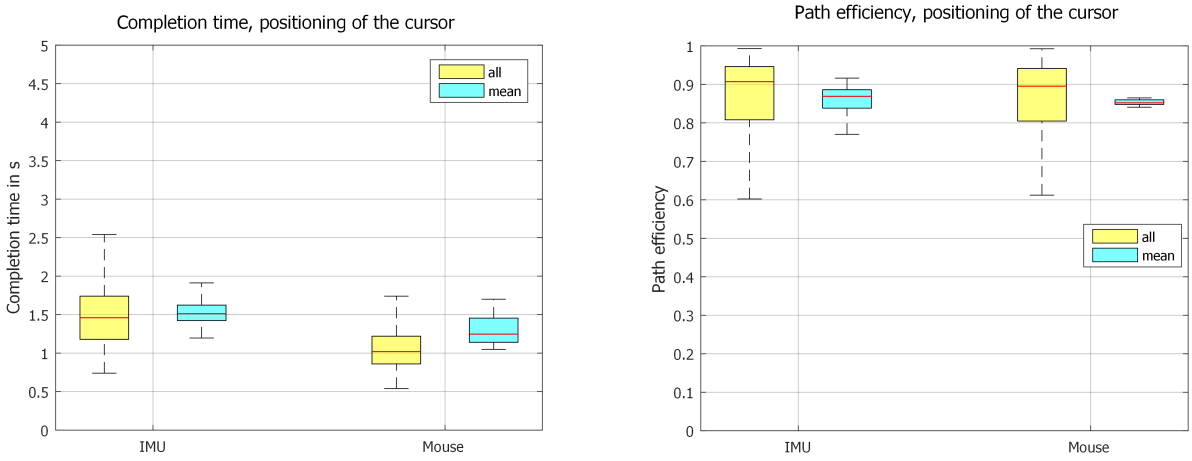

(a) (b)

Figure 6.13: Comparison of the achieved completion time (a) and the achieved path efficiency (b) during the cursor positioning task using the orientation-based control scheme (IMU) and a computer mouse.

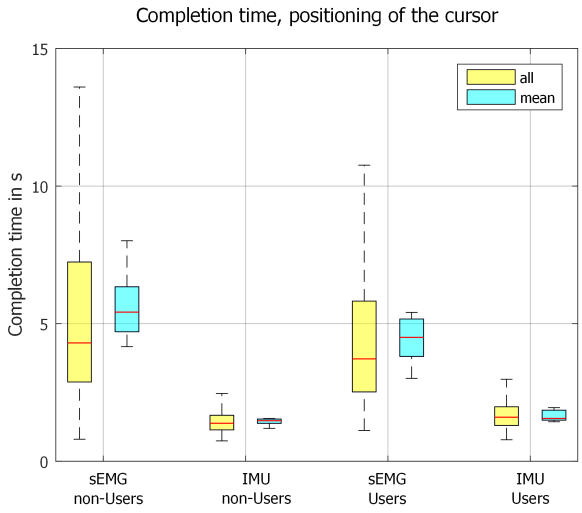

Figure 6.14: Comparison of the achieved completion time during the cursor positioning task using the orientation-based control (IMU) and the four-channel control (sEMG). Participants are split into groups of prosthesis users and non-users.

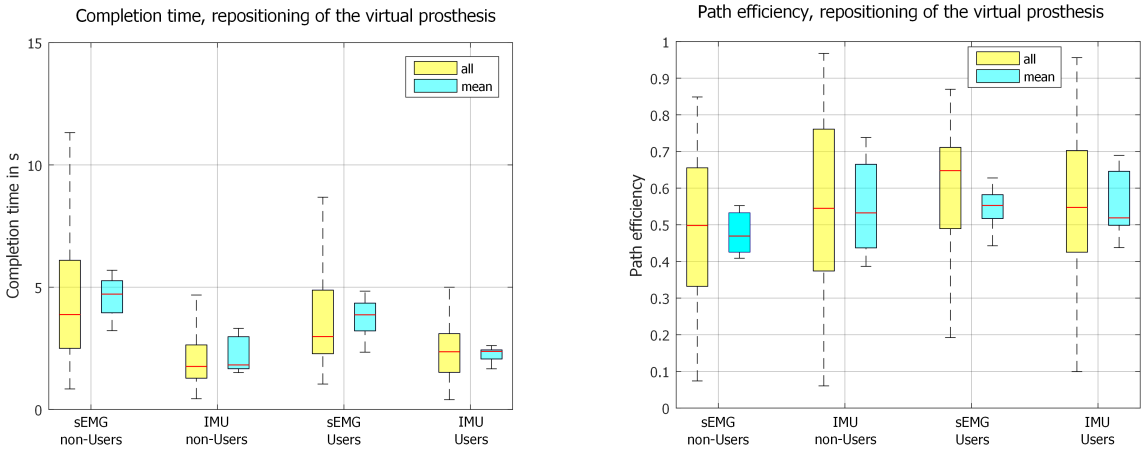

(a) (b)

Figure 6.15: Comparison of the achieved completion time (a) and the achieved path efficiency (b) during the repositioning task of the virtual prosthesis using the orientation-based control (IMU) and the four-channel control (sEMG). Participants are split into groups of prosthesis users and non-users.

Evaluation of the Questionnaire

The evaluation of the questionnaires is effected separately for prosthesis users and non-prosthesis users. However, the ratings of the two groups show a similar image. Fig. (6.16) summarizes the results concerning the cursor positioning task. The evaluation shows that the participants had no difficulties solving the given task with the orientation-based control scheme; furthermore, the participants stated having less problems handling the orientation-based control scheme and obtaining the necessary accuracy (size of the targets) compared to the usage of the four-channel (sEMG) control; these results conform to the quantitative results (completion time, path efficiency). The required range of the arm movement was judged as being "Comfortable" by the majority. All participants that had answered the question with "Rather comfortable" rated the required arm movement in the following sub-question as "Rather too big".

Fig. (6.17) summarizes the results concerning the repositioning task of the virtual prosthesis. Both types of regulation of the virtual prosthesis are in principle being rated positively by both groups. The group of non-prosthesis users therein assessed the two control concepts as very similar; the group of prosthesis users assessed the orientation-based control scheme as being more intuitive and handable with less difficulties. As before, the required range of the arm movement is perceived as "Comfortable" by the majority. Also in this test, the participants that had answered "Rather comfortable" rated the arm movement as being "Rather too big".

The last part of the questionnaire examines (i) whether prosthesis users could imagine to incorporate the orientation-based control scheme in their daily life and (ii) how they evaluate the usability of both control concepts against each other (only prosthesis users were questioned for that purpose). The results are summarized in Fig. (6.18). According to the participants, the orientation-based control scheme provides a more accurate and quicker positioning of the prosthesis. Both aspects were judged as important by the participants. An implementation of the proposed control scheme into daily life is imaginable for the participants in positioning wrist joints; grasping however is not imaginable for them. Conversations that took place after the test stated following reason: The sEMG-based control concept allows controlling the exerted force, as the force is proportional to how intensely the muscles are being contracted. With the proposed orientation-based control scheme a regulation of the excited force would not be given due to a non-existent feedback.

able-bodied subjects, cursor positioning task

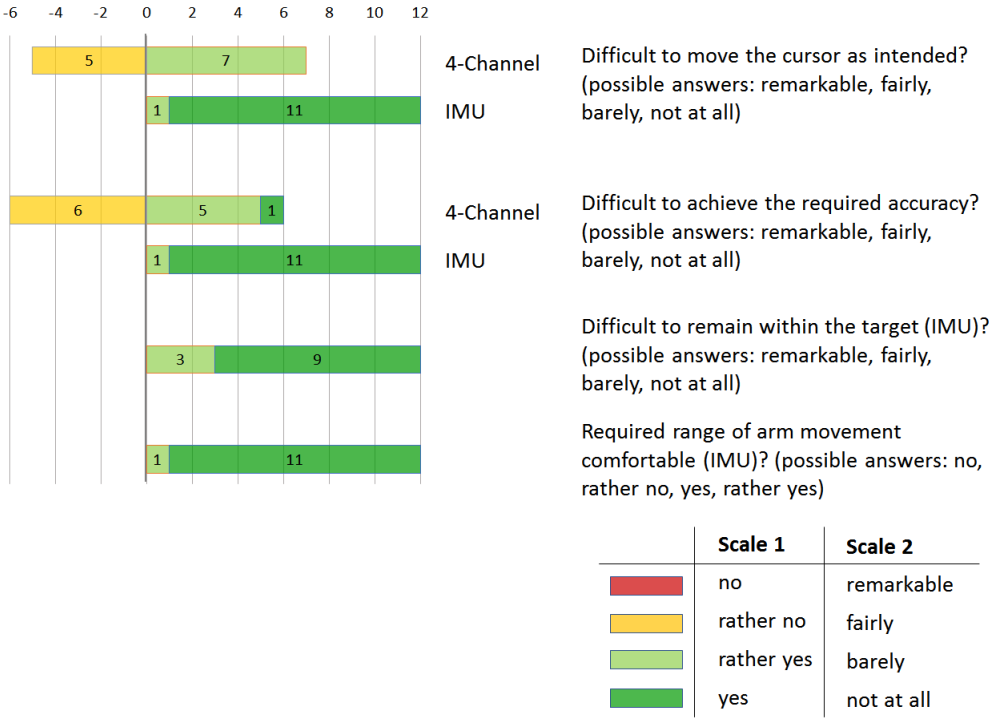

disabled subjects, cursor positioning task

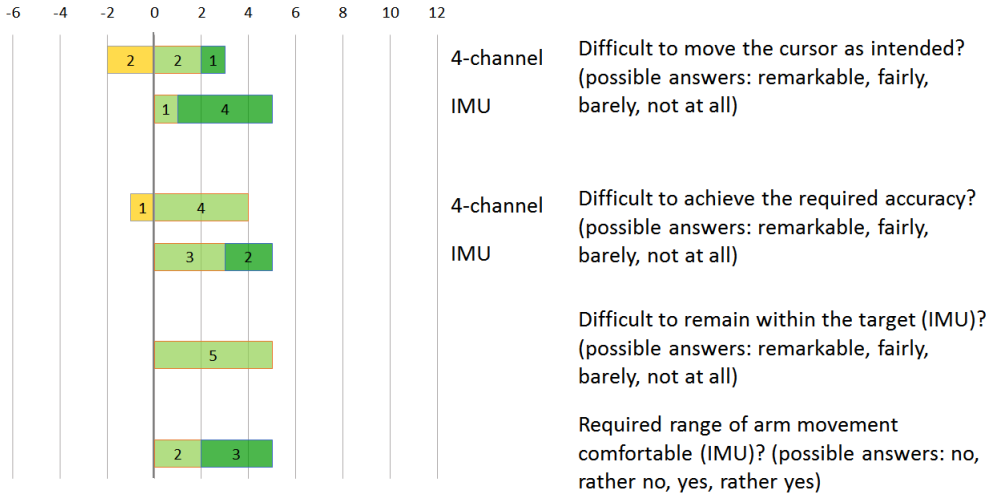

Figure 6.16: Comparison of the participants' perception of the four-channel control (sEMG) and the orientation-based control (IMU) regarding the cursor positioning task. The evaluation of the questionnaires is effected separately for prosthesis users and non-prosthesis users.

able-bodied subjects, repositioning of the virtual prosthesis

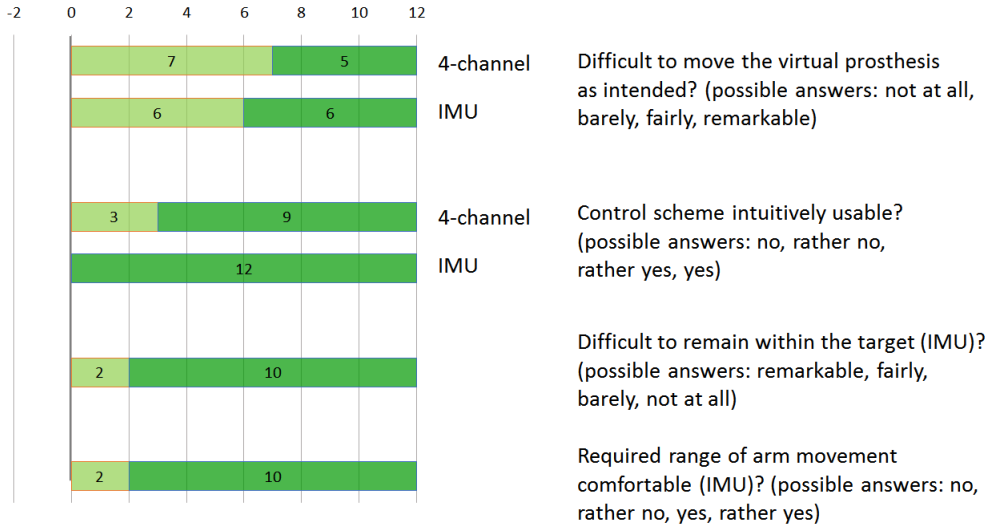

disabled subjects, repositioning of the virtual prosthesis

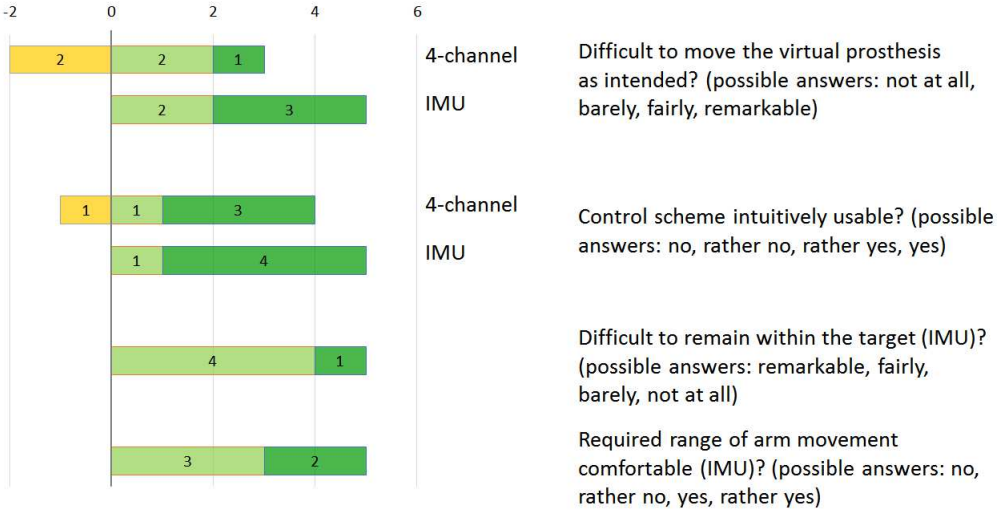

Figure 6.17: Comparison of the participants' perception of the four-channel control (sEMG) and the orientation-based control (IMU) regarding the repositioning task of the virtual prosthesis. The evaluation of the questionnaires is effected separately for prosthesis users and non-prosthesis users.

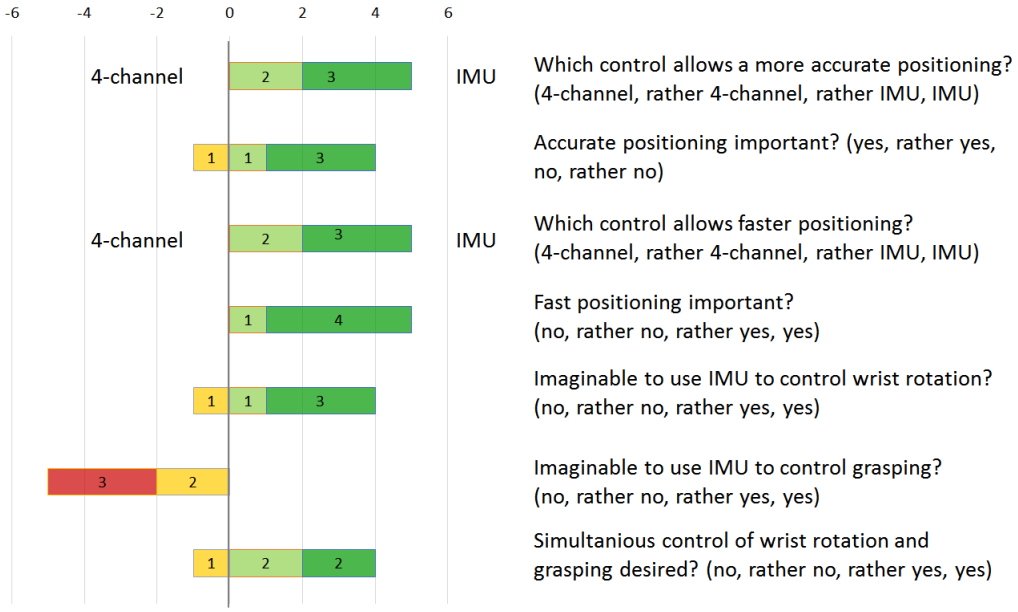

Figure 6.18: Results of the gathered feedback from prosthesis users on (i) how they evaluate the usability of the orientation-based control and the four-channel control against each other and (ii) if they could imagine to incorporate the orientation-based control scheme into their daily life.

6.3.2 Single-DoF Test

Experimental Protocol

All participants followed the same test procedure, which took about 45 minutes. At first, the experiment using the sEMG-based control was conducted. An Ottobock employee - with experience with the adjustment procedure - adjusted the four-channel control. This was followed by a guided training in order to (i) ensure that the adjustment allows the user to move the cursor in a controlled way and (ii) to allow the user to recall how to use the four-channel control. During this training process the participant was asked to move the cursor to a certain position indicated by the test conductor by pointing on various spots on the horizontal coordinate axis with a pencil. Immediately after the training process the experiment using the four-channel control took place. Three runs were executed, with 30 trials per run. After each run the participant was offered a break.

After a break of a couple of minutes the IMU sensor casing was donned on the participant's dominant hand and the measurement of the orientation of the sensor frame relative to the forearm frame (p. 32) was executed. After explaining how the cursor can be moved using the one-dimensional IMU-based control scheme a short training process took place during which the participant was asked to move the cursor toward about ten different locations again indicated by a pencil. Although all participants had already used the IMU-based

control scheme this guided training was conducted to familiarize the participant with the control of a single DoF and to recall how to manipulate the required DoF using the IMU-based control scheme. During the test - which took part immediately after the training - the participants were confronted with the same 90 trials, again split into three runs. Again, after each run a break was offered.

As in the previous test, the participants were monitored during performing the test to ensure that no software problems occurred and to answer questions that may have come up.

Performance Evaluation

Fig. (6.19) shows the achieved completion time using the four-channel control and the orientation-based control.

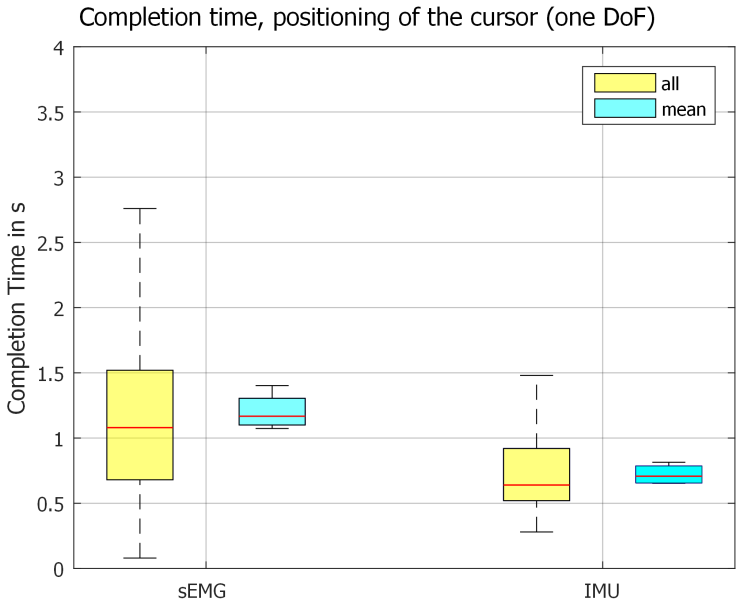

Figure 6.19: Comparison of the achieved completion time using the orientation-based control (IMU) and the four-channel control (sEMG) during the one-dimensional cursor positioning task. Only non-prosthesis users took part in the test.

6.3.3 Long Term Test

Experimental Protocol

This test was conducted at five days in one working week and at four additional days in the week after. At every day both subjects followed the same test procedure, which took

about 25 minutes. After donning the IMU casing at the participant's dominant hand, the sensor position was calibrated (p. 32). Subsequently the participants were asked to execute single-DoF movements as a pure flexion and pure rotation; this ensured that the participants were able to control the virtual prosthesis as intended. After that, the training took place (it was pointed out that during the training no data is recorded), which took about ten minutes; this was followed by the test after a break of a couple of minutes, which also took about ten minutes.

Performance Evaluation

Fig. (6.20)(a) and Fig. (6.20)(b) show the development of the performance of the two participants over nine days.

6.3.4 Discussion

This subchapter discusses the results of the conducted user tests. After an interpretation of the measured performance concerning the positioning of two joints, the gathered feedback of the participants is reviewed. This is followed by a discussion of the measured performance during the single-DoF test and the long term test.

The two-DoF user test was conducted in order to (i) assess the overall usability of the proposed IMU control scheme regarding the positioning of two joints and (ii) to assess how the IMU control compares to the conventional four-channel control (sEMG). To evaluate whether the participants are able to position two DoF using the proposed IMU-control scheme in a controlled way, at first an experiment was conducted in which the participants had to position a cursor vertically and horizontally using the IMU control scheme and a computer mouse. A computer mouse was chosen as reference as it represents a highly accepted and sophisticated input device. The measured path efficiency turned out to be very similar using the IMU control scheme and the computer mouse (Fig. (6.13)(b)) and therefore it is concluded that the participants were able to manipulate the cursor as intended. However, using the mouse the participants reached the desired positions considerably faster (Fig. (6.13)(a)). This could be caused by a lower physical burden as the mouse is moved only a few centimeters while the entire forearm must be rotated using IMU control.

The experiment in which a cursor has to be positioned was further conducted using the four-channel control. The comparison of the completion time with the IMU control (Fig. (6.14)) shows that the participants were able to position the cursor considerably faster using the IMU control (1.6s vs. 4.5s, mean of means achieved by prosthesis-users). These results are most likely caused by the two major advantages of the IMU control: by using the IMU control scheme (i) the user is able to manipulate the two DoF simultaneously and (ii) the user directly manipulates the position – the desired physical parameter – instead of the velocity. Further, when using the four-channel control the maximum angular velocity

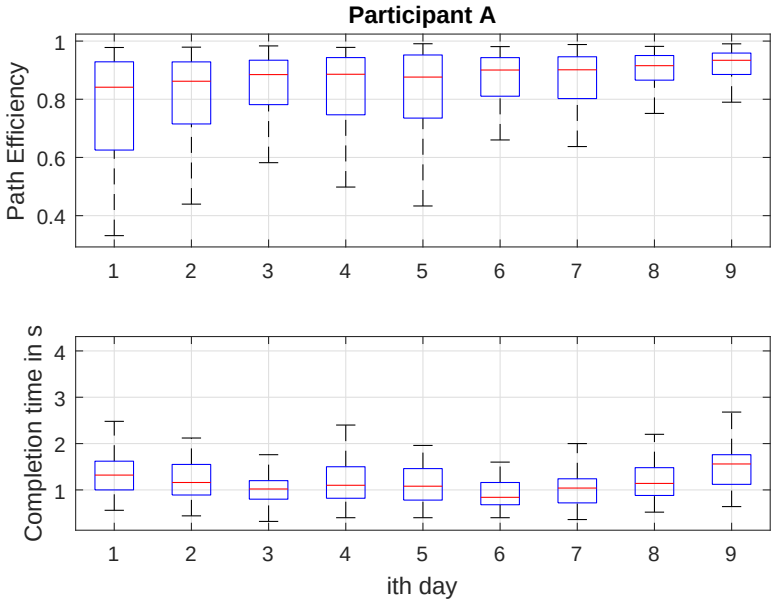

(a)

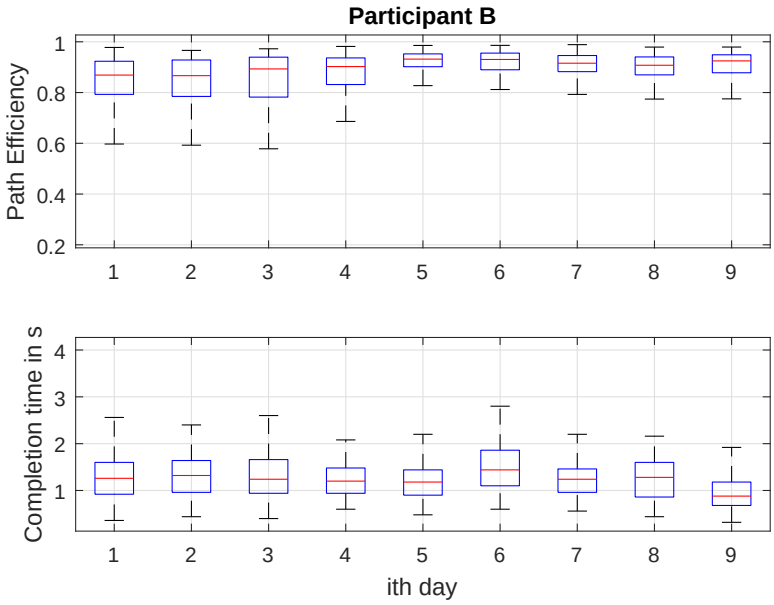

(b)

Figure 6.20: Development of the control performance measured over nine days.

is limited (Chap. 3.2) as the maximum possible velocity is a compromise between speed and accuracy. Most likely this also increases the time needed to reach targets when large displacements of the cursor or joint angles are required.

In order to evaluate the applicability of the IMU control for positioning prosthesis joints an experiment was conducted in which the participants were asked to reposition a virtual prosthesis from different start configurations into its neutral position. Fig. (6.15)(a) reports the completion time measured using the four-channel control and IMU control. The time needed to reposition the prosthesis joints using the IMU control is still considerably shorter compared to the four-channel control (2.3s vs. 3.8s, mean of means achieved by prosthesis-users). However, the difference is not as clearly pronounced as during the cursor positioning task. Compared with the cursor positioning task the path efficiency (Fig. (6.15)(b)) is considerably lower which leads to the conclusion that the participants were not able to capitalize the possibility of a simultaneous control using the IMU control. This shows that the participants were not able to immediately use (without a longer training) the IMU control intuitively to reposition the virtual prosthesis. This can be caused by a non-intuitive mapping of the forearm's orientation to joint angles as well as by difficulties in the interpretation of the position of the three-dimensional prosthesis from the two-dimensional visualization.

The evaluation of the questionnaire in Fig. (6.18) shows that the prosthesis users were generally speaking very liberally towards a possible control of the wrist joints on the basis of the introduced control scheme. Grasping by means of the new control scheme though was not imaginable for the participants. It was not perceived as a problem that the usage of the control scheme requires movements of the forearm. The participants' throughout positive feedback was mainly based on the intuitive usability of the control over prosthesis angles (instead of speed). This combined with the simultaneous control of the two degrees of freedom resulted in a considerably more "dynamic" control. Further, the possibility to position the joints in a faster and more accurate way was experienced as a plus. Of the five participants, three perceived the required range of movement of the arm as "Rather Comfortable", two of them rated it being "Comfortable"; those who rated "Rather Comfortable", stated that the range of movement is "rather too big".

To investigate how the IMU control compares to the four-channel control when only one joint is controlled, a test was conducted where a cursor had to be moved only horizontally. As only one DoF is manipulated this test assesses the differences of both control concepts isolated from the possibility of a simultaneous control of two DoF. Fig. (6.19) compares the completion time using the IMU control and four-channel control. The results show that the IMU control also allows a faster positioning when a single joint is controlled (mean of means: 0.7 vs. 1.16). These results are also most likely caused by the advantage of controlling the position directly. Also the limited speed while using the four-channel control could have an impact when large displacements are required.

During the two-DoF experiment in which the participants were asked to reposition a virtual prosthesis, the participants did not capitalize the possibility of a simultaneous

control but rather positioned the two joints sequentially. In the last user test it was assessed how the performance develops under training. For that purpose, the participants repeated the repositioning experiment over nine days (with changing start configurations). Fig. (6.20) shows that the path efficiency increases fast and reaches a high value close to the path efficiency achieved during the cursor positioning task within a short time of use. This suggests that the possibility of a simultaneous control will be utilized after a short training time.

7 Conclusion and Outlook

This thesis examined the development and assessment of an alternative control concept for upper limb prosthesis based on forearm movements which are tracked using inertial measurements. The basic idea was to link relative changes of the position or orientation of the forearm to movements of prosthesis joints when the control mode is activated – while activation and deactivation of the said control mode is (intended to be) provided via sEMG. Having a later product realization in mind, a single IMU placed on the forearm was used for tracking, making it possible to integrate the sensor within the prosthesis.

To examine the viability of such a control concept, at first the achievable accuracy of position and orientation tracking systems was investigated. As a useful and workable system should allow positioning of prosthesis joints within a few seconds, in particular the uprising error within a couple of seconds was examined. Subsequently an orientation-based control scheme was developed and a test framework was implemented. Using this framework, user tests were conducted in order to investigate advantages and disadvantages of the proposed control scheme compared to a conventional sEMG control.

Reflection of Results

The achievable accuracy of orientation and position tracking was determined for the Bosch BMX055 – a state of the art IMU with excellent properties. It was shown that the white sensor noise of the accelerometer and the gyroscope represents the dominant error source and allows a suitable estimation of the uprising drifts.

Orientation tracking by integrating the angular velocity leads to a stable but non-attractive error solution. In contrast, position tracking by double integration of the accelerations (without any aiding sensor information) leads to an unstable error dynamic and therefore to a rapidly growing displacement error. The dominant error source is given by the gyroscope noise, as an error in the estimated vertical leads to a projection of the Earth's gravity onto the horizontal plane which leads to large error within the horizontal plane.

It was shown that the orientation tracking error remains in the range of tenths of a degree for a considered time span of five seconds. On the contrary, after five seconds the displacement error caused by the accelerometer noise is in the range of several centimeters and the error caused by the gyroscope noise is in the range of 1m. Even though the error caused by the gyroscope noise can be reduced by utilizing additional attitude information obtained by the accelerometer, it was concluded that a control scheme based on position tracking is hardy feasible.

Subsequently an orientation-based control scheme was developed which allows the positioning of two prosthesis joints simultaneously. User tests showed that the proposed

control scheme allows a more precise and faster positioning of prosthesis joints compared to a conventional sEMG control. Though the control scheme requires an arm movement that might be considered a disadvantage at first sight, the participants did not perceive this as problematic, and rated the required range of arm movements as reasonable. The participants evaluated the proposed control scheme as being a potential improvement over the conventional control with respect to wrist rotation and flexion/extension. However, they preferred the conventional sEMG control for grasping.

Study Limitations and Outlook

In this work, it was not evaluated how an inertial behavior of a physical prosthesis affects the control quality of the proposed control scheme. Instead the virtual prosthesis moved towards the specified configuration instantaneously. For further work, it is suggested to incorporate the proposed control scheme into a physical prosthesis allowing it to interact with the real world, and making tests with a real prosthesis possible. Presently, there are widely-used tests which evaluate control performance through interaction with physical objects and performing daily life activities such as the Southampton Hand Assessment Procedure and the Box and Blocks Test [52]. Furthermore, a prototype would allow prosthesis users to apply the proposed control scheme for an extended span of time. This would provide users with the opportunity to evaluate the control concept, along with the practicality of use in their everyday lives.

A Appendix

A.1 Questionnaire results: able-bodied participants

About the participant

Age: 22, 30, 21, 26, 22, 51, 21, 22, 26, 22, 35, 37

Sex: male x 11, female x 1

Dominant hand: right hand x 11, left hand x 1

Do you regularly use a computer mouse as an input device?: yes x 12

Do you use 3D applications on your PC (CAD programs, computer games)?: no x 6, yes x 6

Do you already have experience using the four-channel control?:

- No: 9
- Yes, I have tried the four-channel control already several times: 3
- Yes, I handle the four-channel control in irregular intervals: 0
- Yes, I handle the four-channel control on a daily base: 0

Cursor positioning task, four-channel control (sEMG)

Was the explication of functioning of the control scheme comprehensible?

- Completely comprehensible: 12
- Rather comprehensible: 0
- Rather incomprehensible: 0
- Completely incomprehensible: 0
  - If not “completely comprehensible”: What was incomprehensible?

Was the time of practicing sufficient to get accustomed to the control scheme?

- Completely sufficient: 10
- Rather sufficient: 1
- Rather insufficient: 1
- Insufficient: 0

Was the explication of the test procedure comprehensible?

- Completely comprehensible: 12
- Rather comprehensible: 0
- Rather incomprehensible: 0
- Completely incomprehensible: 0
  - If not "completely comprehensible": What was incomprehensible?

Was it difficult to move the cursor as you intended to?

- Not at all: 0
- Barely: 6
- Fairly: 6
- Remarkably: 0
  - If not "Not at all": what were the problems?
    - switching the channel reliably x 3
    - slow movements -> unintentional channel switching
    - unintentional channel switching

5. Was it difficult to move the cursor with the required accuracy (size of the target)?

- Not at all: 1
- Barely: 5
- Fairly: 6
- Remarkably: 0

Did you experience pain during or after the termination of the test (e.g. caused by stress or an unnatural hand posture)?

- Yes: 2
- No: 10
  - If "yes", please describe them in more detail:
    - stress of the wrist joint x 2

Did you notice any delayed reaction or bucking (interruptions, jumps) of the cursor during the execution of the test?

- Yes: 0
- Rather yes: 0
- Rather no: 1
- no: 11
  - If not "no", when did it occur?
    - bucking at one time

Repositioning of the virtual prosthesis, four-channel control (sEMG)

Was the explication of the functioning of the control scheme comprehensible?

- Completely comprehensible: 12
- Rather comprehensible: 0
- Rather incomprehensible: 0
- Completely incomprehensible: 0
  - If not "completely comprehensible": What was incomprehensible?

Was the time of practicing sufficient to get accustomed to the control scheme?

- Completely sufficient : 10
- Rather sufficient: 1

- Rather insufficient: 1
- Insufficient: 0

Was it difficult to transfer the requested movement of the prosthesis into the necessary muscle signals?

- Not at all: 5
- Barely: 6
- Fairly: 1
- Remarkably: 0
  - If not "not at all": What were the reasons?
    - reliable channel switching
    - unintended channel switching x 2
    - fine adjustment of wrist rotation

Do you think you could handle the control scheme with more ease after some reruns of the test?

- Yes: 6
- Rather yes: 6
- Rather no: 0
- No: 0

Do you think you could use the control scheme after some practice intuitively without thinking about the functioning?

- Yes: 9
- Rather yes: 3
- Rather no: 0
- No: 0

3D visualization: Could you clearly recognize the initial configuration of the virtual prosthesis?

- Yes: 7
- Rather yes: 5
- Rather no: 0
- No: 0

Did you experience pain during or after the termination of the test (e.g. caused by stress or an unnatural hand posture)?

- Yes: 2
- No: 10
  - If "yes", please describe them in more detail:
    - stress of the wrist joint x 2

Did you notice any delayed reaction or bucking (interruptions, jumps) of the virtual prosthesis during the execution of the test?

- Yes: 0
- Rather yes: 0
- Rather no: 0
- No: 12
  - If not "no", when did it occur?

Cursor positioning task, orientation-based control (IMU)

Was the explication of the functioning of the control scheme comprehensible?

- Completely comprehensible: 12
- Rather comprehensible: 0
- Rather incomprehensible: 0
- Completely incomprehensible: 0
  - If not "completely comprehensible": What was incomprehensible?

Was the time of practicing sufficient to get accustomed to the control scheme?

- Completely sufficient: 11
- Rather sufficient: 1
- Rather insufficient: 0
- Insufficient: 0

Was the explication of the test procedure comprehensible?

- Completely comprehensible: 12
- Rather comprehensible: 0
- Rather incomprehensible: 0
- Completely incomprehensible: 0
  - If not "completely comprehensible": What was incomprehensible?

Was it difficult to move the cursor as you intended to?

- Not at all: 11
- Barely: 1
- Fairly: 0
- Remarkably: 0
  - If not "Not at all": what were the problems?
    - was not explained in more detail by the participant

Was it difficult to move the cursor with the required accuracy (size of the target)?

- Not at all: 11
- Barely: 1
- Fairly: 0
- Remarkable: 0

Was it difficult to remain in the targets?

- Not at all: 9
- Barely: 3
- Fairly: 0
- Remarkable: 0

Was the required range of movement of the forearm in a comfortable scale?

- Yes: 11
- Rather yes: 1
- Rather no: 0
- No: 0
  - If not “yes”, the required range was
    - too big: 0
    - rather too big: 1
    - Rather too small: 0
    - Too small: 0

Did you experience pain during or after the termination of the test (e.g. caused by stress or an unnatural hand posture)?

- Yes: 1
- No: 11
  - If “yes”, please describe them in more detail:
    - was not explained in more detail by the participant

Did you notice any delayed reaction or bucking (interruptions, jumps) of the cursor during the execution of the test?

- Yes: 0
- Rather yes: 0
- Rather no: 1
- No: 11
  - If not “no”, when did it occur?
    - one time short bucking - was not detrimental

Repositioning of the virtual prosthesis, orientation-based control (IMU)

Was the explication of the functioning of the control scheme comprehensible?

- Completely comprehensible: 12
- Rather comprehensible: 0
- Rather incomprehensible: 0
- Completely incomprehensible: 0
  - If not "completely comprehensible": What was incomprehensible?

Was the time of practicing sufficient to get accustomed to the control scheme?

- Completely sufficient: 11
- Rather sufficient: 1
- Rather insufficient: 0
- Insufficient: 0

Was it difficult to transfer the requested movement of the prosthesis into the necessary muscle signals?

- Not at all: 6
- Barely: 6
- Fairly: 0
- Remarkably: 0
  - If not "Not at all": what were the problems?
    - estimation of which joint has to be moved how far
    - not enough practice
    - sometimes handling of the control not intuitive

Do you think you could handle the control scheme with more ease after some reruns of the test?

- Yes: 12

- Rather yes: 0
- Rather no: 0
- No: 0

5. Did you have to focus to keep the virtual prosthesis in the target posture?

- Not at all: 10
- Barely: 2
- Fairly: 0
- Remarkable: 0

Was the required range of movement of the forearm in a comfortable scale?

- Yes: 10
- Rather yes: 2
- Rather no: 0
- No: 0
  - If not "yes", the required range was
    - too big: 0
    - rather too big: 2
    - rather too small: 0
    - too small: 0

During the test it was necessary to change two angles to get to the target. Did you feel like you changed them successively or simultaneously?

- Simultaneously: 3
- Rather simultaneously: 9
- Rather successively: 0
- Successively: 0

Did you experience pain during or after the termination of the test (e.g. caused by stress or an unnatural hand posture)?

- Yes: 1
- No: 11
  - If “yes”, please describe them in more detail:
    - was not explained in more detail by the participant

Did you notice any delayed reaction or bucking (interruptions, jumps) of the virtual prosthesis during the execution of the test?

- Yes: 0
- Rather yes: 0
- Rather no: 2
- No: 10
  - If not “no”, when did it occur?
    - maybe once (not shure)
    - second run, one time

A.2 Questionnaire results: disabled participants

About the participant

Age: 28, 28, 31, 35, 29

Sex: male x 5

Dominant hand: right hand x 2, left hand x 3

Do you regularly use a computer mouse as an input device?: yes x 3, no x 2

Do you use 3D applications on your PC (CAD programs, computer games)?: no x 5

How long does the amputation date back?: 06/2010, 3 years, 5 year, since birth, 2 year

For how long have you been provided with a prosthesis?: 07/2010, 2.5 years, 5 years, 1997, 1.5 years

With which kind of prosthesis have you been provided?: Michelangelo hand, Michelangelo hand / Sensor-Speed, Michelangelo hand, Axon - Bus, Michelangelo hand

For how many hours a day do you wear your prosthesis?: 14, 2-12, 14-15, 10-15, 5-12

Which method do you use for channel switching (4-channel, co-contraction, etc.)?:

- grasping mode: co-contraction + long opening, short impulse, long opening, co-contraction, 4-channel
- opening/closing to wrist rotation: 4-channel, not in use, co-contraction, 4-channel, 4-channel
- wrist rotation to opening closing: 4-channel, not in use, co-contraction, 4-channel, 4-channel

Are you satisfied with the current control of your prosthesis? What could be improved?

- yes very satisfied
- Wrist rotation is not in use because using the 4-channel control unintended rotations occurred. However active control of wrist rotation would be desirable.
- reliability of channel switching

Do you already have experience using the four-channel control?

- No: 2
- Yes, I have tried the four-channel control already several times: 0
- Yes, I handle the four-channel control in irregular intervals: 0
- Yes, I handle the four-channel control on a daily base: 3

Cursor positioning task, four-channel control (sEMG)

Was the explication of the functioning of the control scheme comprehensible?

- Completely comprehensible: 5
- Rather comprehensible: 0
- Rather incomprehensible: 0
- Completely incomprehensible: 0
  - If not “completely comprehensible”: What was incomprehensible?

Was the time of practicing sufficient to get accustomed to the control scheme?

- Completely sufficient: 3

- Rather sufficient: 2
- Rather insufficient: 0
- Insufficient: 0

Was the explication of the test procedure comprehensible?

- Completely comprehensible: 5
- Rather comprehensible: 0
- Rather incomprehensible: 0
- Completely incomprehensible: 0
  - If not "completely comprehensible": What was incomprehensible?

Was it difficult to move the cursor as you intended to?

- Not at all: 1
- Barely: 2
- Fairly: 2
- Remarkable: 0
  - If not "Not at all", what were the problems?
    - reliable channel switching
    - fine adjustment of movements

Was it difficult to move the cursor with the accuracy (size of the target)?

- Not at all: 0
- Barely: 4
- Fairly: 1
- Remarkable: 0

Did you experience pain during or after the termination of the test (e.g. caused by stress or an unnatural hand posture)?

- Yes: 0

- No: 5
  - If "yes", please describe them in more detail:

Did you notice any delayed reaction or bucking (interruptions, jumps) of the cursor during the execution of the test?

- Yes: 0
- Rather yes: 0
- Rather no: 4
- No: 1
  - If not "no", when did it occur?

Repositioning of the virtual prosthesis, four-channel control (sEMG)

Was the explication of the functioning of the control scheme comprehensible?

- Completely comprehensible: 5
- Rather comprehensible: 0
- Rather incomprehensible: 0
- Completely incomprehensible: 0
  - If not "completely comprehensible": What was incomprehensible?

Was the time of practicing sufficient to get accustomed to the control scheme?

- Completely sufficient: 4
- Rather sufficient: 1
- Rather insufficient: 0
- Insufficient: 0

Was it difficult to transfer the requested movement of the prosthesis into the necessary muscle signals?

- Not at all: 1

- Barely: 2
- Fairly: 2
- Remarkable: 0
  - If not "not at all": What were the reasons?
    - channel switching
    - overrun of the required position several times

Do you think you could handle the control scheme with more ease after some reruns of the test?

- Yes: 1
- Rather yes: 2
- Rather no: 2
- No: 0

Do you think you could use the control scheme after some practice intuitively without thinking about the functioning?

- Yes: 3
- Rather yes: 1
- Rather no: 1
- No: 0

3D visualization: Could you clearly recognize the initial configuration of the virtual prosthesis?

- Yes: 3
- Rather yes: 1
- Rather no: 1
- No: 0

Did you experience pain during or after the termination of the test (e.g. caused by stress or an unnatural hand posture)?

- Yes: 0
- No: 5
  - If "yes", please describe them in more detail:

Did you notice any delayed reaction or bucking (interruptions, jumps) of the virtual prosthesis during the execution of the test?

- Yes: 0
- Rather yes: 1
- Rather no: 1
- No: 3
  - If not "no", when did it occur?
    - during very fine movements

Cursor positioning task, orientation-based control (IMU)

Was the explication of the functioning of the control scheme comprehensible?

- Completely comprehensible: 5
- Rather comprehensible: 0
- Rather incomprehensible: 0
- Completely incomprehensible: 0
  - If not "completely comprehensible": What was incomprehensible?

Was the time of practicing sufficient to get accustomed to the control scheme?

- Completely sufficient: 4
- Rather sufficient: 1
- Rather insufficient: 0
- Insufficient: 0

Was the explication of the test procedure comprehensible?

- Completely comprehensible: 5
- Rather comprehensible: 0
- Rather incomprehensible: 0
- Completely incomprehensible: 0
    - If not "completely comprehensible": What was incomprehensible?

Was it difficult to move the cursor as you intended to?

- Not at all: 4
- Barely: 1
- Fairly: 0
- Remarkable: 0
    - If not "Not at all", what were the problems?

Was it difficult to move the cursor with the required accuracy (size of the target)?

- Not at all: 3
- Barely: 2
- Fairly: 0
- Remarkable: 0

Was it difficult to remain in the targets?

- Not at all: 0
- Barely: 5
- Fairly: 0
- Remarkable: 0

Was the required range of movement of the forearm in a comfortable scale?

- Yes: 3
- Rather yes: 2

- Rather no: 0
- No: 0
  - If not "yes", the required range was
    - too big: 0
    - rather too big: 2
    - rather too small: 0
    - too small: 0

Did you experience pain during or after the termination of the test (e.g. caused by stress or an unnatural hand posture)?

- Yes: 1
- No: 4
  - If "yes", please describe them in more detail:
    - exhausting which results in light discomfort in the shoulder

Did you notice any delayed reaction or bucking (interruptions, jumps) of the cursor during the execution of the test?

- Yes: 0
- Rather yes: 0
- Rather no: 1
- No: 4
  - If not "no", when did it occur?

Repositioning of the virtual prosthesis, orientation-based control (IMU)

Was the explication of the functioning of the control scheme comprehensible?

- Completely comprehensible: 5
- Rather comprehensible: 0
- Rather incomprehensible: 0

- Completely incomprehensible: 0
  - If not "completely comprehensible": What was incomprehensible?

Was the time of practicing sufficient to get accustomed to the control scheme?

- Completely sufficient: 5
- Rather sufficient: 0
- Rather insufficient: 0
- Insufficient: 0

Was it difficult to transfer the requested movement of the prosthesis into the necessary muscle signals?

- Not at all: 4
- Barely: 1
- Fairly: 0
- Remarkable: 0
  - If not "Not at all": what were the problems?
    - estimation of which joint has to be moved how far

Do you think you could use the control scheme after some practice intuitively without thinking about the functioning?

- Yes: 4
- Rather yes: 1
- Rather no: 0
- No: 0

Did you have to focus to keep the virtual prosthesis in the target posture?

- Not at all: 1
- Barely: 4
- Fairly: 0

- Remarkable: 0

Was the required range of movement of the forearm in a comfortable scale?

- Yes: 3
- Rather yes: 2
- Rather no: 0
- no: 0
  - If not “yes”, the required range was
    - too big: 0
    - rather too big: 2
    - rather too small: 0
    - too small: 0

Do you think you could handle the control scheme with more ease after some reruns of the test?

- Yes: 3
- Rather yes: 1
- Rather no: 1
- No: 0

During the test it was necessary to change two angles to get to the target. Did you feel like you changed them successively or simultaneously?

- Simultaneously: 3
- Rather simultaneously: 2
- Rather successively: 0
- Successively: 0

Did you experience pain during or after the termination of the test (e.g. caused by stress or an unnatural hand posture)?

- Yes: 2

- No: 3
  - If "yes", please describe them in more detail:
    * fatigue of shoulder muscles due to the weight of the prosthesis
    * during execution slight stress in the shoulder

Did you notice any delayed reaction or bucking (interruptions, jumps) of the virtual prosthesis during the execution of the test?

- Yes: 0
- Rather yes: 0
- Rather no: 2
- No: 3
  - If not "no", when did it occur?

Comparison of the four-channel control (sEMG) and orientation-based control (IMU)

With with control scheme was it possible to position the prosthesis joints in a more accurate way?

- with the four-channel control: 0
- rather with the four-channel control: 0
- rather with the orientation-based control: 3
- with the orientation-based control: 2
  - How important is the possibility of positioning the prosthesis' joint in an accurate way to you?
    * Important: 3
    * Rather important: 1
    * Rather unimportant: 1
    * Unimportant: 0

Are the situations in everyday life in which you wish for the possibility of a more accurate positioning of the prosthesis' joints? If yes, what are the situations?: modeling, opening closet (too time-consuming to position the joints accurately)

With which regulation was it possible to position the prosthesis joints quicker?

- with the four-channel control: 0
- rather with the four-channel control: 0
- rather with the orientation-based control: 3
- with the orientation-based control: 2
  - How important is the possibility of quickly positioning the prosthesis' joints to you?
    - Important: 4
    - Rather important: 1
    - Rather unimportant: 0
    - Unimportant: 0

Are the situations in everyday life in which you wish for the possibility of a quicker positioning of the prosthesis joints? If yes, what are the situations?: same answers given as before

For the control of which joints could you in principle imagine using the IMU-based control scheme?

- rotation of the wrist joint:
  - Yes: 3
  - Rather yes: 1
  - Rather no: 1
  - No: 0
- open/closing of the hand:
  - Yes: 0
  - Rather yes: 0
  - Rather no: 3
  - No: 2

Could you imagine the orientation-based control scheme as a substitution of your current control scheme in terms of rotation of the wrist?

- Yes: 2
- Rather yes: 2

- Rather no: 1
- No: 0
  - Annotation: “rather no as an unintended rotation of the wrist could be dangerous in situations like driving a car”

5. Could you imagine the orientation-based control scheme as a substitution of your current control scheme in terms of opening/closing the hand ?

- Yes: 0
- Rather yes: 0
- Rather no: 1
- No: 4
  - Annotation: ”with sEMG control the force is proportional to the contraction level, with the orientation-based control dosing the force would impossible as no feedback exists.”

In principle, it is possible to allow opening/closing of the hand and rotation of the wrist simultaneously. In doing so, the positioning of the joint would be effected via orientation-based control and the positioning of the other joint via sEMG control. Would this simultaneous control of two joints be eligible?

- Yes: 2
- Rather yes: 3
- Rather no: 0
- No: 0
  - Which advantages and disadvantages could this result in?: faster and simultaneous positioning, less mode switching necessary

Which joint would you relate to which regulation type?

- orientation-based control: rotation of the wrist x 5
- sEMG control: opening/closing of the hand x 5

Could you imagine using a system that allows simultaneous opening/closing of the hand sEMG and rotation of the wrist via the orientation-based control scheme?

- Yes: 2
- Rather yes: 2
- Rather no: 1
- No: 0
  - Which advantages and disadvantages could this result in?
    * driving a car: would be bad, if the orientation-based control would be activated unintended
    * movement patter would be faster
    * probably some practice necessary, it has to be possible to activate and deactivate the control thus only in combination with sEMG control

Bibliography

[1] Scheme E., Englehart K., "Electromyogram pattern recognition for control of powered upper-limb protheses: State of the art and challanges for clinical use", Journal of Rehabilitation Research & Development, Vol. 48, Nr. 6, 2011, pp. 643-660

[2] Mayer R., "3D Position Estimation using Inertial Measurement Units for a Novel Control of Upper Limb Prothesis", Diploma Thesis, Institute of Electrodynamics, Microwave and Circuit Engineering, TU Vienna, 2015

[3] Simon A., Hargrove L., Lock B., Kuiken T., "The Target Achievement Control Test: Evaluation real-time myoelectric pattern recognition control of a mutlifunctional upper-limb prothesis", J Rehabil Dev. 2011; 48(6), pp. 619-628

[4] Groves P., "Principles of GNSS, Inertial, and Multisensr Integrated Navigation Systems", Artech House, 2. Edition, 2013

[5] Roman S., "Advanced Linear Algebra", Springer, 3. Edition, 2008

[6] Bremer H., "Vorlesungsskriptum Technische Mechanik 3", JKU Linz, 2. Edition, 2010

[7] Du Val P., "Homographies, Quaternions and Rotations", Oxford University Press, 1964

[8] Wendel J., "Integrierte Navigationssysteme, Sensordatenfusion, GPS und Inertiale Navigationssysteme", Oldenbourg Verlag München, 2. Edition, 2011

[9] Titterton D., Weston J., "Strapdown Inertial Navigation Technology", The American Institute of Aeronautics and Astronautics, 2. Edition, 2004

[10] Dacunha J., "Transition matrix and generalized matrix exponential via the Peano-Baker series", Department of Mathematical Sciences, United States Military Academy, 2005

[11] Ahmed M., Ćuk D., "Strapdown Attitude Algorithms using Quaternion Transition Matrix and Random Inputs", Scientific-Technical Review, Vol.LV,No.1, 2005

[12] M. A. El-Gohary., "Joint Angle Tracking with Inertial Sensors", Dissertation, Department of Electrical and Computer Engineering, Portald State University, 2013

[13] H. A. Abdulla., "Dynamic biomechanical model for assessing and monitoring robot-assisted upper-limb therapy", JRRD, Vol. 44, No. 1, 2007, pp. 43-62

[14] Armenise M., Ciminelli C., Dell'Olio F., Passaro V., "Advances in Gyroscope Technologies", Springer, 2010

[15] Shkel A. (2016, Jan. 18). "Type I and Type II Micromachined Vibrator Gyroscopes", Position, Location, And Navigation Symposium, 2006 IEEE/ION

[16] Zhang G., Wei B., "Advanced Mechatronics and MEMS Devices II", 1. Edition, 2017

[17] Tomaszewski D., Rapinski J., Smieja M., "Analysis of the noise parameters and attitude alignment accuracy of INS conducted with the use of MEMS-based integrated navigation systems", Acta Geodyn. Geomater., Vol. 12, No. 2 (178), 197–208, 2015

[18] Woodman O., "An introduction to inertial navigation, Technical Report Number 696", University of Cambridge [Online]

[19] Panahandeh, G., Skog I., Jansson M., "Calibration of the Accelerometer Triad of an Inertial Measurement Unit, Maximum Likelihood Estimation and Cramer-Rao Bound", 2010, International Conference on indoor positioning and indoor navigation

[20] Tedaldi D., Pretto A., Menegatti M., "A Robust and Easy to Implement Method for IMU Calibration without External Equipments", 2014, IEEE International Conference on Robotics and Automation

[21] Looney M., "A Simple Calibration for MEMS Gyroscopes", July 2010, Electronic Design Europe Magazin (EDN)

[22] Olivares A., Olivares G., Gorriz J. M, Ramirez J., "High-Efficiency Low-Cost Accelerometer-Aided Gyroscope Calibration", 2009, IEEE, International Conference on Test and Measurement

[23] Pretto A., Grisetti G., "Calibration and performance evaluation of low-cost IMUs", 2014, 20th IMEKO TC4 International Symposium

[24] Resnik L., Klinger, Shana L., Etter K., "The DEKA Arm: Its features, functionality, and evolution during the Veterans Affairs Study to Optimize the DEKA Arm", Prosthetics and Orthotics International 38(6): 492-504, 2014

[25] "i-limb quantum Clinician Manuel", http://touchbionics.com. Touch Bionics, July 2015

[26] Woodward R., Shefelbine S., Vaidyanathan R., "Integrated Grip Switching and Grasp Control for Prosthetic Hands Using Fused Inertial and Mechanomyography Measurement", Swarm/Human Blended Intelligence Workshop (SHBI), 2015

[27] Scheme E., Fougner A., Chan A.D.C., Englehart K., "Examining the Adverse Effects of Limb Position on Pattern Recognition Based Myoelectric Control ", 32nd Annual International Conference of the IEEE EMBS, 2010

[28] Fougner A, Scheme E, Chan AD, Kyberd PJ, Englehart K, Stavdahl, "Adverse effects of limb position on myoelectric control of upper-limb prostheses", Proceedings of the 22nd International Conference of the Society for Medical Innovation and Technology; 2010

[29] Churko J. M., Mehr A., Linassi G., Dinh A., "Sensor Evaluation for Tracking Upper Extremity Prosthesis Movements in a Virtual Environment", 31st Annual International Conference of the IEEE, 2009

[30] Dermitzakis K., Hernandez A., Pfeifer R., "Gesture recognition in upper-limb prosthetics: A viability study using Dynamic Time Warping and gyroscopes", 33rd Annual International Conference of the IEEE, 2011

[31] Aggarwal P., Syed Z., Niu X., El-Sheimy N., "Cost-effective Testing and Calibration of Low Cost MEMs Sensors for Integrated Positioning, Navigation and Mapping Systems", Shapping the Change XXIII FIG Congress, Munich, Germany, October 8-13, 2006

[32] Wahba G., "A least-square estimate of spacecraft attitude", SIAM Review, 7:409, 1965

[33] Sabatini A., "Kalman-Filter-Based Orientation Determination Using Inertial/Magnetic Sensors: Observability Analysis and Performance Evaluation", Sensors 2011, 11, 9182-9206

[34] Madgwick S. (Online), "An efficient orientation filter for inertial and inertial/magnetic sensor arrays", Access: https://www.samba.org/tridge/UAV/madgwick_internal_report.pdf

[35] Veltnik P., Bussmann H., de Vries W., Martens W., Van Lummel R., "Detection of static and dynamic activities using uniaxial accelerometers", 1996, IEEE Trans. Rehabiil. Eng., pp. 375-385

[36] Bachman E., Yun X., Perterson C., "An Investigation of the Effects of Magnetic Variations on Inertialklagnetic Orientation Sensors", Prodlnga on the 2004 IEEE International Conference on Robotics and Automation, New Orleans, 2004

[37] Marins J., Yun X., Bachman E., McGhee R., Zysa M., "An Extended Kalman Filter for Quaternion-Based Orientation Estimation Using MARG Sensors", 2001, IEEE/RSJ International Conference on Intelligent Robots and Systems, pp. 2003-2009

[38] Madgwick S., Harrison A., Vaidyanathan R., "Estimation of IMU and MARG orientation using a gradient descent algorithm", 2011, IEEE International Conference on Rehabilitation Robotics

[39] W. Lie, J. Wang, "Effective Adaptive Kalman Filter for MEMS-IMU/Magnetometers Integrated Attitude and Heading Reference Systems", 2013, The Journal of Navigation, 66, pp. 99–113

[40] Sabatini A.: "Quaternion-Based Extended Kalman Filter for Determining Orientation by Inertial and Magnetic Sensing", 2006, IEEE TRANSACTIONS ON BIOMEDICAL ENGINEERING, VOL. 53, NO. 7

[41] R. Mahony, Hamel T., Pflimlin J., "Nonlinear Complementary Filters on the Special Orthogonal Group" IEEE Transactions on Automatic Control, Institute of Electrical and Electronics Engineers, 2008, 53 (5), pp.1203-1217

[42] Zhao F., van Wachem B.G.M., "A novel Quaternion integration approach for describing the behaviour of non-squerical particles", Springerlink, 2013

[43] V. Bistrovs, "Analyse of MEMS Based Inertial Sensors Parameters for Land Vehicle Navigation Application," Scientific Journal of RTU: Telecommunications and Electronics, vol. 8, 2008, pp. 43–47

[44] Neto P., Ries J.N., "3-D Estimation from Inertial Sensing: Minimizing the Error from the Process of Double Integration of Accelerations", Industrial Electronics Society, IECON 2013 - 39th Annual Conference of the IEEE

[45] Nebot E., Durrant-Whyte H., "Initial Calibration and Alignment of Low Cost Inertial Navigation Units for Land Vehicle Applications", Journal of Robotics Systems, Vol. 16, No. 2, 1999, pp. 81-92.

[46] Stančić R. and Graovac S., Land Vehicle Navigation System Based on the Integration of Strap-Down INS and GPS, ELECTRONICS, VOL. 15, NO. 1, 2011, pp. 54-61

[47] Baudoin Y., Habib M., "Using robots in hazardous environments", Woodhead Publishing, 1. Edition, 2011, p. 273

[48] A. Olivares, J. Ramírez, J. M. Górriz, G. Olivares, and M. Damas, "Detection of (In)activity Periods in Human Body Motion Using Inertial Sensors: A Comparative Study," Sensors, vol. 12, no. 5, pp. 5791–5814, 2012.

[49] Tantamjarik E., Tanprasert T.,"Distance Measurement with Smartphone using Acceleration Model of Hand Movement", 2016, 8th International Conference on Knowledge and Smart Technology (KST)

[50] Matejček M., Šostronek M., "Computation and Evaluation Allan Variance Results", 2016, New Trends in Signals Processing (NTSP)

[51] Marinov M., Petrov Z., "Allan Variance Analysis on Error Characters of Low-Cost MEMS Accelerometer MMA8451Q", International Conference of Science Paper AFASES, 2014

[52] B. Calli, A. Walsman, A. Singh, S. Srinivasa, P. Abbeel and A. M. Dollar, "Benchmarking in Manipulation Research: Using the Yale-CMU-Berkeley Object and Model Set," in IEEE Robotics & Automation Magazine, vol. 22, no. 3, pp. 36-52, Sept. 2015

Eidesstattliche Erklärung

Ich erkläre an Eides statt, dass ich die vorliegende Diplomarbeit selbstständig und ohne fremde Hilfe verfasst, andere als die angegebenen Quellen und Hilfsmittel nicht benutzt bzw. die wörtlich oder sinngemäß entnommenen Stellen als solche kenntlich gemacht habe. Die vorliegende Diplomarbeit ist mit dem elektronisch übermittelten Textdokument identisch.

Wien, am 29.08.2017 Vorname Nachname